Symmetry, magnetism and phase coexistence in Superconducting Iron Chalcogenides $A_yFe_{2-x}Se_2$ (A=K, Cs, Rb)

Vladimir Pomjakushin
Laboratory for Neutron Scattering, PSI, Switzerland

Laboratory for Neutron Scattering

Bosak, Krzton-Maziopa, Conder, Pomjakushina, Pomjakushin Svitlyk, Chernyshov

---

Ekaterina Pomjakushina, Anna Krzton-Maziopa, Kazimierz Conder *Laboratory for Developments and Methods, PSI, Switzerland*
Dmitry Chernyshov, Volodymir Svitlyk *Swiss-Norwegian Beam Lines at ESRF, France*
Alexey Bosak, *ESRF, France*
Vladimir Pomjakushin *Laboratory for Neutron Scattering, Paul Scherrer Institute PSI*

Laboratory for Neutron Scattering

Bosak, Krzton-Maziopa, Conder, Pomjakushina, Pomjakushin Svitlyk, Chernyshov

Ekaterina Pomjakushina, Anna Krzton-Maziopa, Kazimierz Conder ***Laboratory for Developments and Methods, PSI, Switzerland***

Dmitry Chernyshov, Volodymir Svitlyk *Swiss-Norwegian Beam Lines at ESRF, France*

Alexey Bosak, *ESRF, France*

Vladimir Pomjakushin *Laboratory for Neutron Scattering, Paul Scherrer Institute PSI*

Laboratory for Neutron Scattering

Bosak, Krzton-Maziopa, Conder, Pomjakushina, Pomjakushin

Svitlyk, Chernyshov

Ekaterina Pomjakushina, Anna Krzton-Maziopa, Kazimierz Conder *Laboratory for Developments and Methods, PSI, Switzerland*

Dmitry Chernyshov, Volodymyr Svitlyk ***Swiss-Norwegian Beam Lines at ESRF, France***

Alexey Bosak, *ESRF, France*

Vladimir Pomjakushin *Laboratory for Neutron Scattering, Paul Scherrer Institute PSI*

Laboratory for Neutron Scattering

Bosak, Krzton-Maziopa, Conder, Pomjakushina, Pomjakushin Svitlyk, Chernyshov

Ekaterina Pomjakushina, Anna Krzton-Maziopa, Kazimierz Conder *Laboratory for Developments and Methods, PSI, Switzerland*
Dmitry Chernyshov, Volodymir Svitlyk *Swiss-Norwegian Beam Lines at ESRF, France*
Alexey Bosak, ***ESRF, France***
Vladimir Pomjakushin *Laboratory for Neutron Scattering, Paul Scherrer Institute PSI*

Laboratory for Neutron Scattering

Bosak, Krzton-Maziopa, Conder, Pomjakushina, Pomjakushin Svitlyk, Chernyshov

---

Ekaterina Pomjakushina, Anna Krzton-Maziopa, Kazimierz Conder *Laboratory for Developments and Methods, PSI, Switzerland*
Dmitry Chernyshov, Volodymir Svitlyk *Swiss-Norwegian Beam Lines at ESRF, France*
Alexey Bosak, *ESRF, France*
Vladimir Pomjakushin *Laboratory for Neutron Scattering, Paul Scherrer Institute PSI*

High temperature iron arsenides and selenides/ telurides superconductors. T_c up to 55K

X-Fe-As pnictides[1] and X-Fe-Se chalcogenides[2]

where X= Li, LaO, Ba, none, ...

---

[1] compounds of P, As, Sb, Bi
[2] compounds of S, Se, Te

High temperature iron arsenides and selenides/ telurides superconductors. T_c up to 55K

X-Fe-As pnictides[1] and X-Fe-Se chalcogenides[2]

where X= Li, LaO, Ba, none, ...

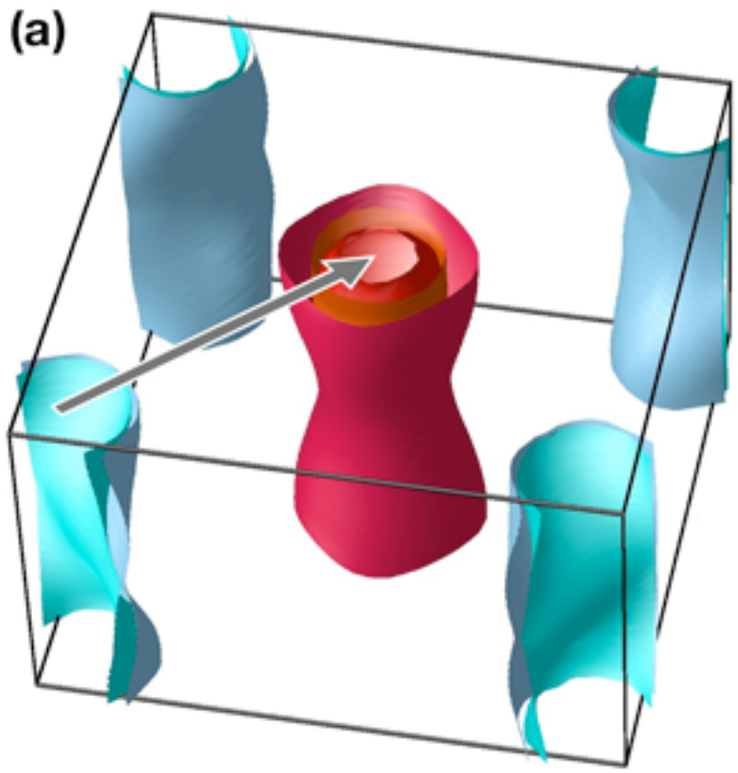

I.Mazin, Physics 4, 26 (2011)

Iron-based high-temperature superconductors were discovered in January 2008

Towards the end of 2010: the s± superconducting pairing

Calculated Fermi surfaces representative of Ba(Fe1.94Co0.06)2As2
Experimentally observed spin excitation with the same wave vector [1/2,1/2,0] or (π,π)

---

[1] compounds of P, As, Sb, Bi
[2] compounds of S, Se, Te

An unexpected surprise!
$K_yFe_{2-x}Se_2$ superconductor Tc=30K

Jiangang Guo et al, (November 2010)

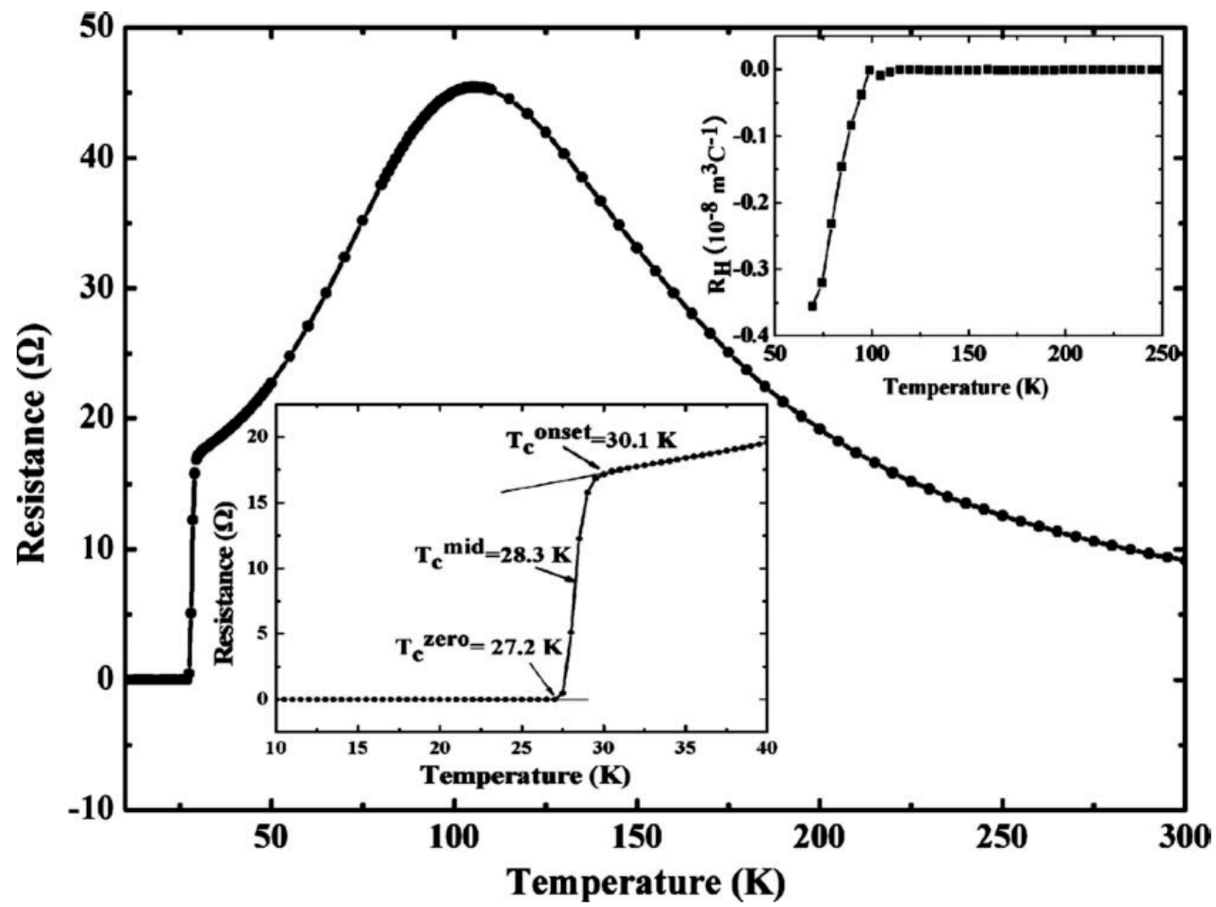

FIG. 3. The temperature dependence of electrical resistance for the $K_{0.8}Fe_2Se_2$ crystal sample. The lower inset shows the details of

1. No (π,π)-resonance!
2. AFM at room T!

Second member $Cs_yFe_{2-y}Se_2$ had been grown by

A Krzton-Maziopa, E Pomjakushina, K.Conder (December 2010)

in Laboratory of Developement and Methods at Paul Scherrer institute PSI, Switzerland

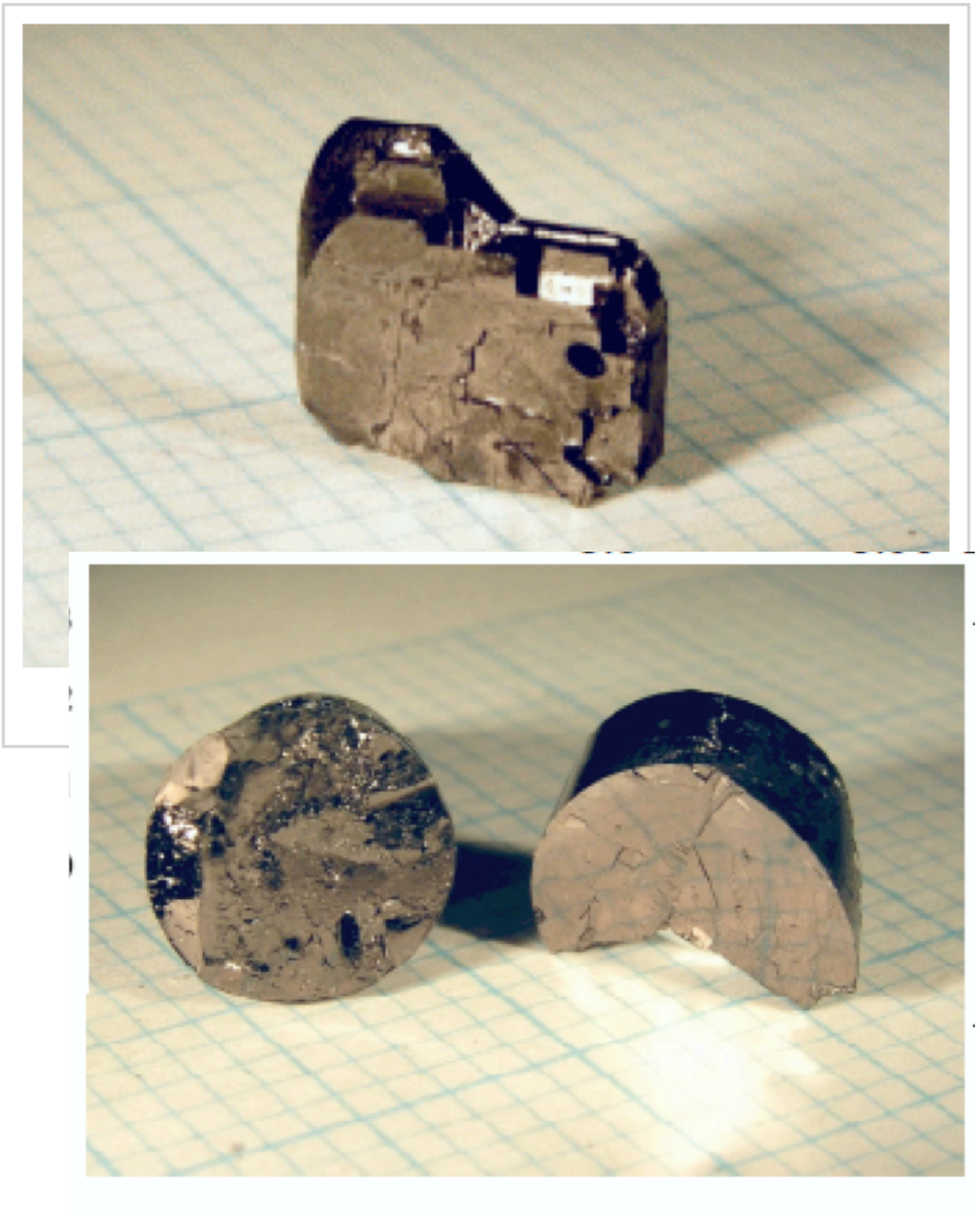

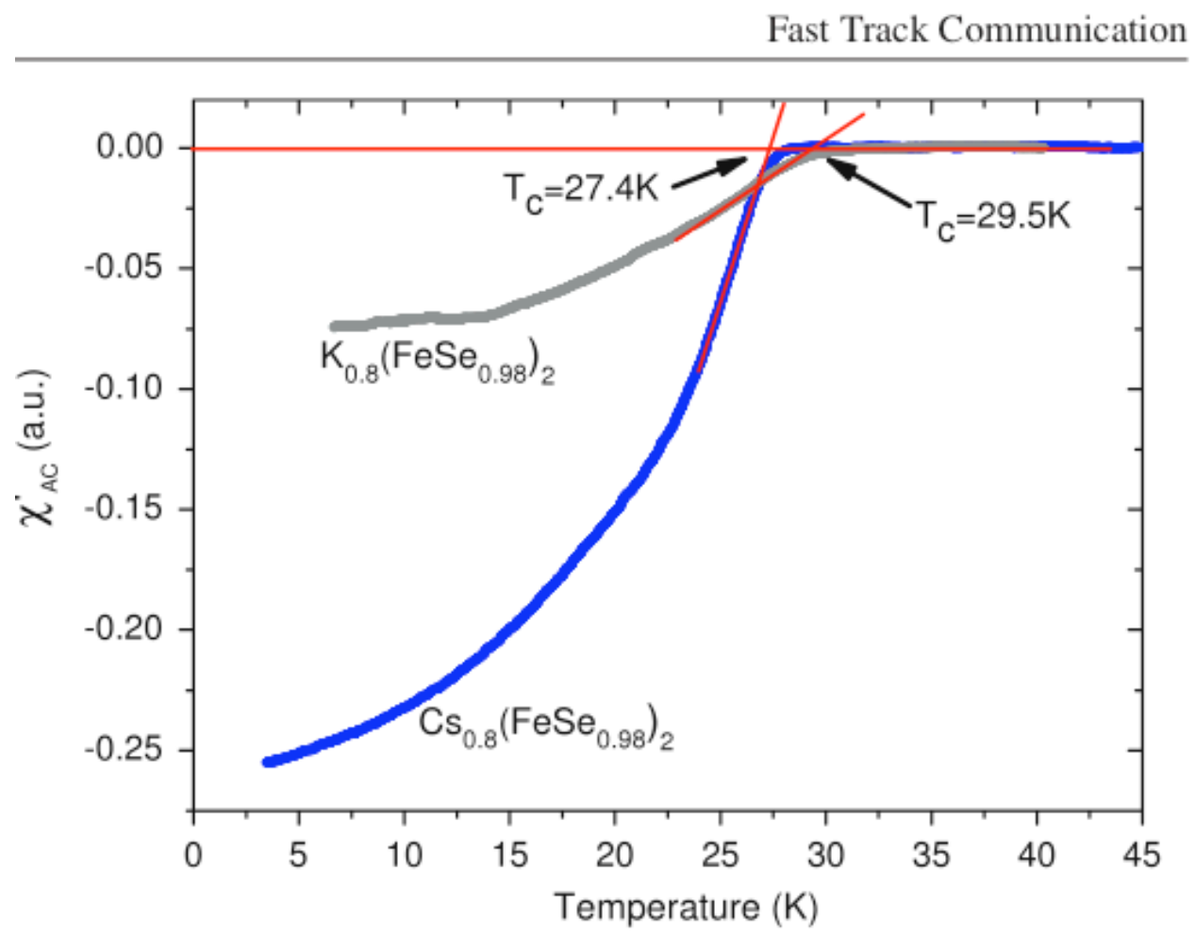

The simplest structure "11" FeSe, T_c=8K

P4/nmm. T<100K *Cmma*

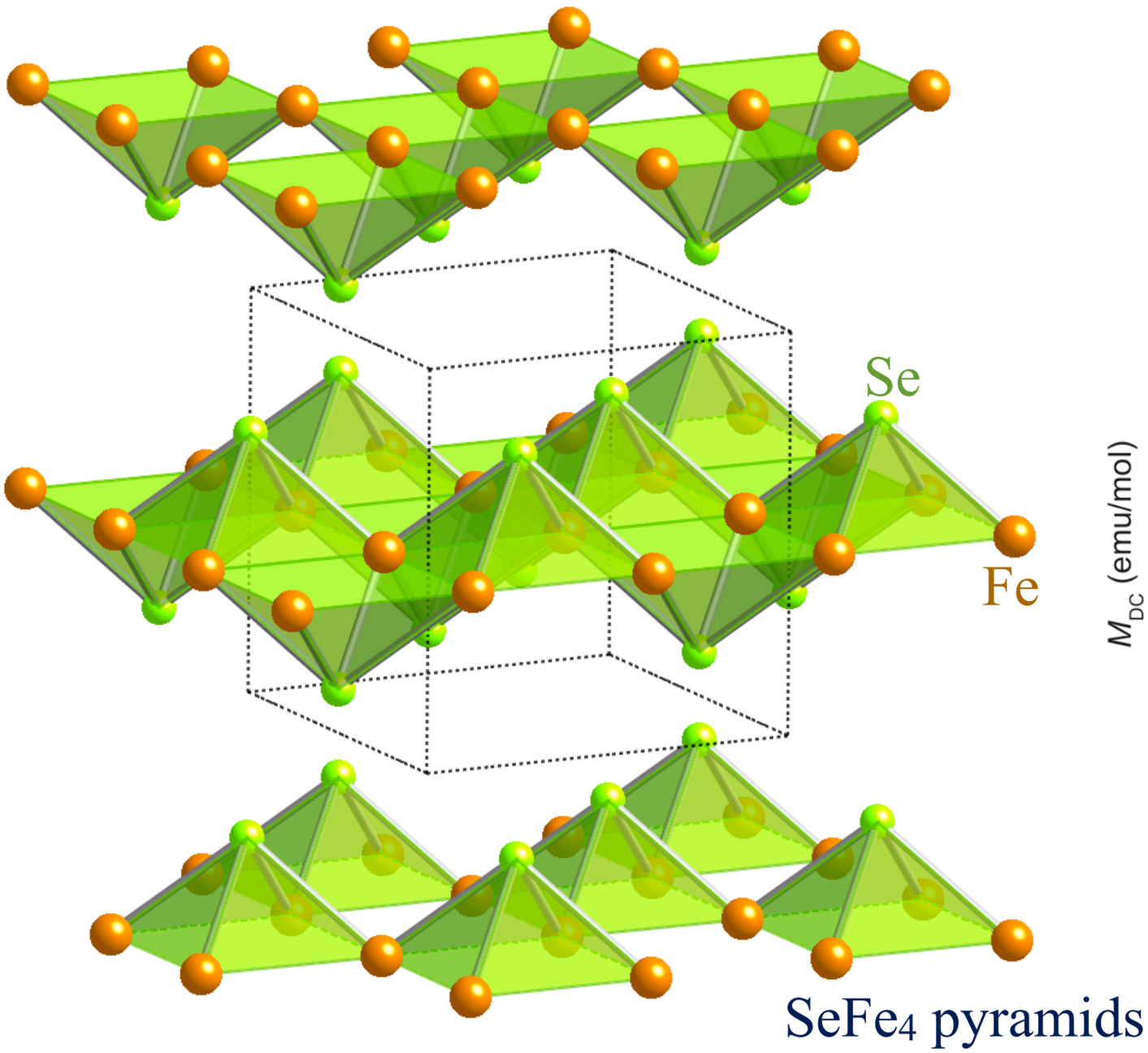

$Fe_1Se_{0.974(5)}$

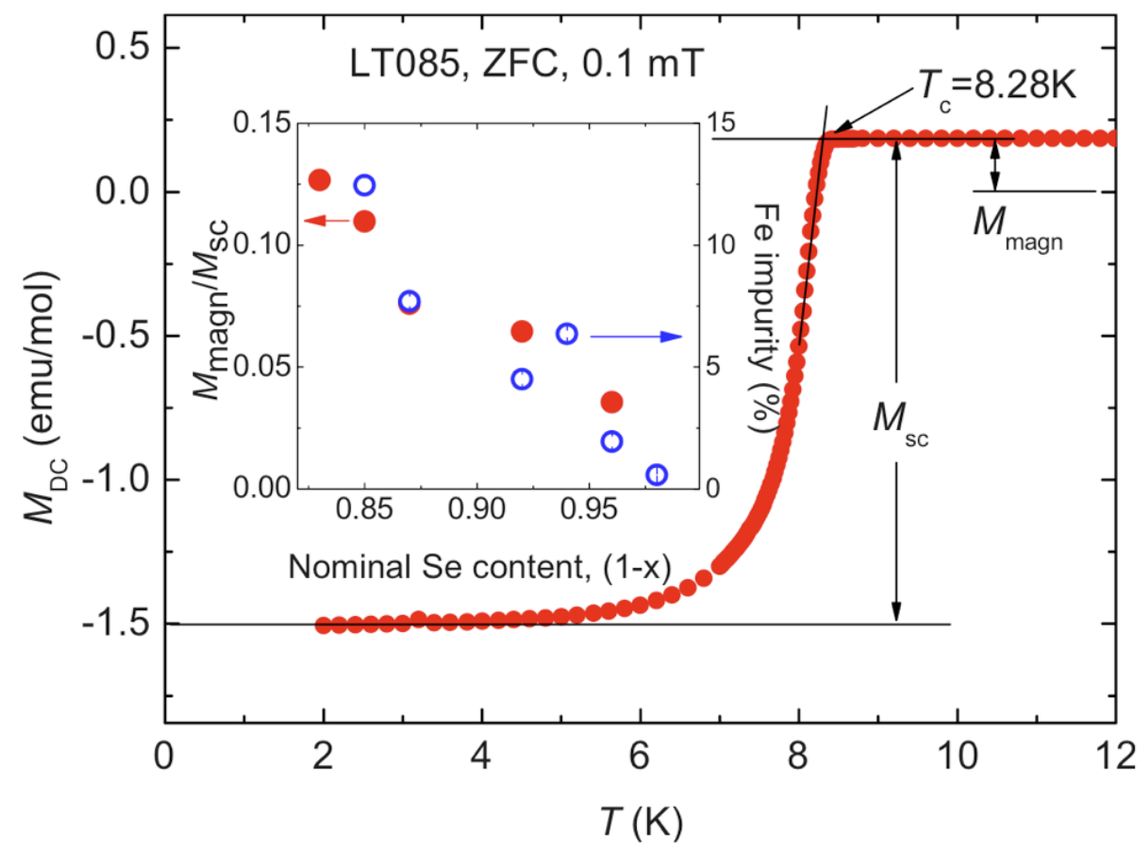

Nomenclature

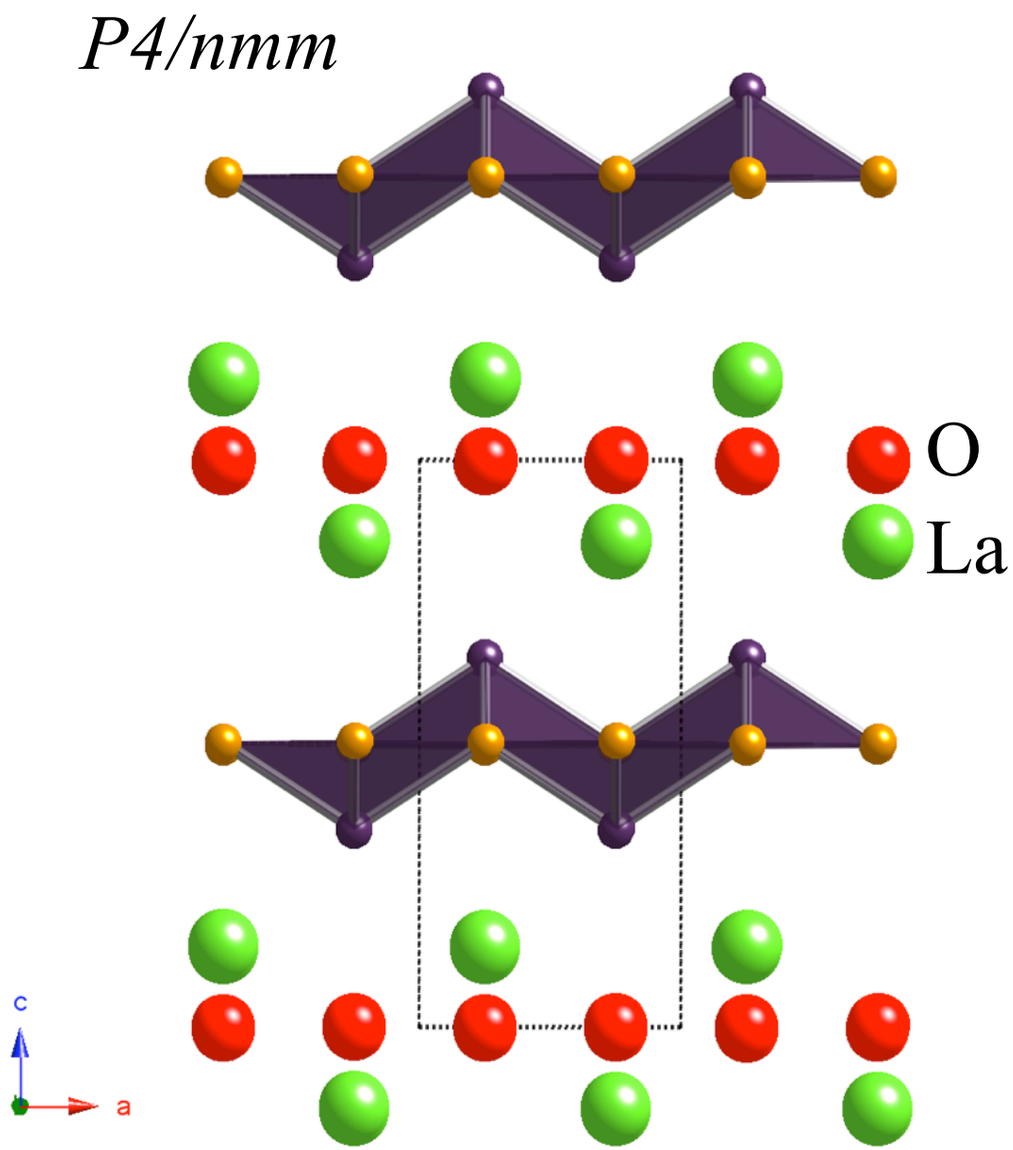

1111

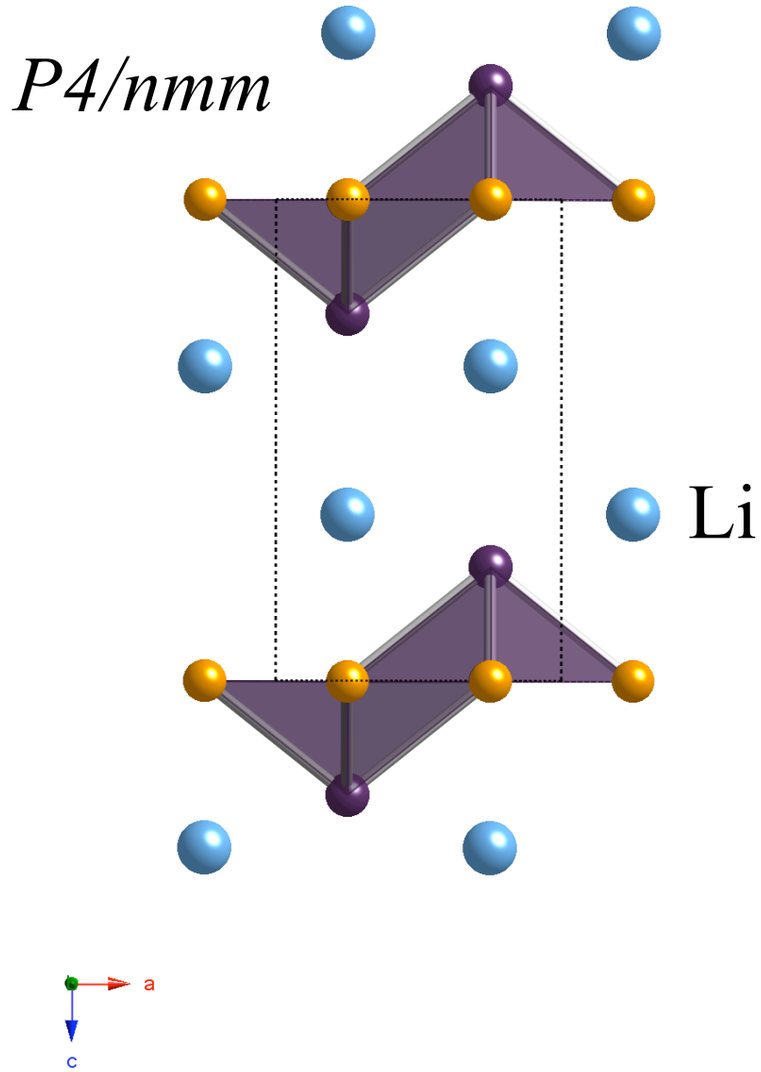

111

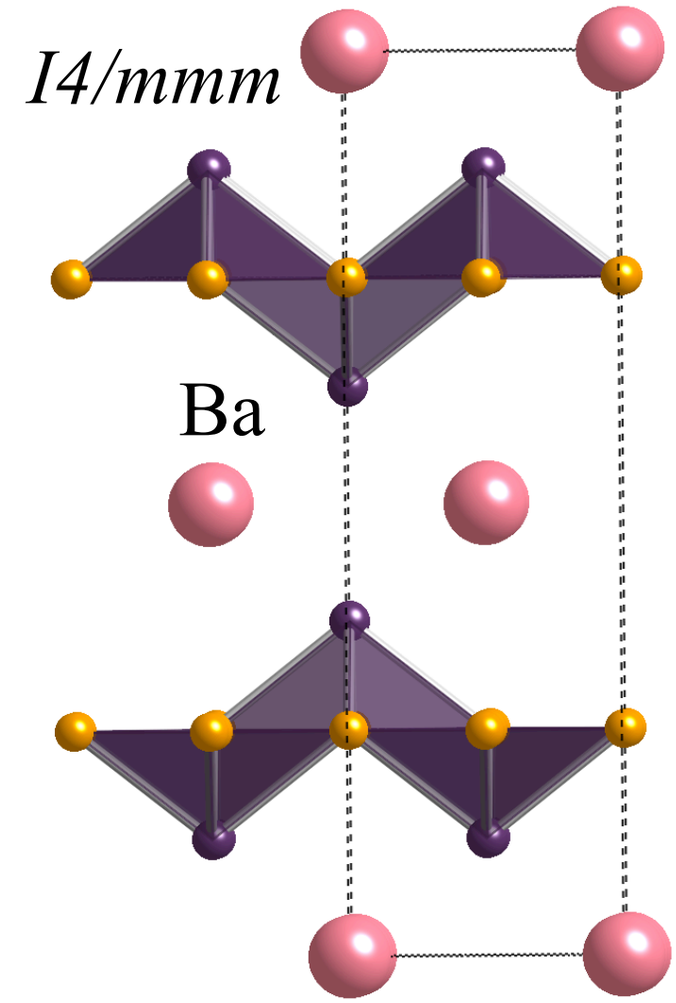

122

11	Fe_1-$(SeTe)_1$	(T_c^{max} =14K)
1111	La_1O_1-Fe_1As_1	(T_c^{max}=55K)
111	Li_1-Fe_1As_1	(T_c^{max} =18K)
122	Ba_1-Fe_2As_2	(T_c^{max} =38K)

$Fe_1Se_{0.974(5)}$ → "$A_1Fe_2Se_2$": $A_yFe_{2-x}Se_2$ (A=K, Cs, Rb)

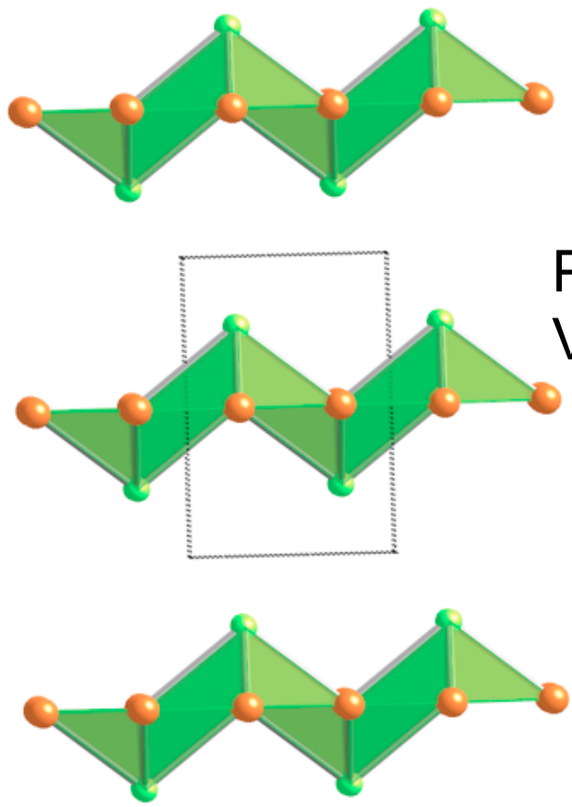

P4/nmm → (1/2,1/2,1/2)+ I4/mmm -> I4/m

Volume x2 x5

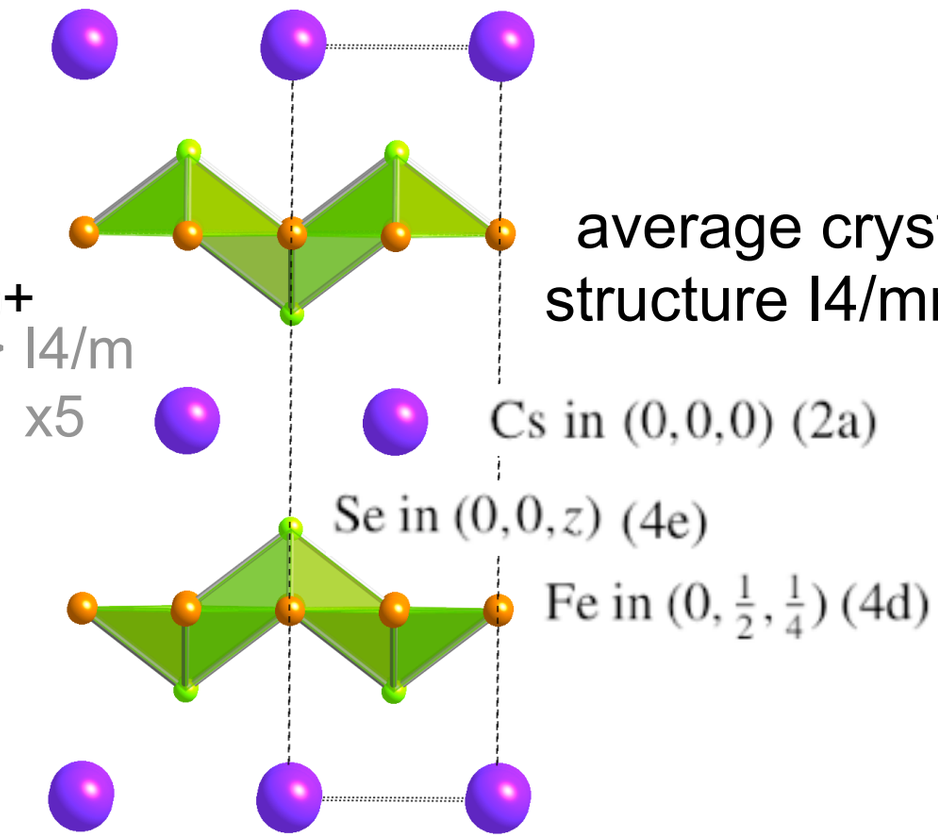

average crystal structure I4/mmm

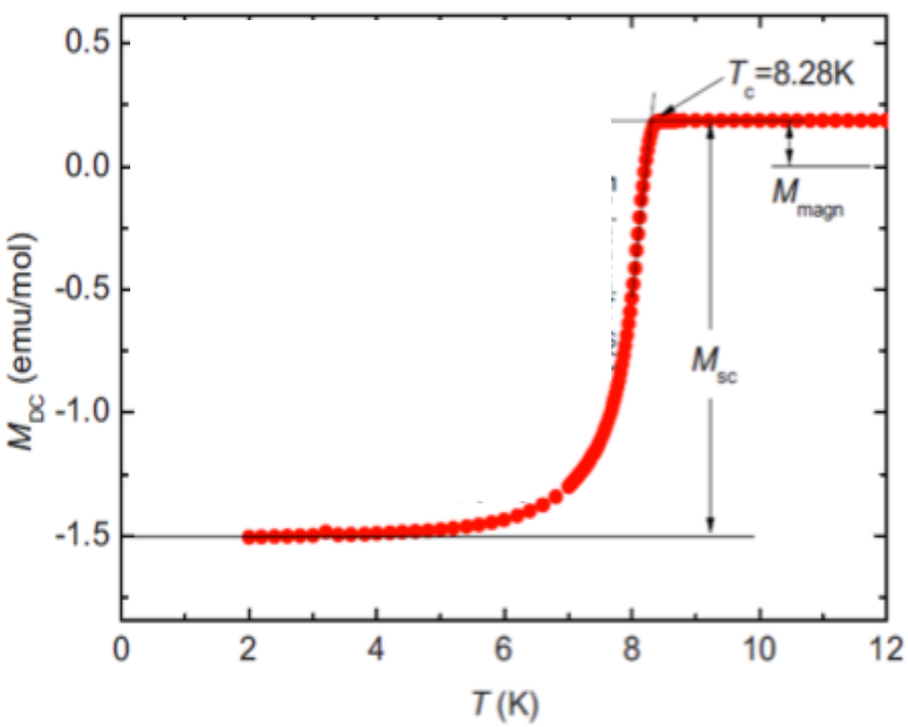

3 times increase in Tc →

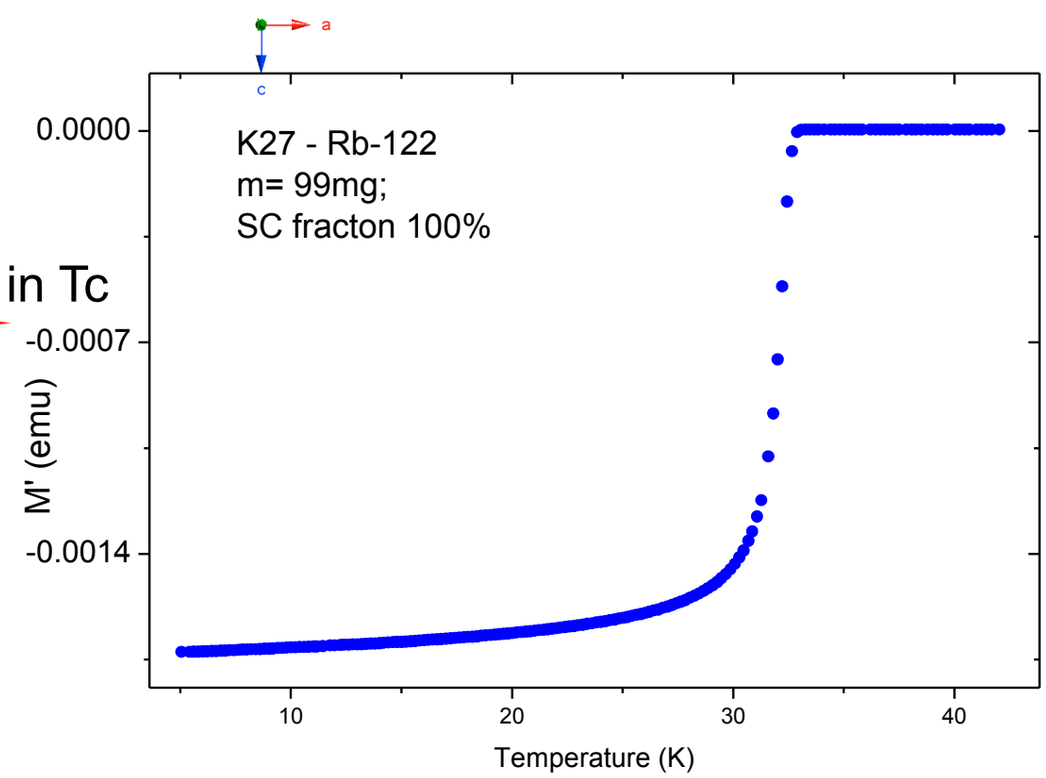

Superconducting $A_yFe_{2-x}Se_2$ are fundamentally different from perviously known 122

Superconducting $A_yFe_{2-x}Se_2$ are fundamentally different from perviously known 122

- Not single phase even in form of single crystal, opposite to all previously known 122 Ba-Fe2As2. From diffraction, uSR, microscopy,...

Superconducting $A_yFe_{2-x}Se_2$ are fundamentally different from perviously known 122

- Not single phase even in form of single crystal, opposite to all previously known 122 Ba-Fe2As2. From diffraction, uSR, microscopy,...
- Symmetry is lower than I4/mmm

Superconducting $A_yFe_{2-x}Se_2$ are fundamentally different from perviously known 122

- Not single phase even in form of single crystal, opposite to all previously known 122 Ba-Fe2As2. From diffraction, uSR, microscopy,...
- Symmetry is lower than I4/mmm
- It possesses bulk AFM. Up to $3\mu_B$ /Fe

Superconducting $A_yFe_{2-x}Se_2$ are fundamentally different from perviously known 122

- Not single phase even in form of single crystal, opposite to all previously known 122 Ba-Fe2As2. From diffraction, uSR, microscopy,...
- Symmetry is lower than I4/mmm
- It possesses bulk AFM. Up to $3\mu_B$ /Fe

- There is a strong temptation to assign SC to one of the phases with "I4/mmm 122"-structure

Superconducting $A_yFe_{2-x}Se_2$ are fundamentally different from perviously known 122

- Not single phase even in form of single crystal, opposite to all previously known 122 Ba-Fe2As2. From diffraction, uSR, microscopy,...
- Symmetry is lower than I4/mmm
- It possesses bulk AFM. Up to $3\mu_B$ /Fe

- There is a strong temptation to assign SC to one of the phases with "I4/mmm 122"-structure
- Single phase 122 material AyFe2-xSe2 (A=K,Rb,Cs) does not exist at room temperature and below.

Single crystal diffraction @ ESRF, France

beamline ID29 PILATUS 6M

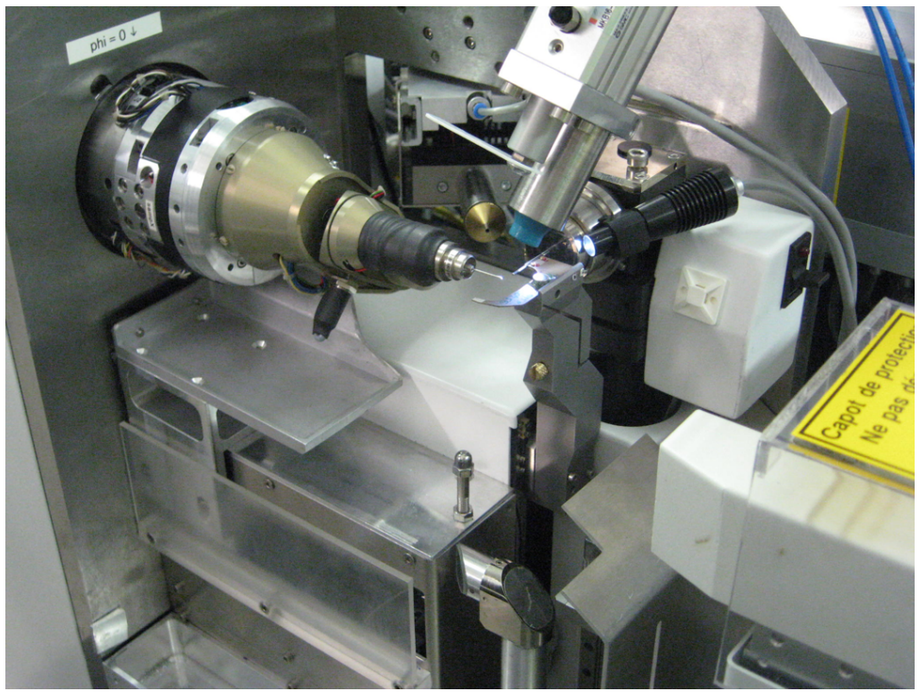

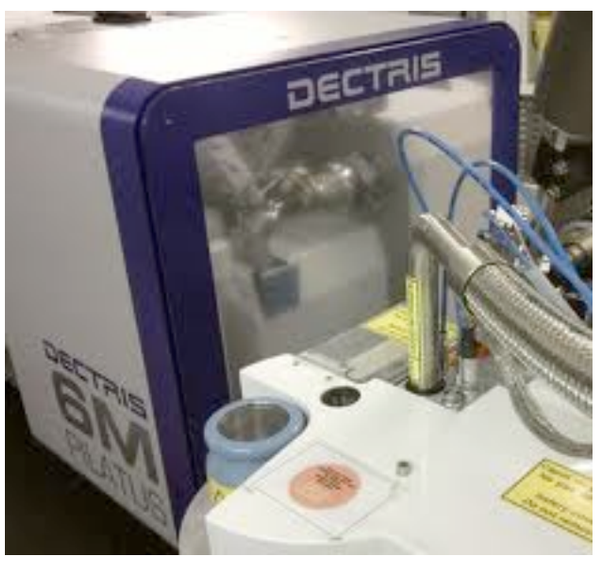

SNBL beamline BM1A with a MAR345 detector

Powder neutron diffraction @ HRPT/SINQ, Paul Scherre Institute, Switzerland

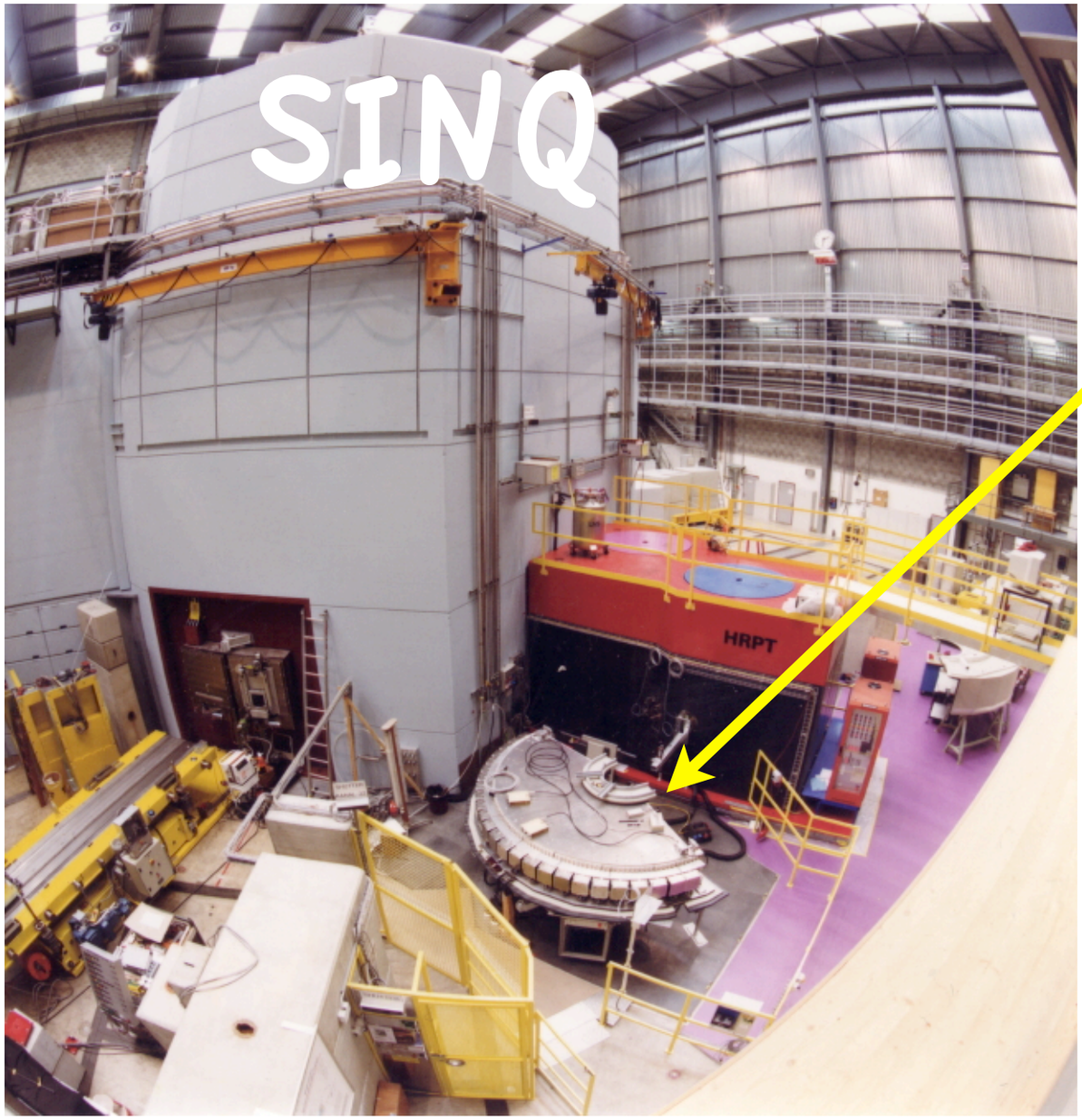

1600 channels 3He detector

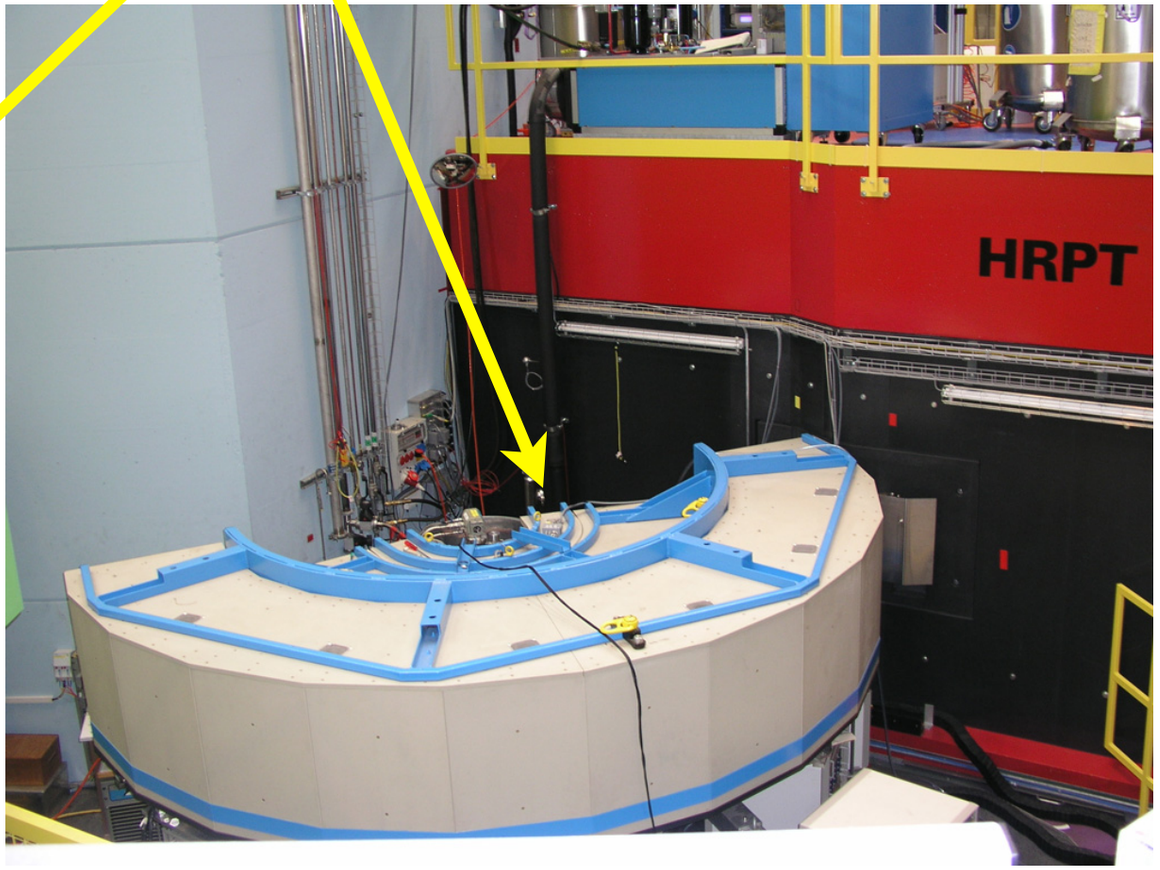

Differential scanning calorimetry. Identifying the transitions.

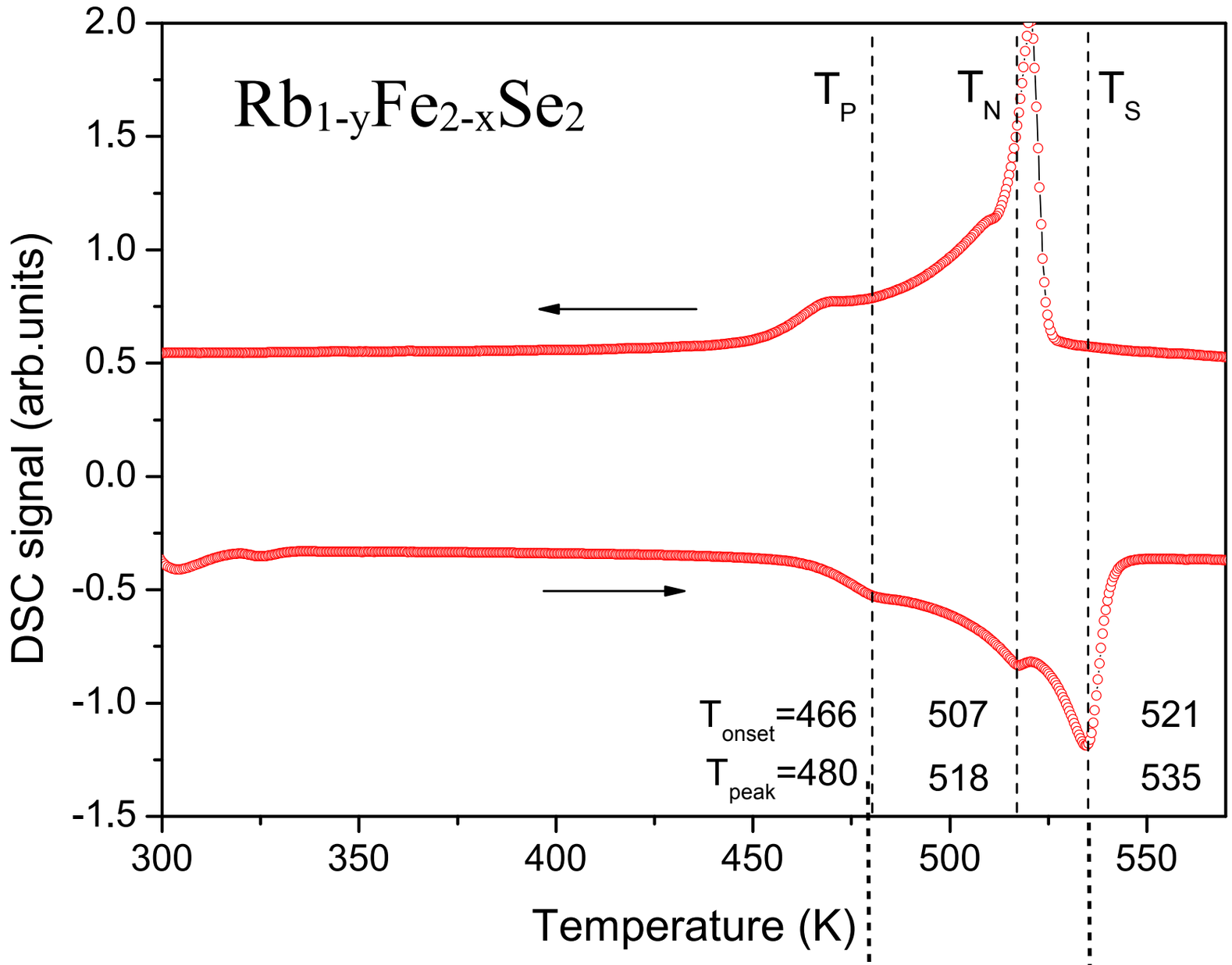

Crystal growth @ >1000K

separation of minority vacancy disordered phase about 10% fraction

I4/m, vacancy ordered $\sqrt{5}\times\sqrt{5}$

I4/mmm, vacancy disordered, 122 phase as growth

Differential scanning calorimetry. Identifying the transitions.

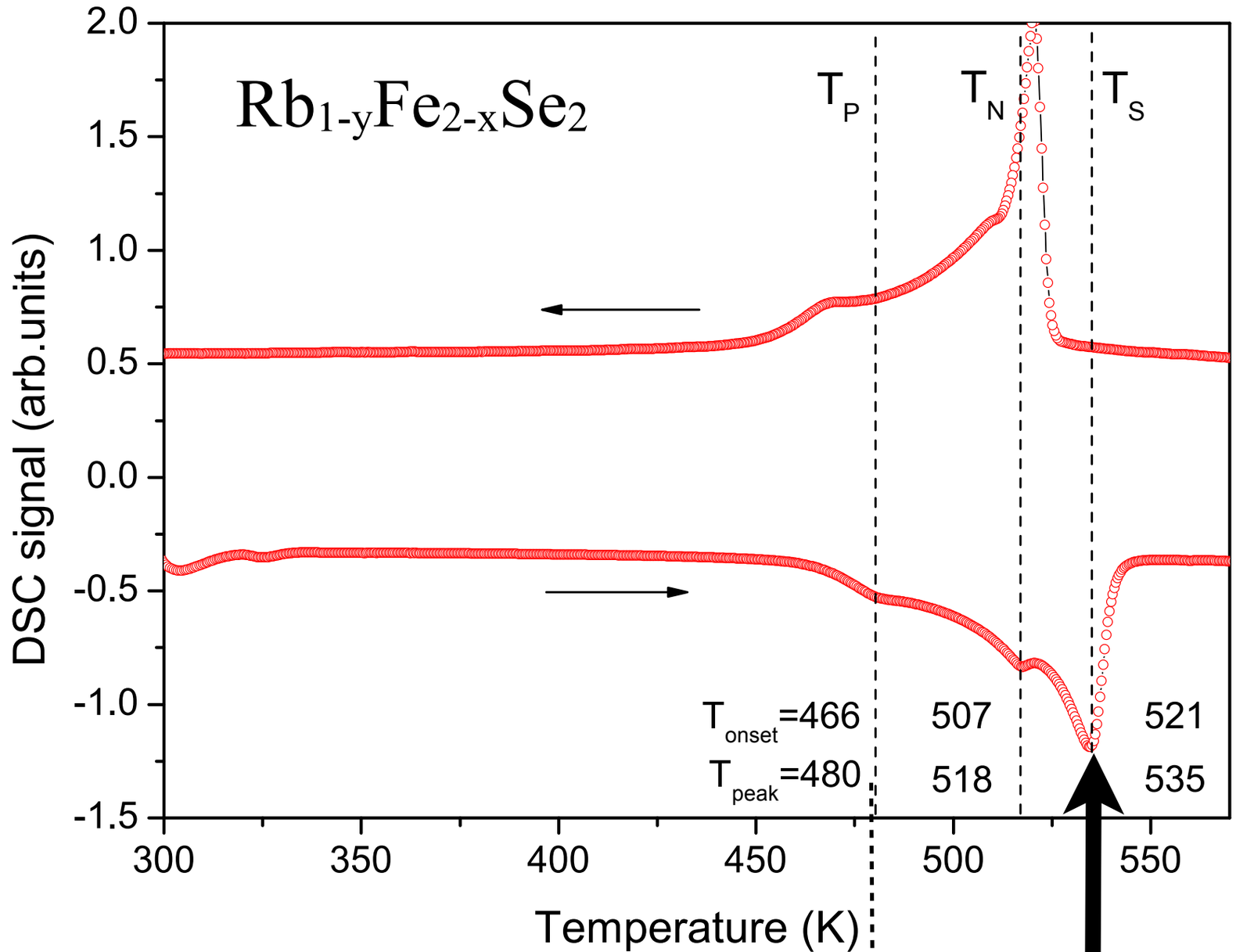

Crystal growth @ >1000K

separation of minority vacancy disordered phase about 10% fraction

I4/m, vacancy ordered $\sqrt{5}\times\sqrt{5}$

I4/mmm, vacancy disordered, 122 phase as growth

Differential scanning calorimetry. Identifying the transitions.

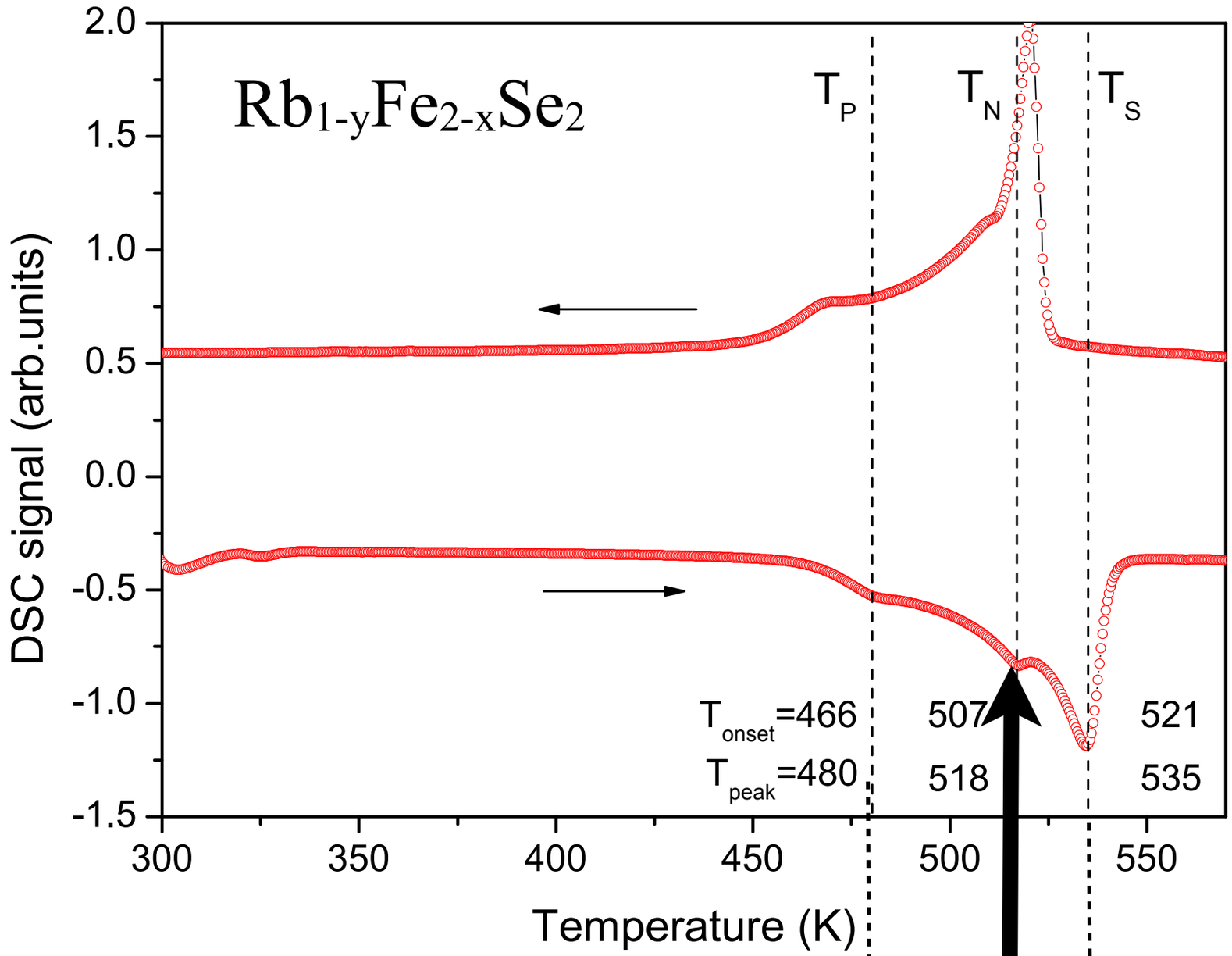

Crystal growth @ >1000K

separation of minority vacancy disordered phase about 10% fraction

I4/m, vacancy ordered $\sqrt{5}\times\sqrt{5}$

I4/mmm, vacancy disordered, 122 phase as growth

Differential scanning calorimetry. Identifying the transitions.

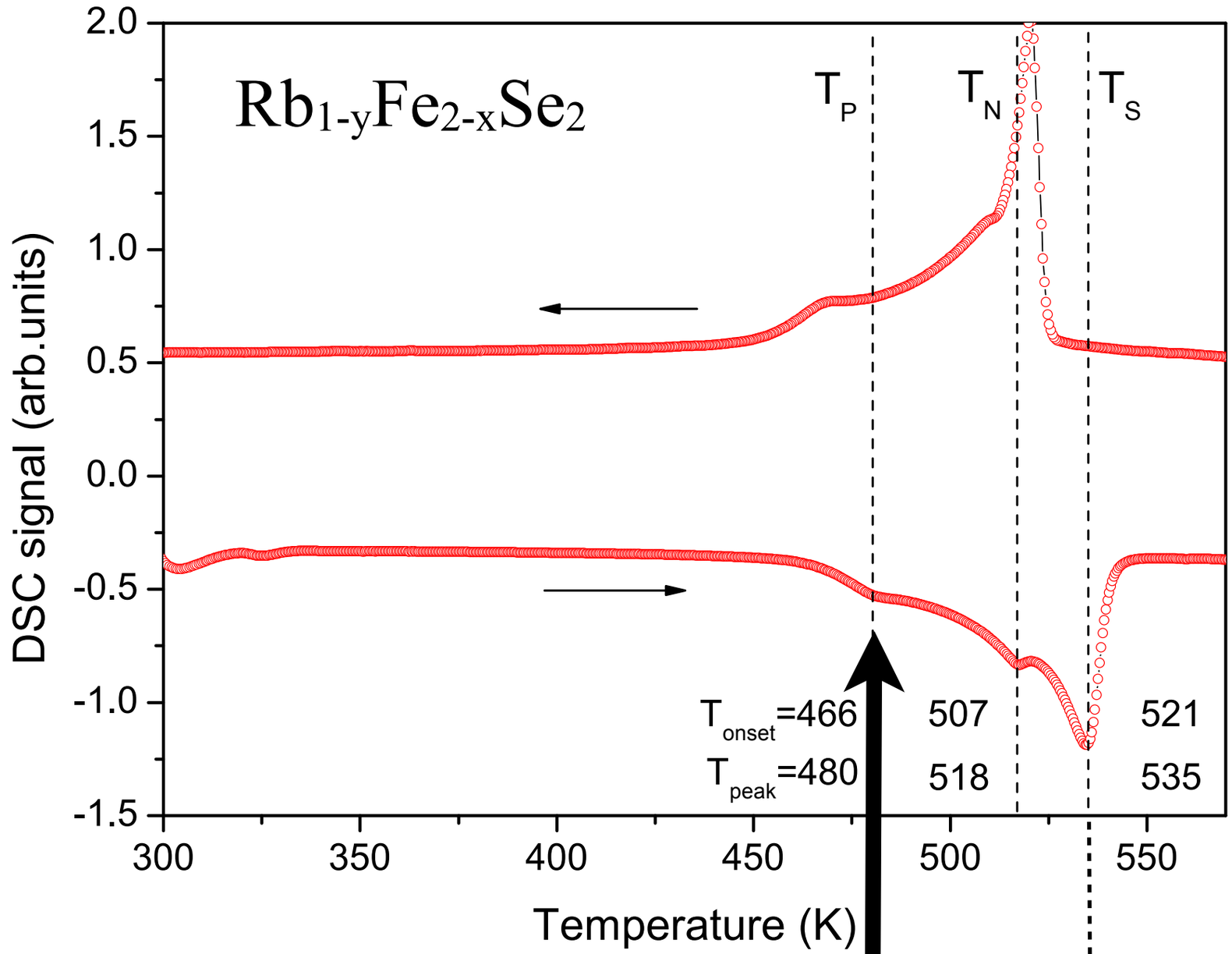

Crystal growth @ >1000K

separation of minority vacancy disordered phase about 10% fraction

I4/m, vacancy ordered $\sqrt{5}\times\sqrt{5}$

I4/mmm, vacancy disordered, 122 phase as growth

A diffraction view on phase separation: I. Main (90%) phase (A)

Reciprocal space reconstruction from single crystal x-ray @ SNBL/ESRF

the mesh is for the parent I4/mmm cell
T=300K, (hk0) plane of $Cs_yFe_{2-x}Se_2$

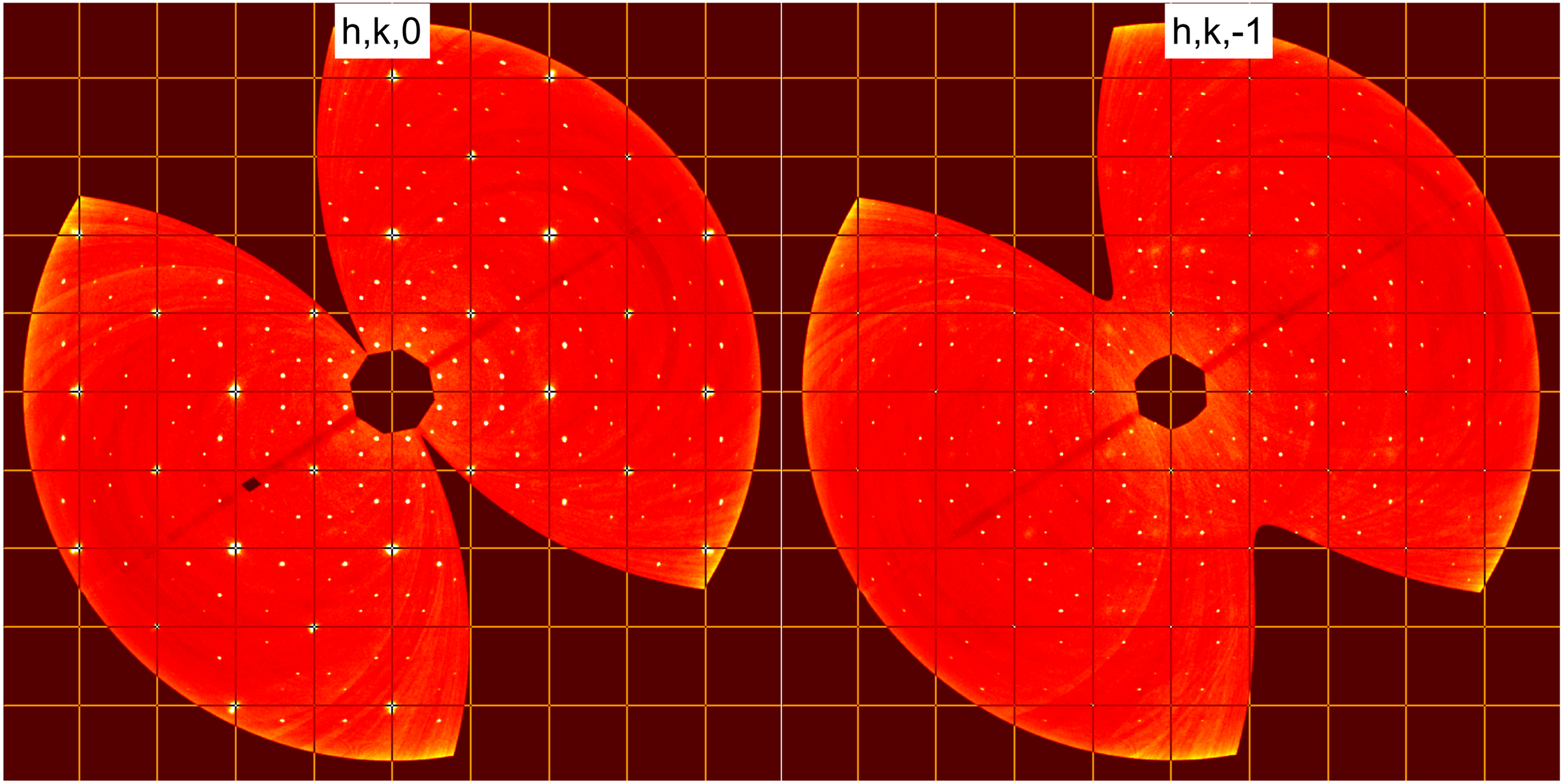

Reciprocal space reconstruction from single crystal x-ray @ SNBL/ESRF

the mesh is for the parent I4/mmm cell
T=300K, (hk0) plane of $Cs_yFe_{2-x}Se_2$

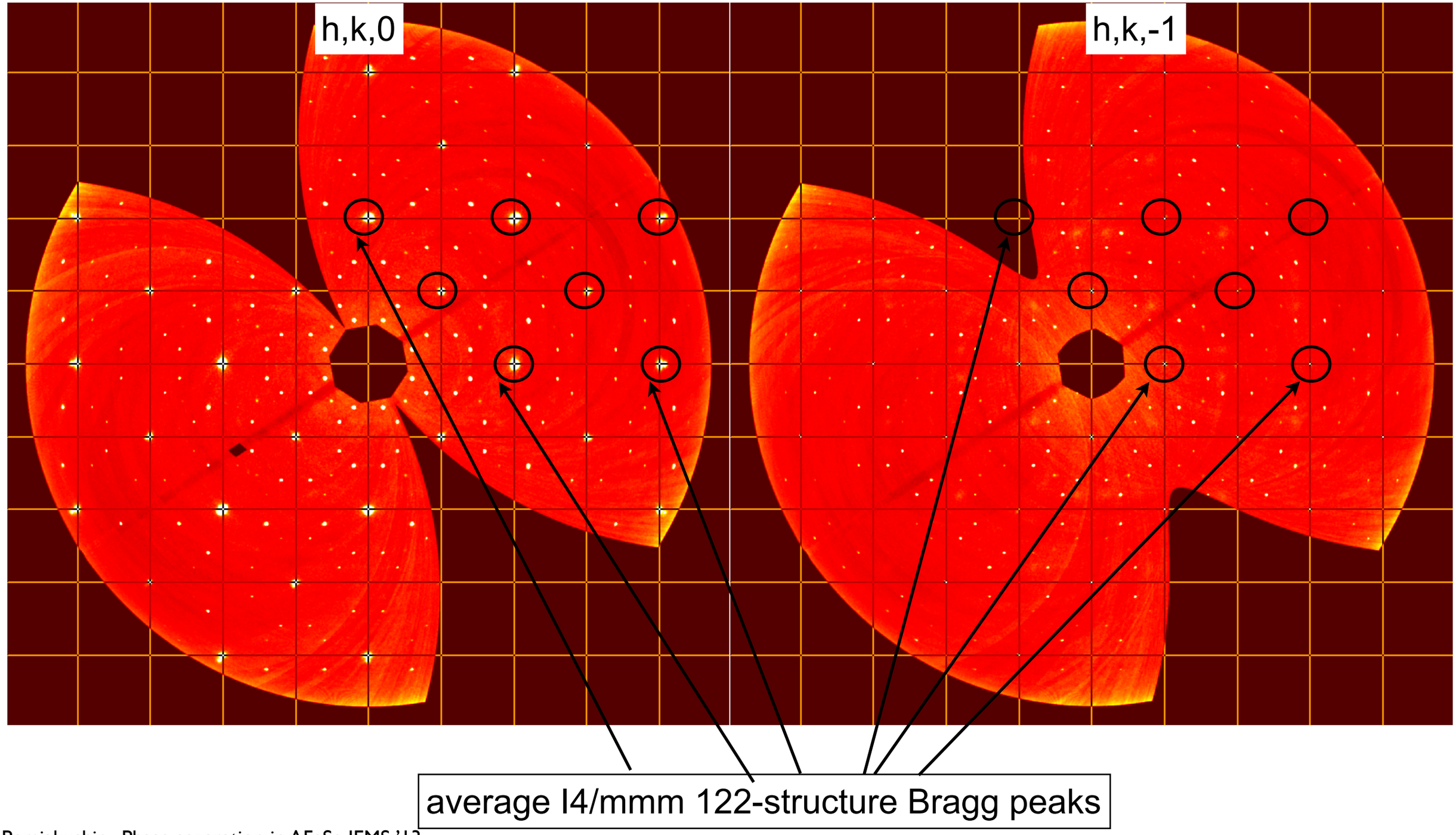

(hk0) slice of reciprocal space. indexing in average I4/mmm structure

the mesh is for the parent I4/mmm cell
T=300K, (hk0) plane of $Cs_yFe_{2-x}Se_2$

4-arms k-vector stars

$$\{\mathbf{k}_1\} = \{[\frac{2}{5}, \frac{1}{5}, 1]\}$$

$$\{\mathbf{k}_2\} = \{[\frac{1}{5}, \frac{2}{5}, \bar{1}]\}$$

superstructure satellites

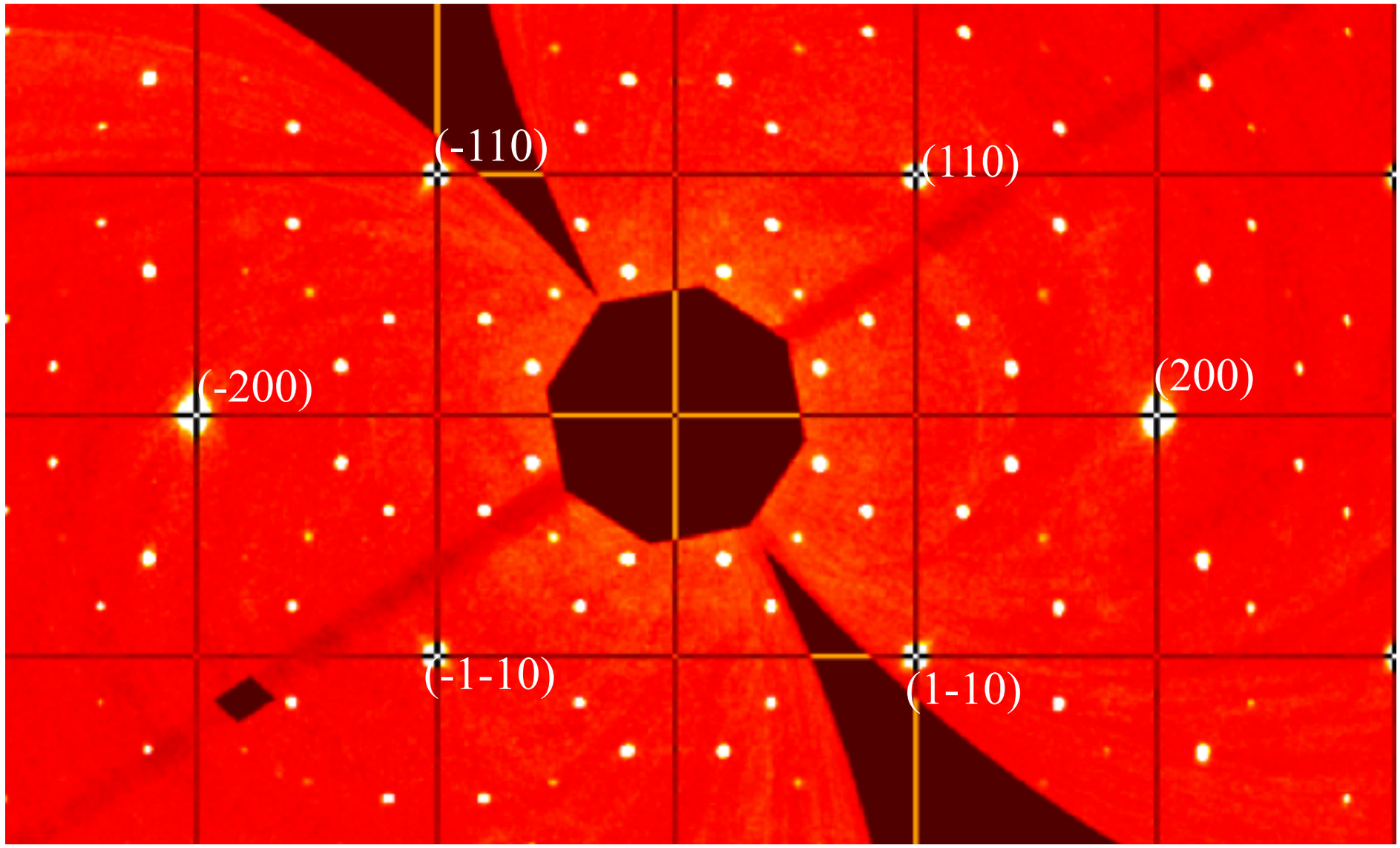

Note: the k-vectors are shown in projection. Their origin is at L=+/-1

(hk0) slice of reciprocal space. indexing in average I4/mmm structure

the mesh is for the parent I4/mmm cell
T=300K, (hk0) plane of $Cs_yFe_{2-x}Se_2$

4-arms k-vector stars

$$\{\mathbf{k}_1\} = \{[\frac{2}{5}, \frac{1}{5}, 1]\}$$

$$\{\mathbf{k}_2\} = \{[\frac{1}{5}, \frac{2}{5}, \bar{1}]\}$$

superstructure satellites

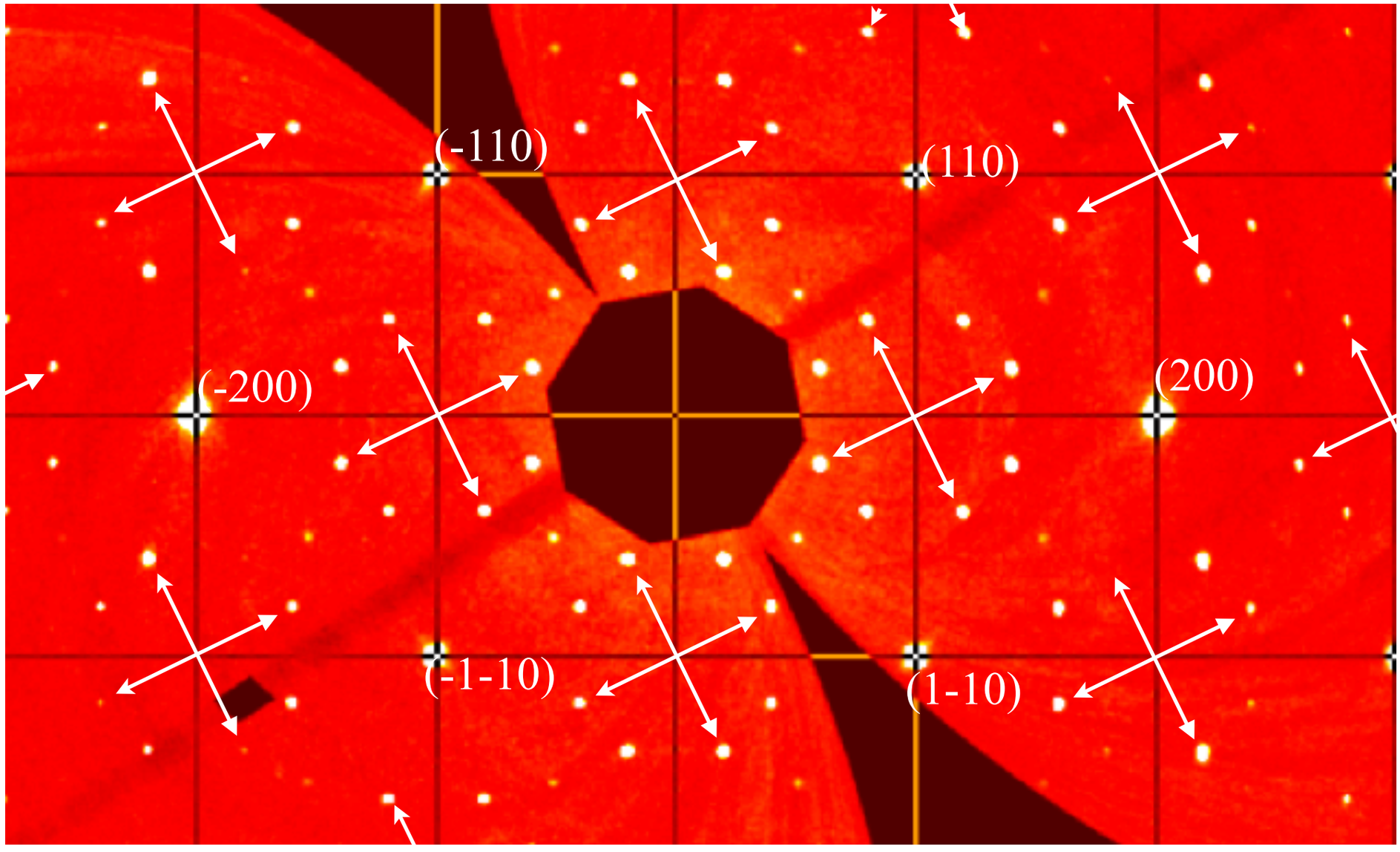

Note: the k-vectors are shown in projection. Their origin is at L=+/-1

(hk0) slice of reciprocal space. indexing in average I4/mmm structure

the mesh is for the parent I4/mmm cell
T=300K, (hk0) plane of $Cs_yFe_{2-x}Se_2$

4-arms k-vector stars

$$\{\mathbf{k}_1\} = \{[\frac{2}{5}, \frac{1}{5}, 1]\}$$

$$\{\mathbf{k}_2\} = \{[\frac{1}{5}, \frac{2}{5}, \bar{1}]\}$$

superstructure satellites

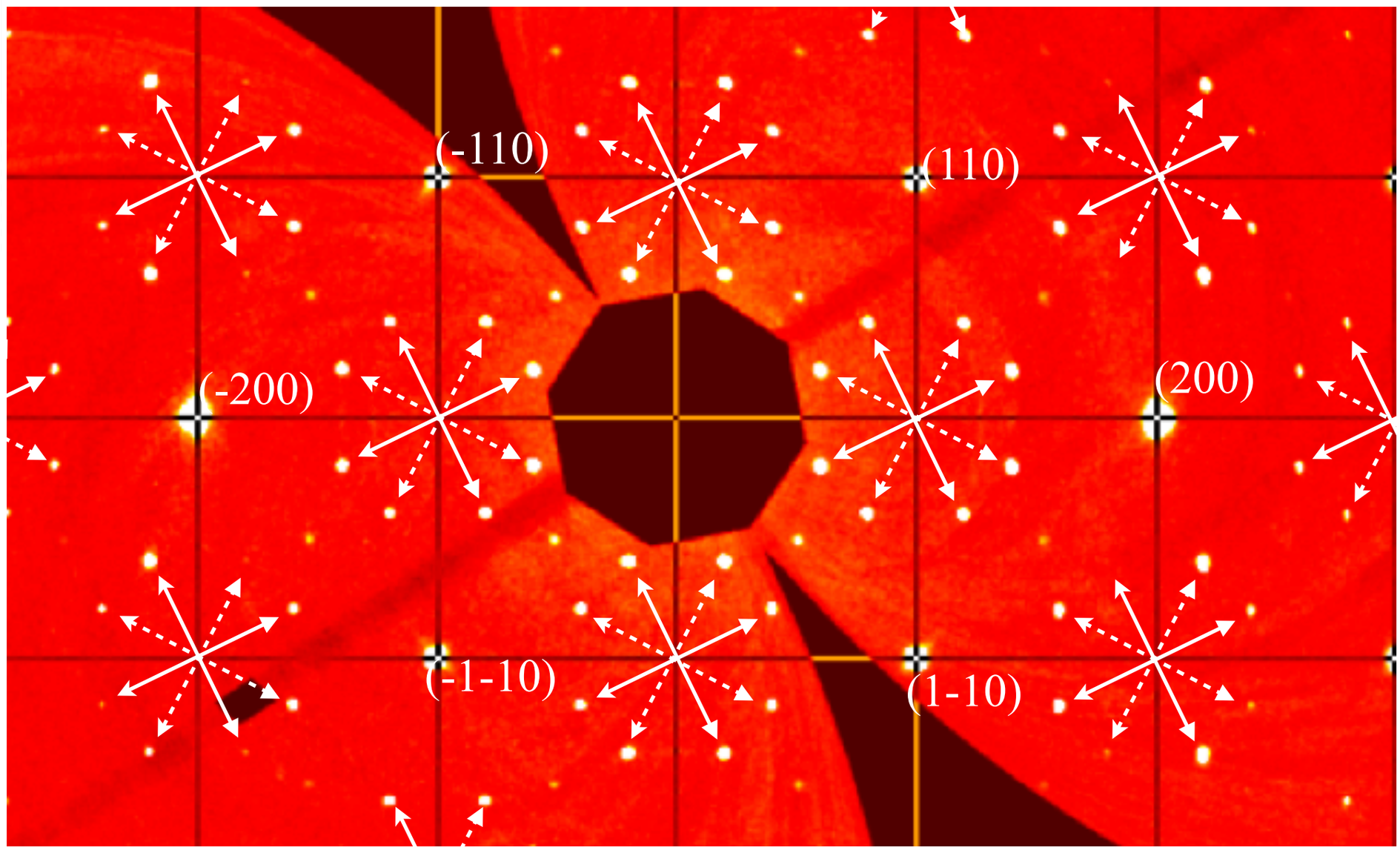

Note: the k-vectors are shown in projection. Their origin is at L=+/-1

I4/m structure of main phase A. Metrics. Two twins.

$$\{\mathbf{k}_1\} = \{[\frac{2}{5}, \frac{1}{5}, 1]\} \longrightarrow \begin{array}{l} \mathbf{A} = 2\mathbf{a} + \mathbf{b} \\ \mathbf{B} = -\mathbf{a} + 2\mathbf{b} \\ \mathbf{C} = \mathbf{c} \end{array}$$

$$\{\mathbf{k}_2\} = \{[\frac{1}{5}, \frac{2}{5}, \bar{1}]\} \longrightarrow \begin{array}{l} \mathbf{A} = 2\mathbf{a} - \mathbf{b} \\ \mathbf{B} = \mathbf{a} + 2\mathbf{b} \\ \mathbf{C} = \mathbf{c} \end{array}$$

$$A \times B = \sqrt{5}a \times \sqrt{5}b$$

(ab) plane projection

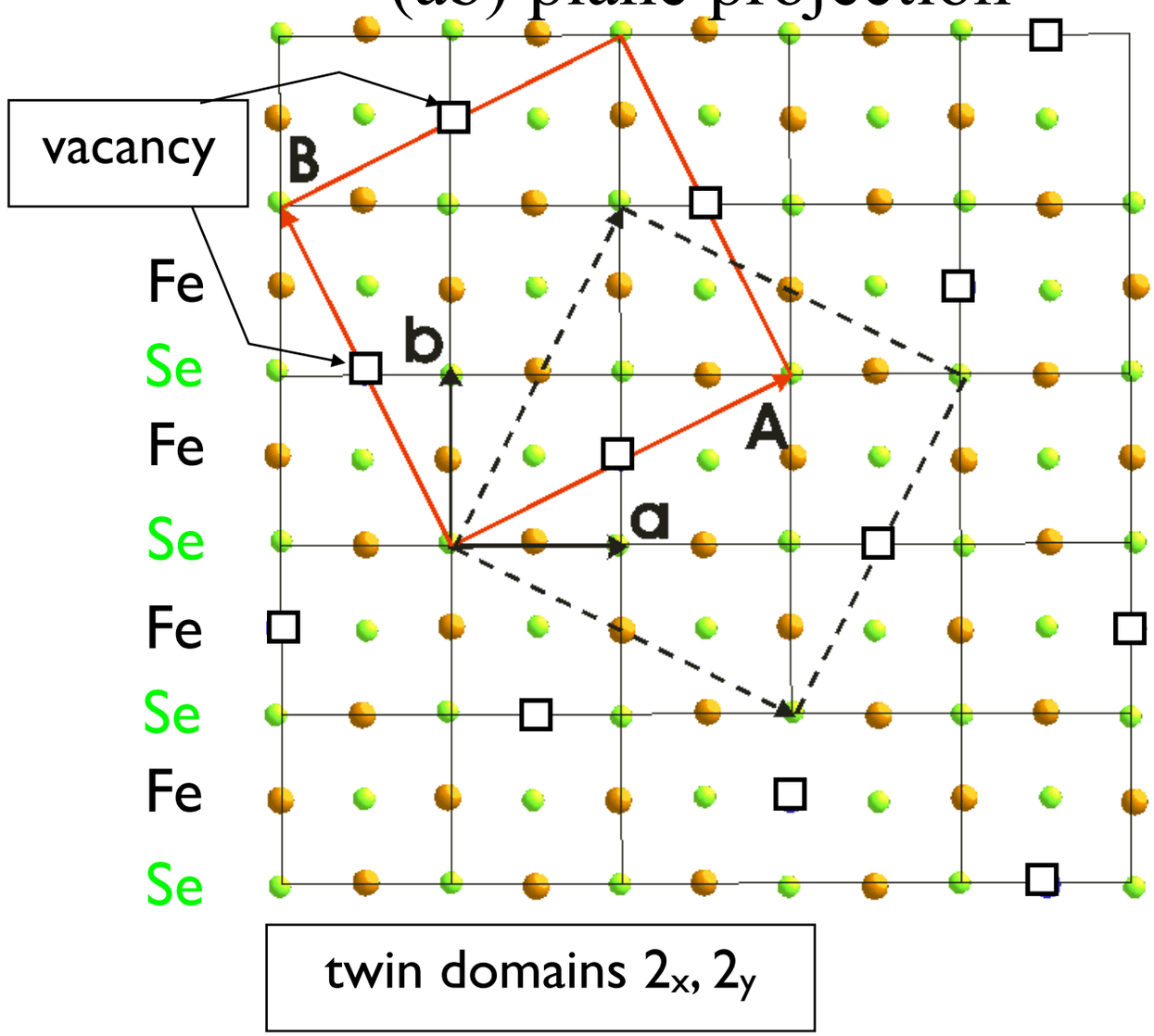

angle between twins
2arctan½ = 53.1deg

I4/mmm -> I4/m Structure details “245”

Position splitting

Cs (2a) (0,0,0) → (2a) (0,0,0) “~~vacancy~~”
Cs (2a) (0,0,0) → (8h) (x,y,0)

Fe (4d) (0, ½, ¼) → (4d) (½,0,¼) “vacancy”
Fe (4d) (0, ½, ¼) → (16i) (x,y,z)

Se (4e) (0,0,z) → (4e) (½, ½,z)
Se (4e) (0,0,z) → (16i) (x,y,z)

I4/mmm -> I4/m Structure details "245"

Position splitting

Cs (2a) (0,0,0) → (2a) (0,0,0) "~~vacancy~~"
Cs (2a) (0,0,0) → (8h) (x,y,0)

Fe (4d) (0, ½, ¼) → (4d) (½,0,¼) "vacancy"
Fe (4d) (0, ½, ¼) → (16i) (x,y,z)

Se (4e) (0,0,z) → (4e) (½, ½,z)
Se (4e) (0,0,z) → (16i) (x,y,z)

$Cs_8Fe_{16}Se_{20} = Cs_2Fe_4Se_5 = Cs_{0.8}Fe_{1.6}Se_2$ real: $A_yFe_xSe_2$

y=0.7-0.85, x=1.60-1.75

I4/mmm -> I4/m Structure details "245"

Position splitting

Cs (2a) (0,0,0) → (2a) (0,0,0) "~~vacancy~~"; (8h) (x,y,0)

Fe (4d) (0, ½, ¼) → (4d) (½,0,¼) "vacancy"; (16i) (x,y,z)

Se (4e) (0,0,z) → (4e) (½, ½,z); (16i) (x,y,z)

$Cs_8Fe_{16}Se_{20} = Cs_2Fe_4Se_5 = Cs_{0.8}Fe_{1.6}Se_2$ real: $A_yFe_xSe_2$

y=0.7-0.85, x=1.60-1.75

---

10 independent distortion modes: 2 order + 8 displacive

Example: distortions for Fe in (*ab*) plane

Dominant mode: order

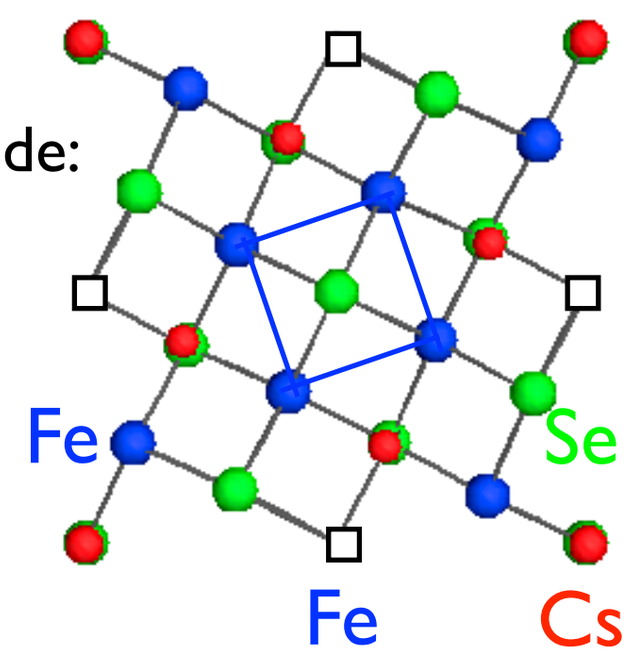

Displacements

E_1

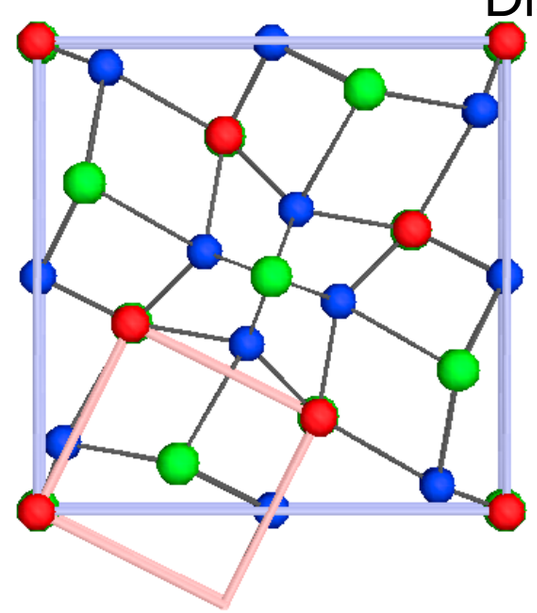

E_2

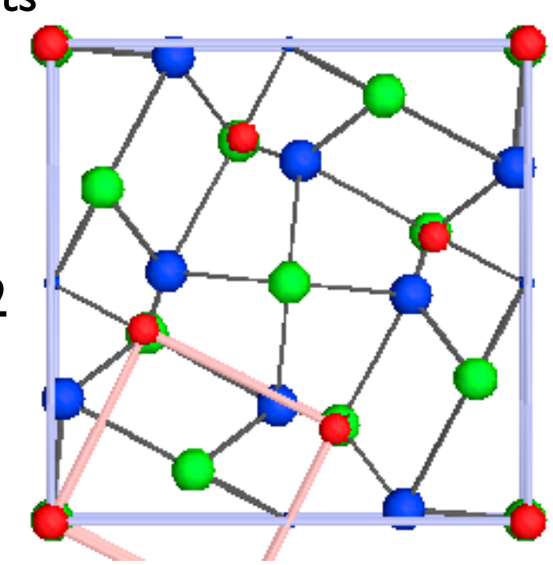

Fe displacements exaggerated for better visibility

Calculated by ISODISTORT stokes.byu.edu/isotropy.html

V. Pomjakushin, Phase separation in AFeSe JEMS '13

A diffraction view on phase separation:
II. Second minority (10%) phase (B) or (MCP)

High resolution synchrotron x-ray, Slices of reciprocal space

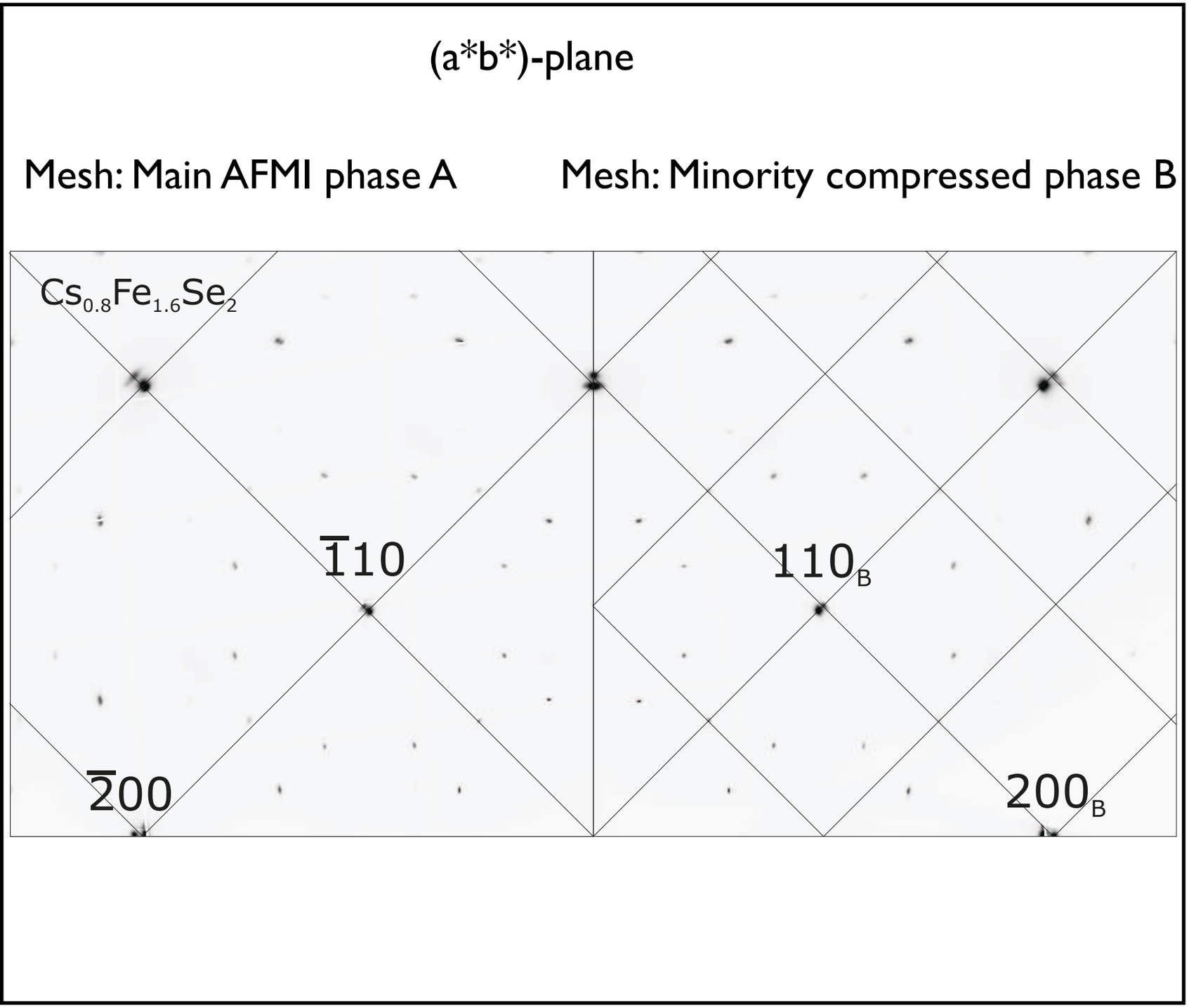

High resolution synchrotron x-ray, Slices of reciprocal space

(a*b*)-plane

Mesh: Main AFMI phase A

Mesh: Minority compressed phase B

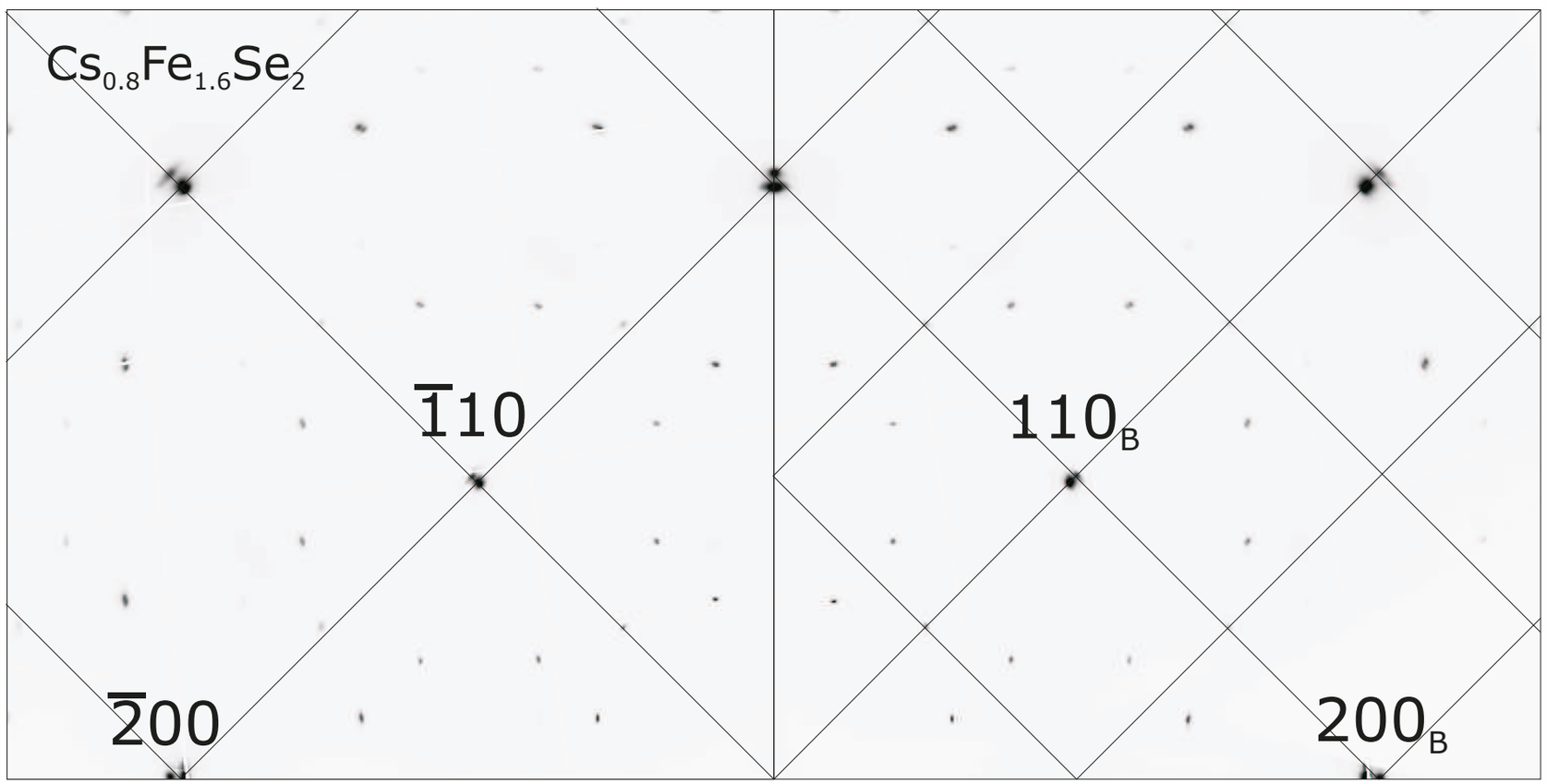

(a*c*)-plane

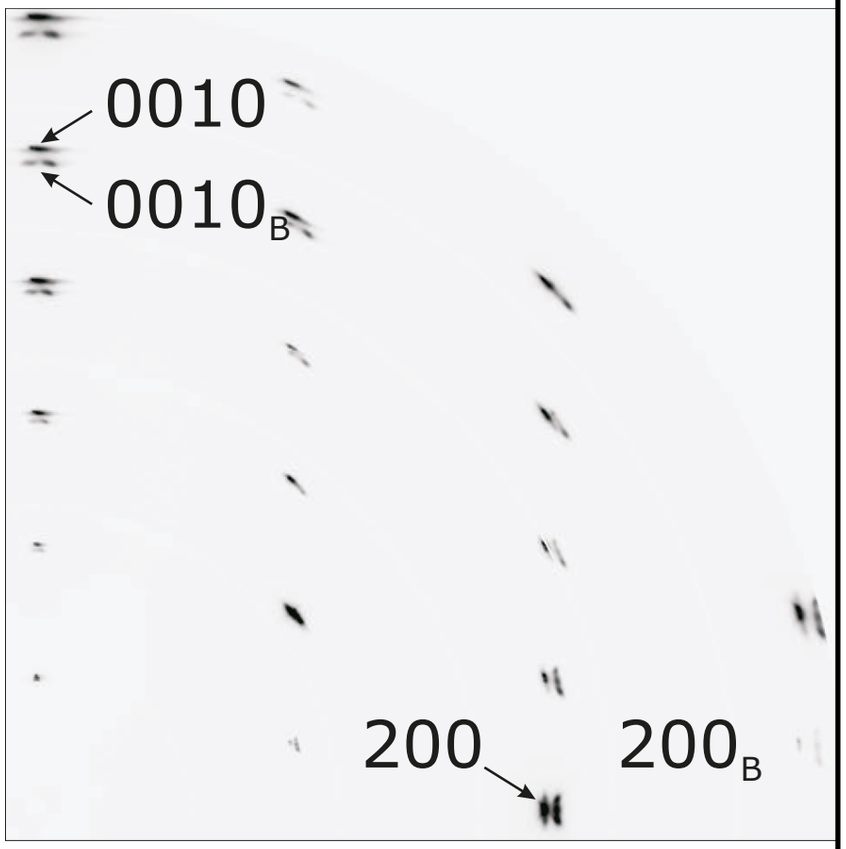

Some projections

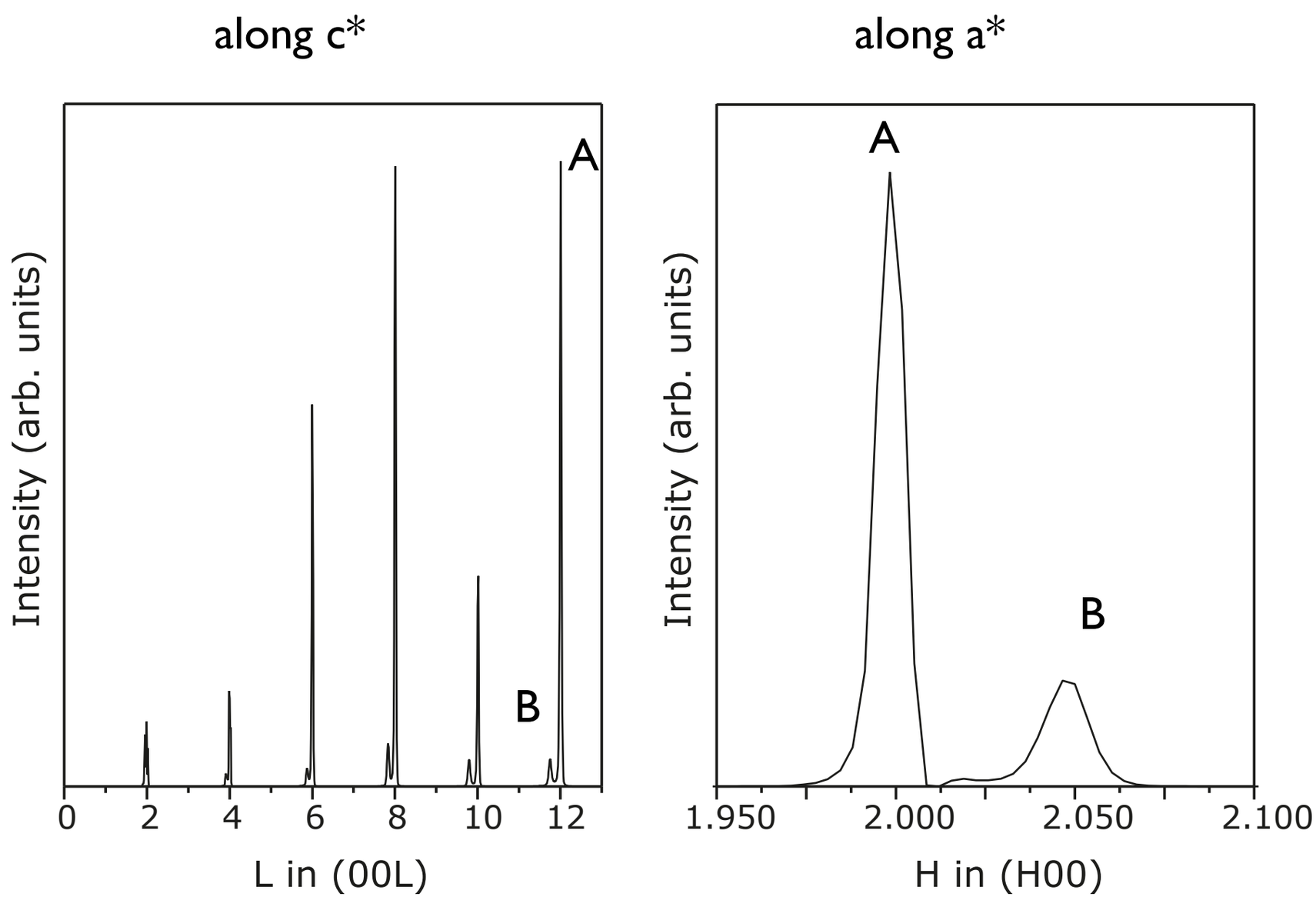

No vacancy ordered satellites from the second phase

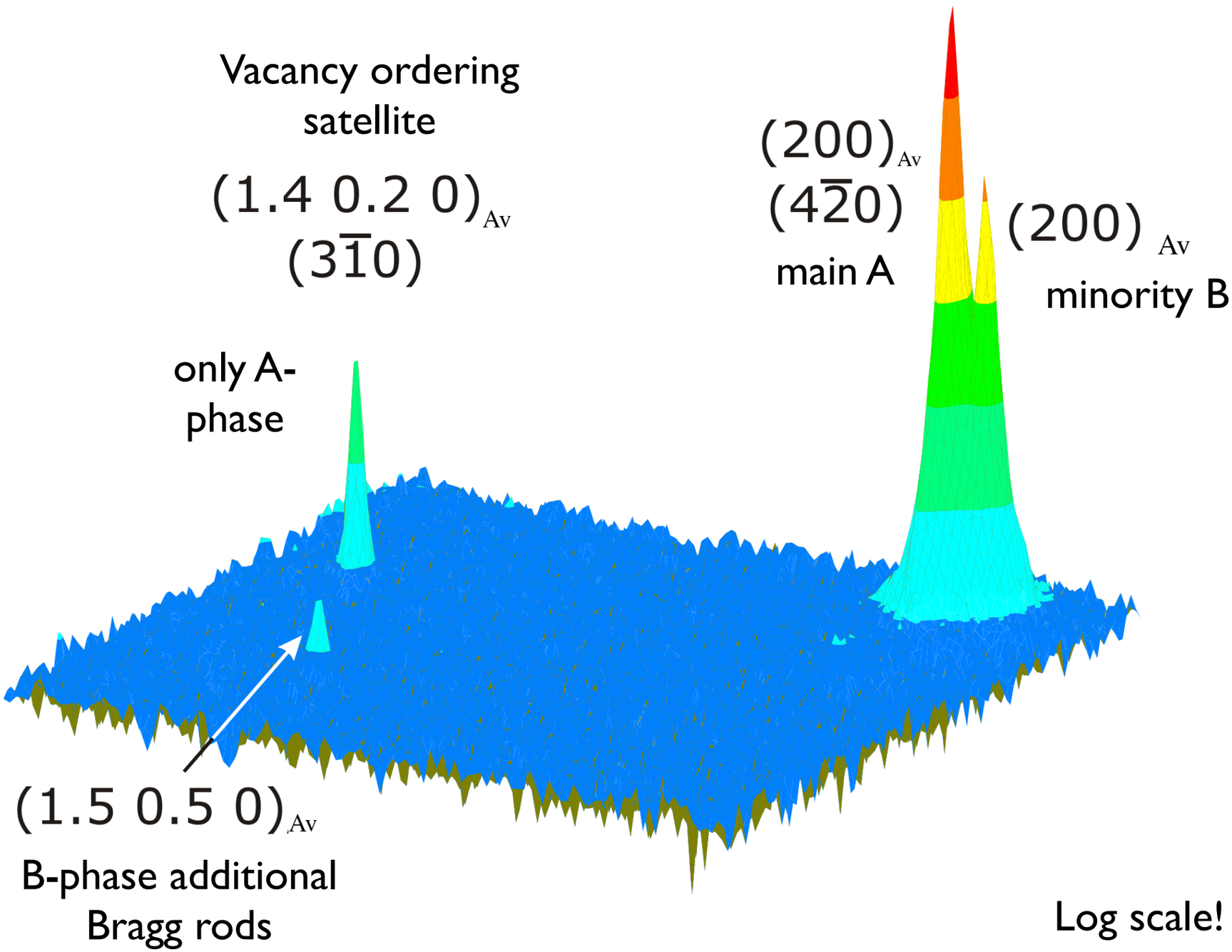

No vacancy ordered satellites from the second phase

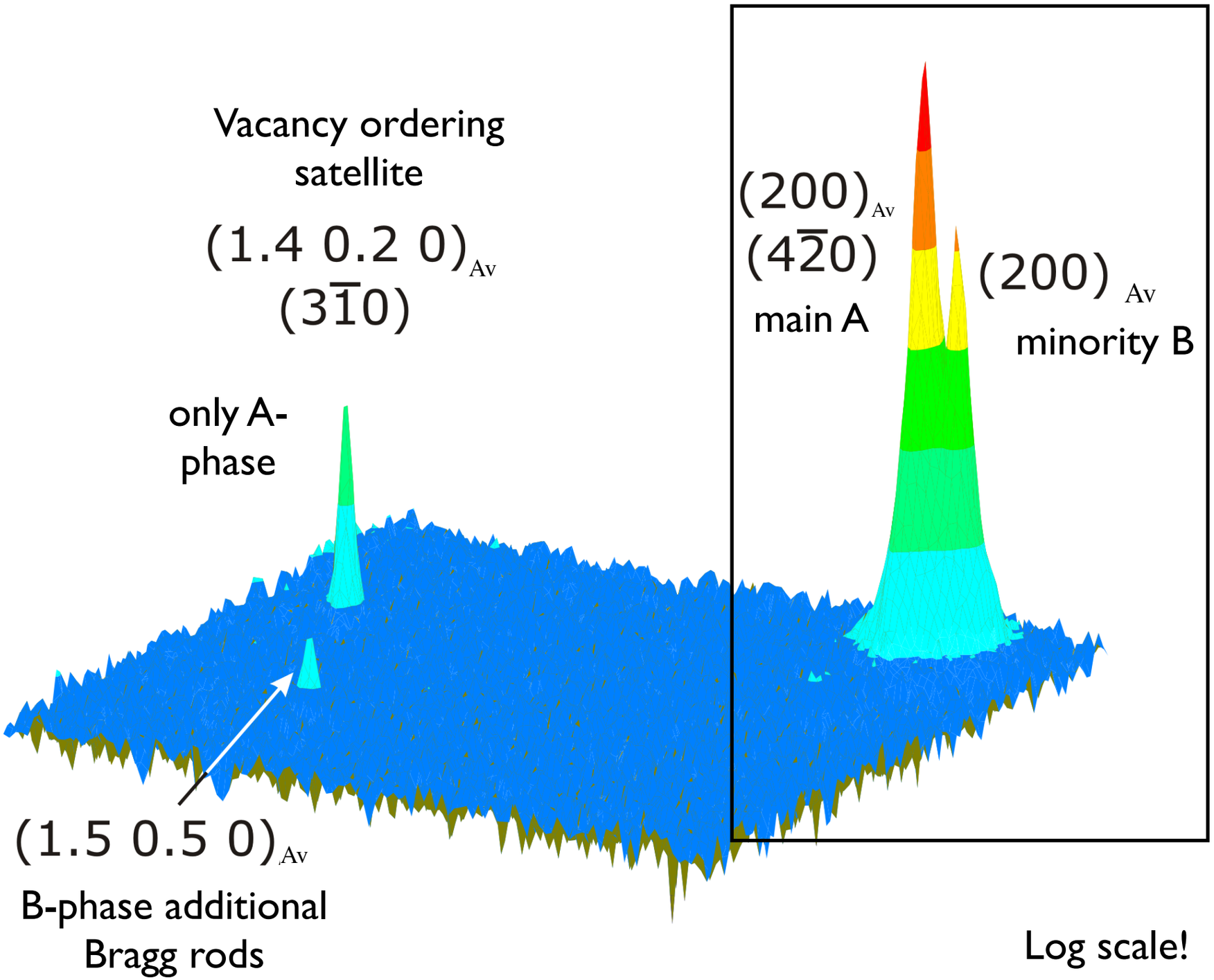

No vacancy ordered satellites from the second phase

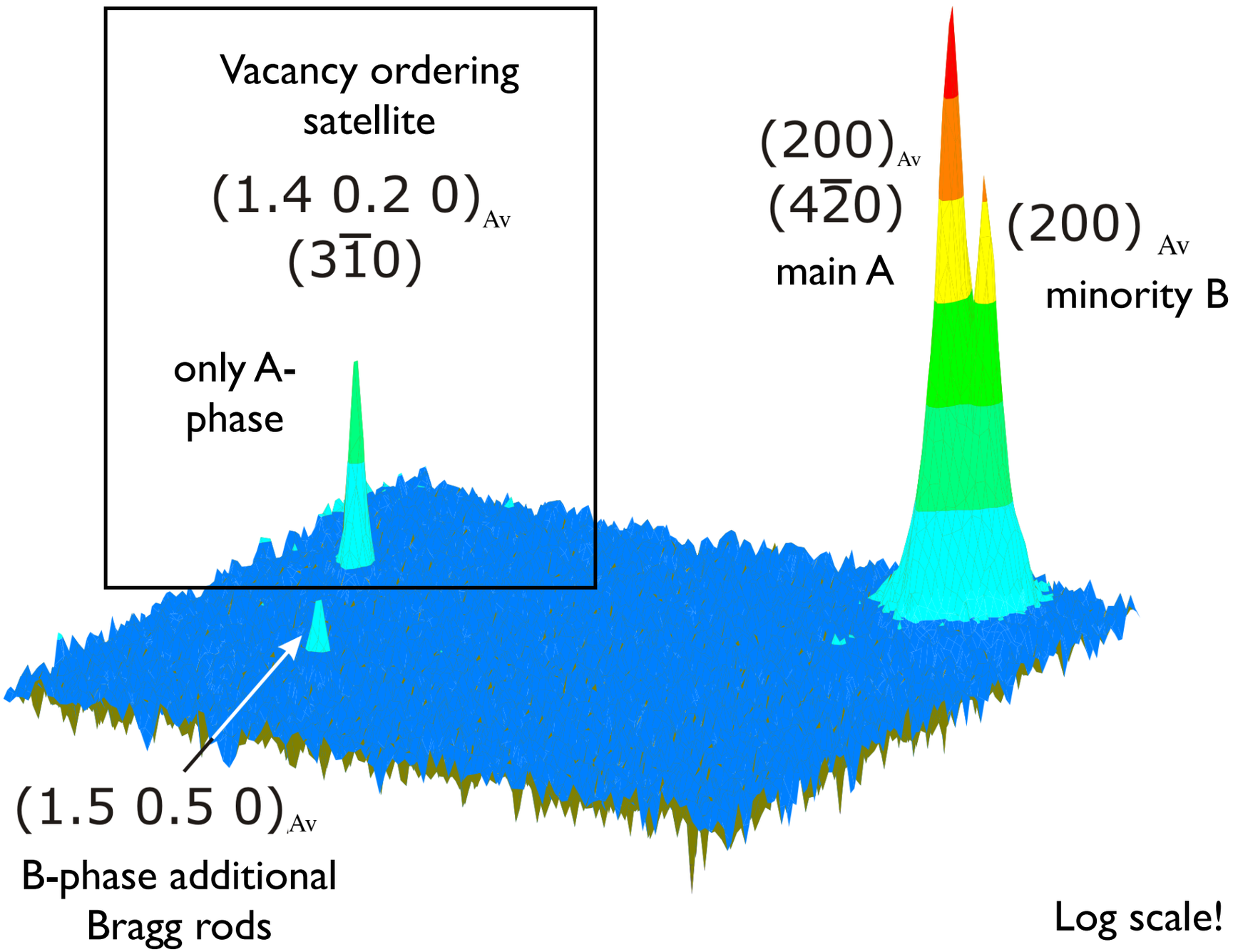

No vacancy ordered satellites from the second phase

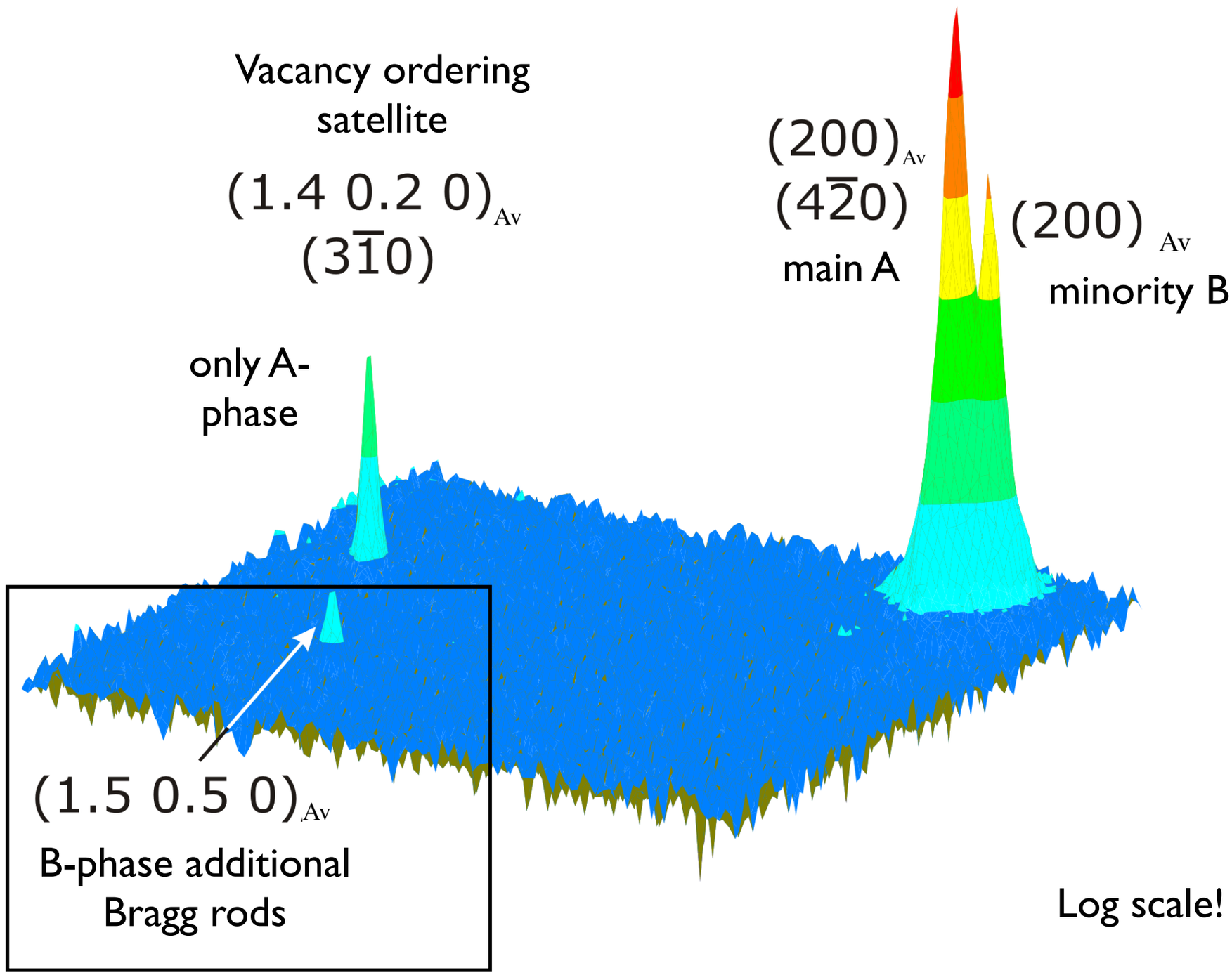

(1/2,1/2,L) rods from phase (B)

(a*b*)-plane

Mesh: Main AFMI phase A

Mesh: Minority compressed phase B

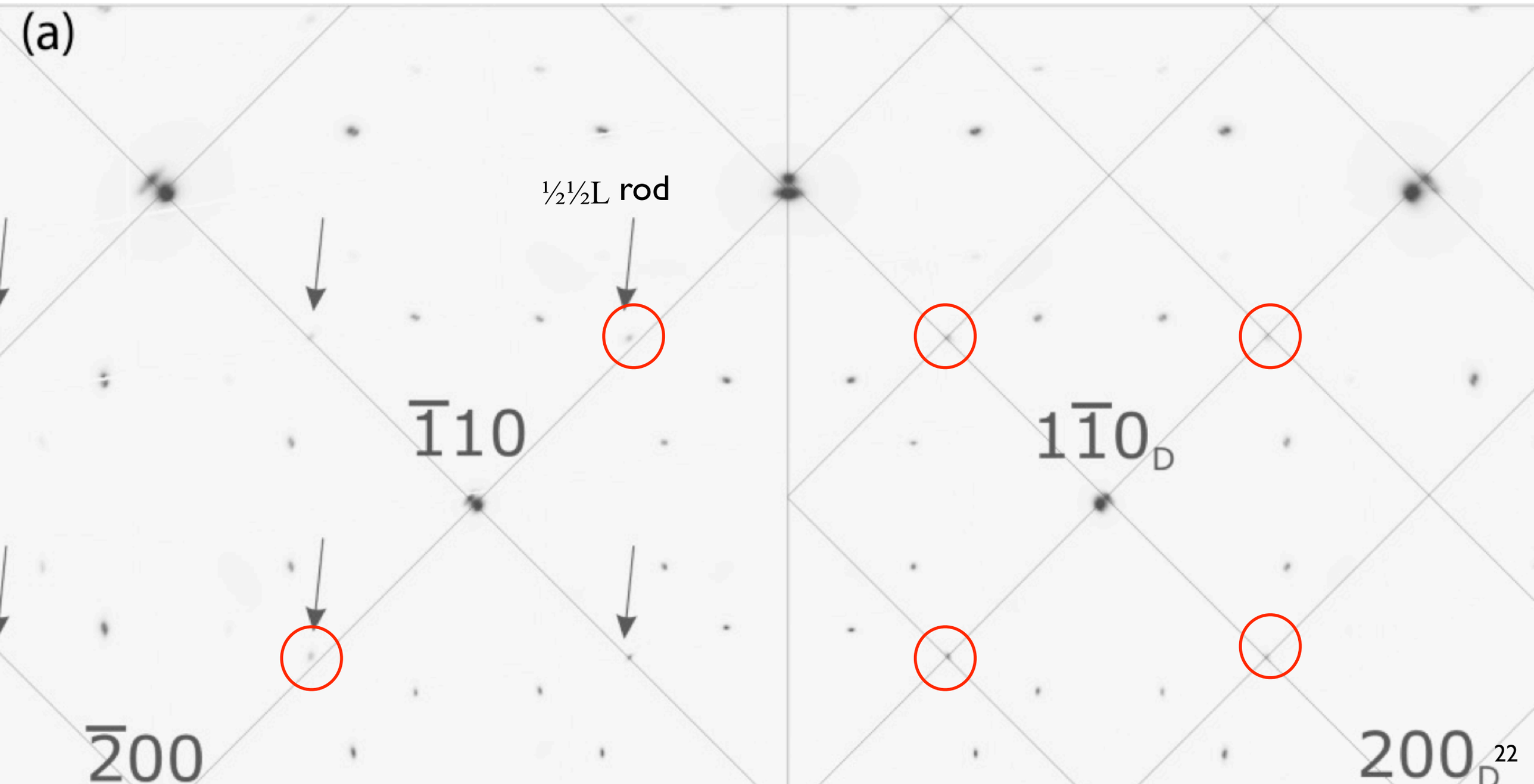

A specific four fold twinning of minority phase B

AFM phase A: I4/m with two twins in ab-plane

Minority phase B: four 100 rotational twins

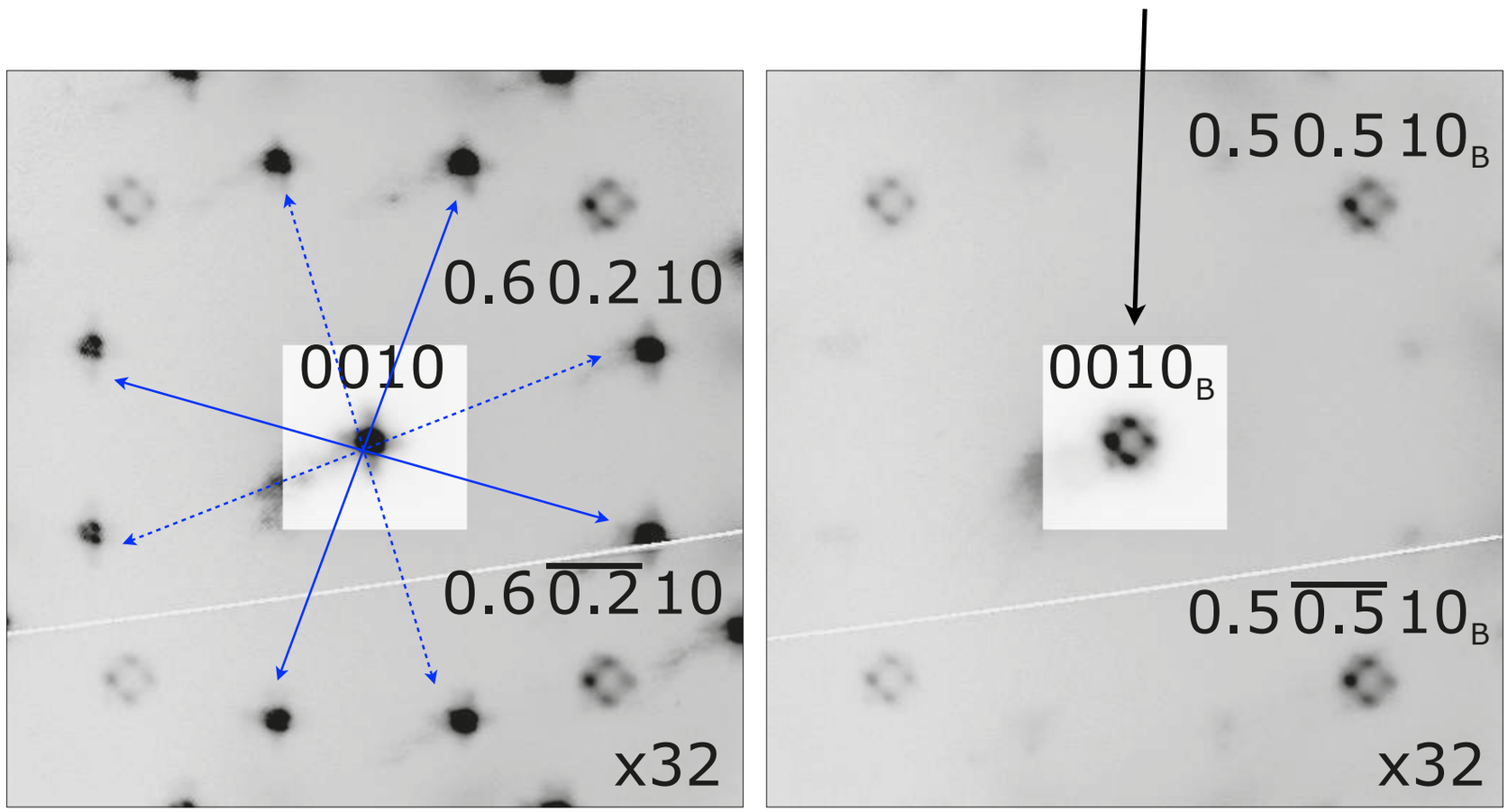

(h,k,10)-plane: best resolution

A specific four fold twinning of minority phase B

AFM phase A: I4/m with two twins in ab-plane

Minority phase B: four 100 rotational twins

Diffraction rods of minority phase B. Also four twins! Log scale

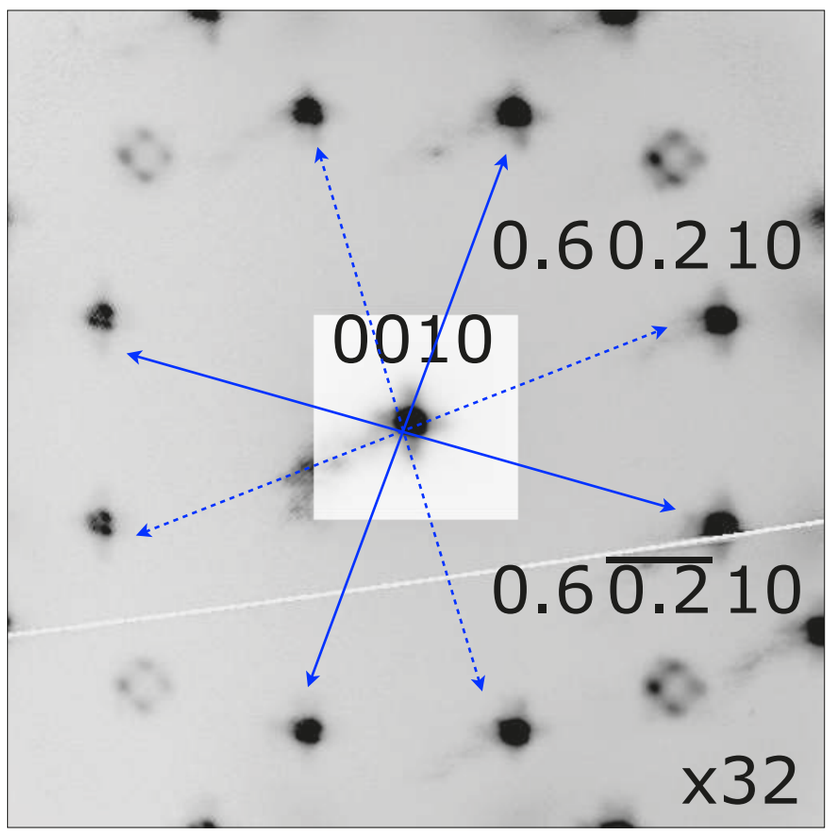

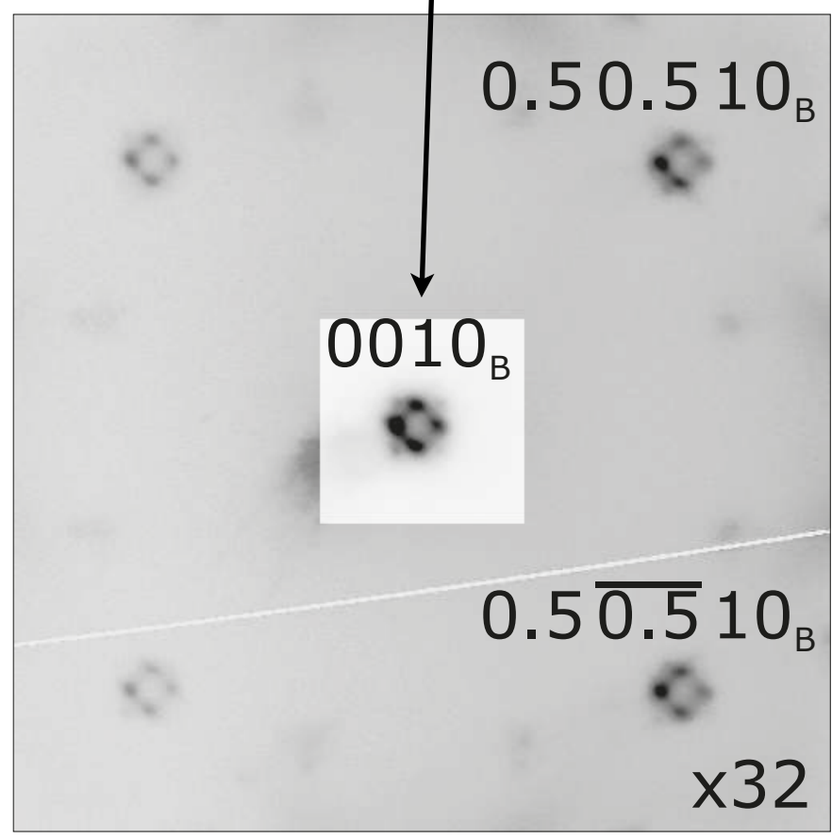

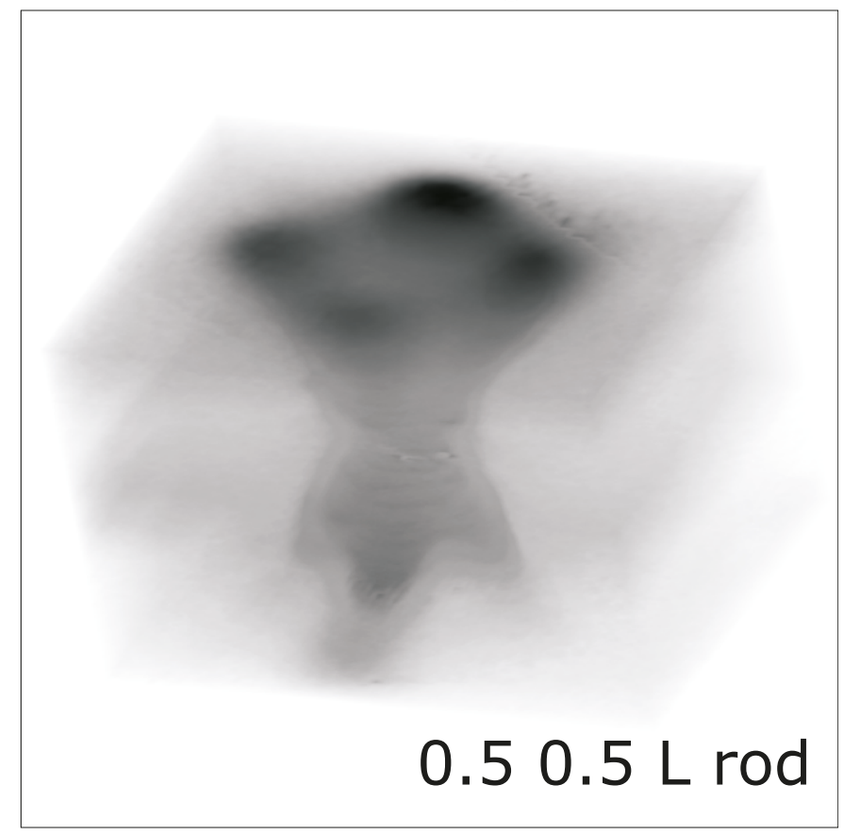

(h,k,10)-plane: best resolution

Origin: in plane 2D ordering of alkali-earth in $A_yFe_xSe_2$

twinning of minority phase B

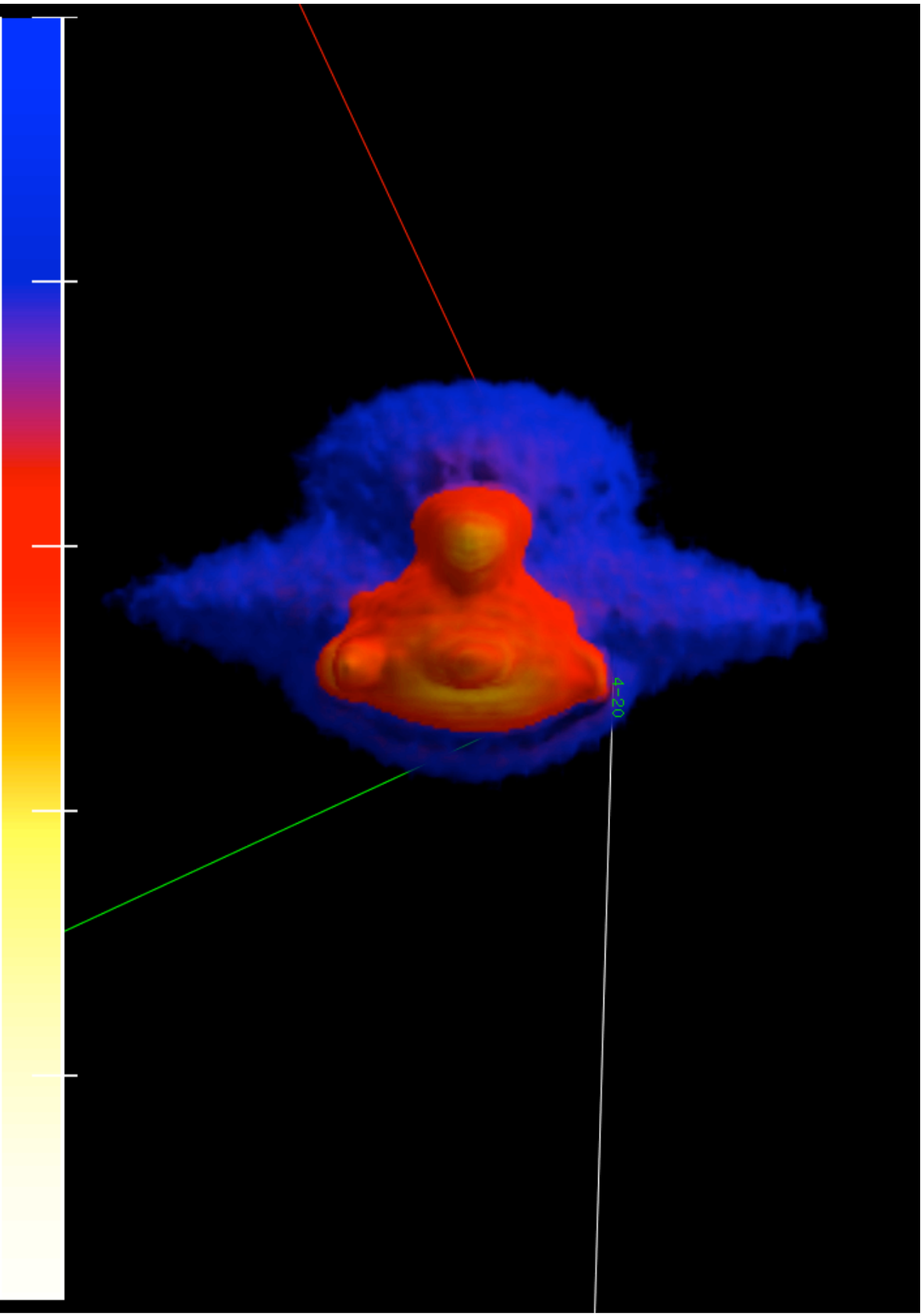

V. Pomjakushin, Phase separation in AFeSe JEMS '13

twinning of minority phase B

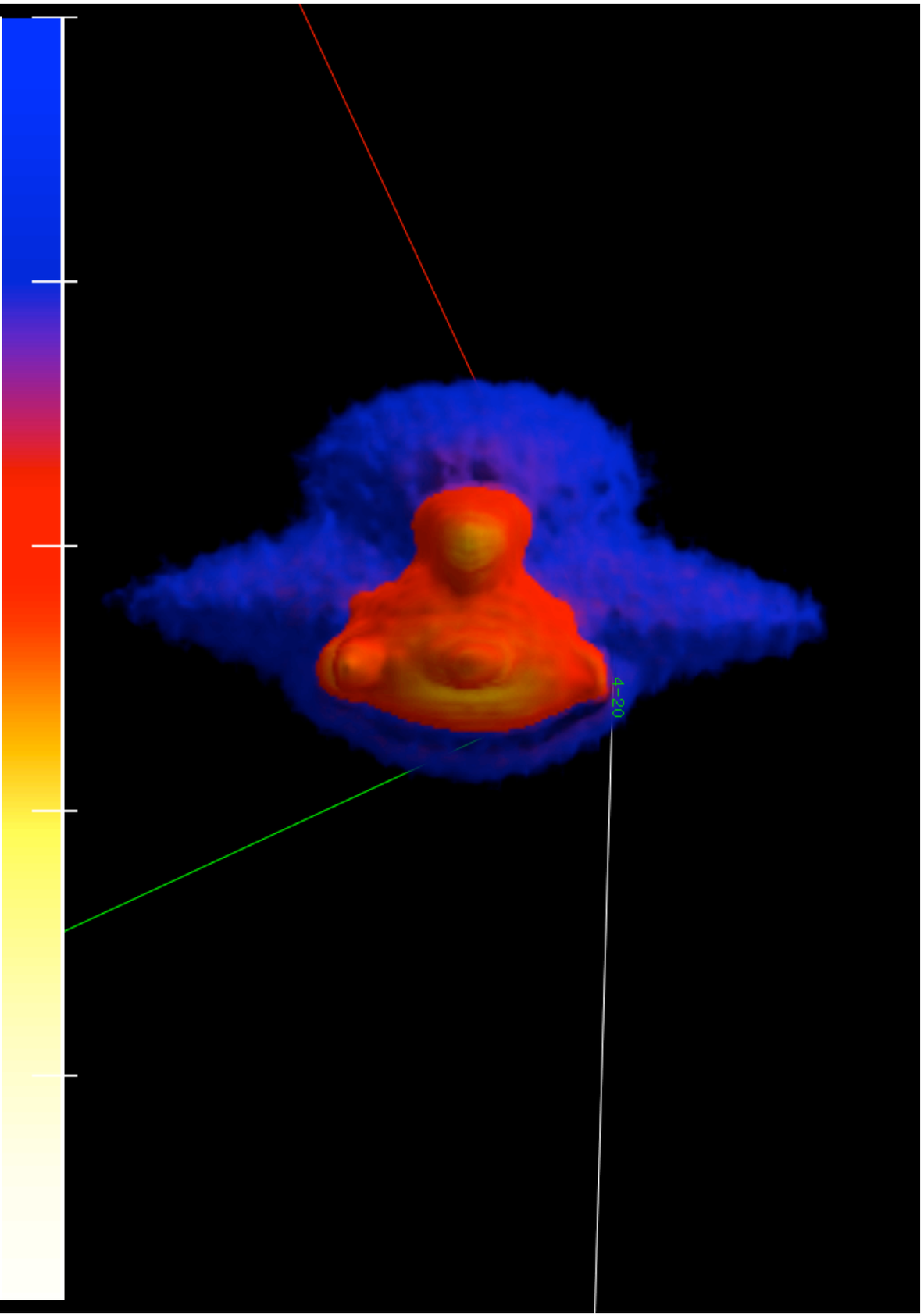

V. Pomjakushin, Phase separation in AFeSe JEMS '13

Looks like a penguin

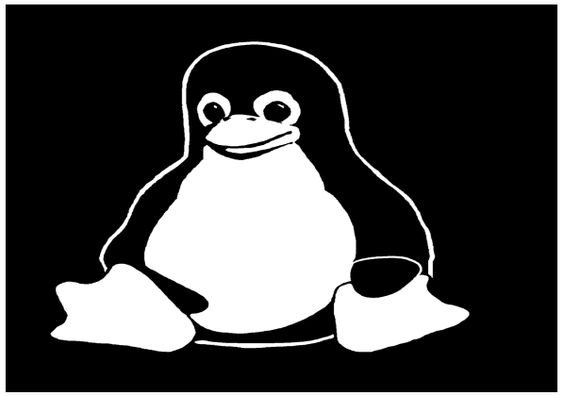

100 rotational twinning for the phase B

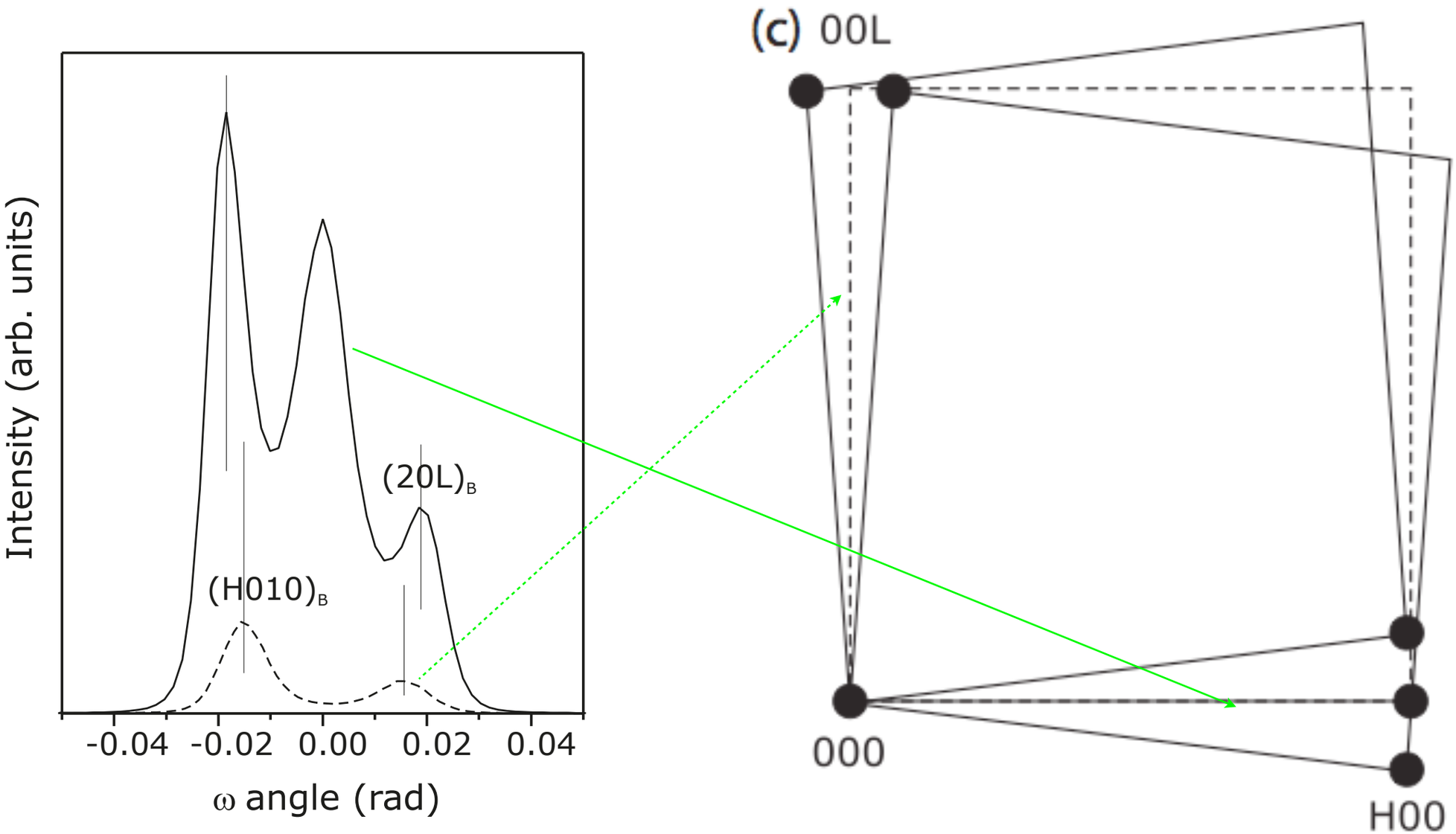

100 rotational twinning for the phase B

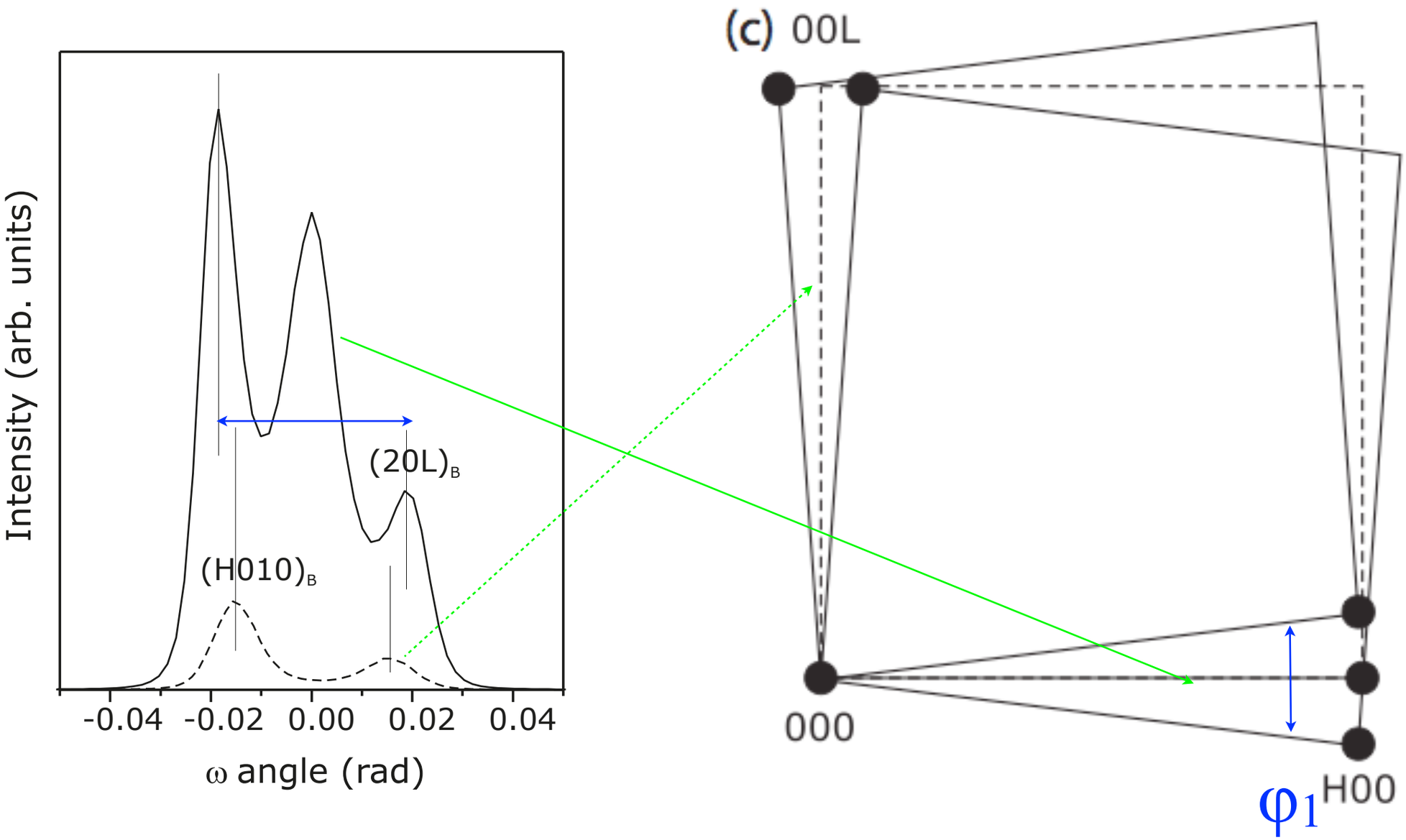

100 rotational twinning for the phase B

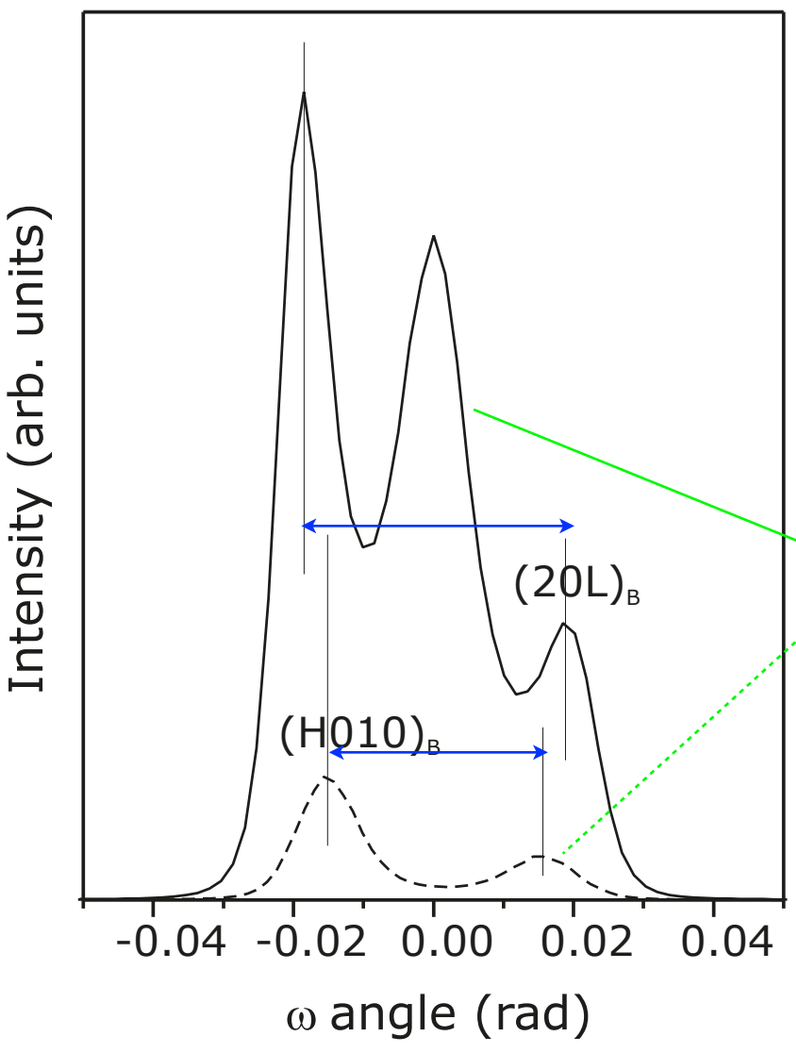

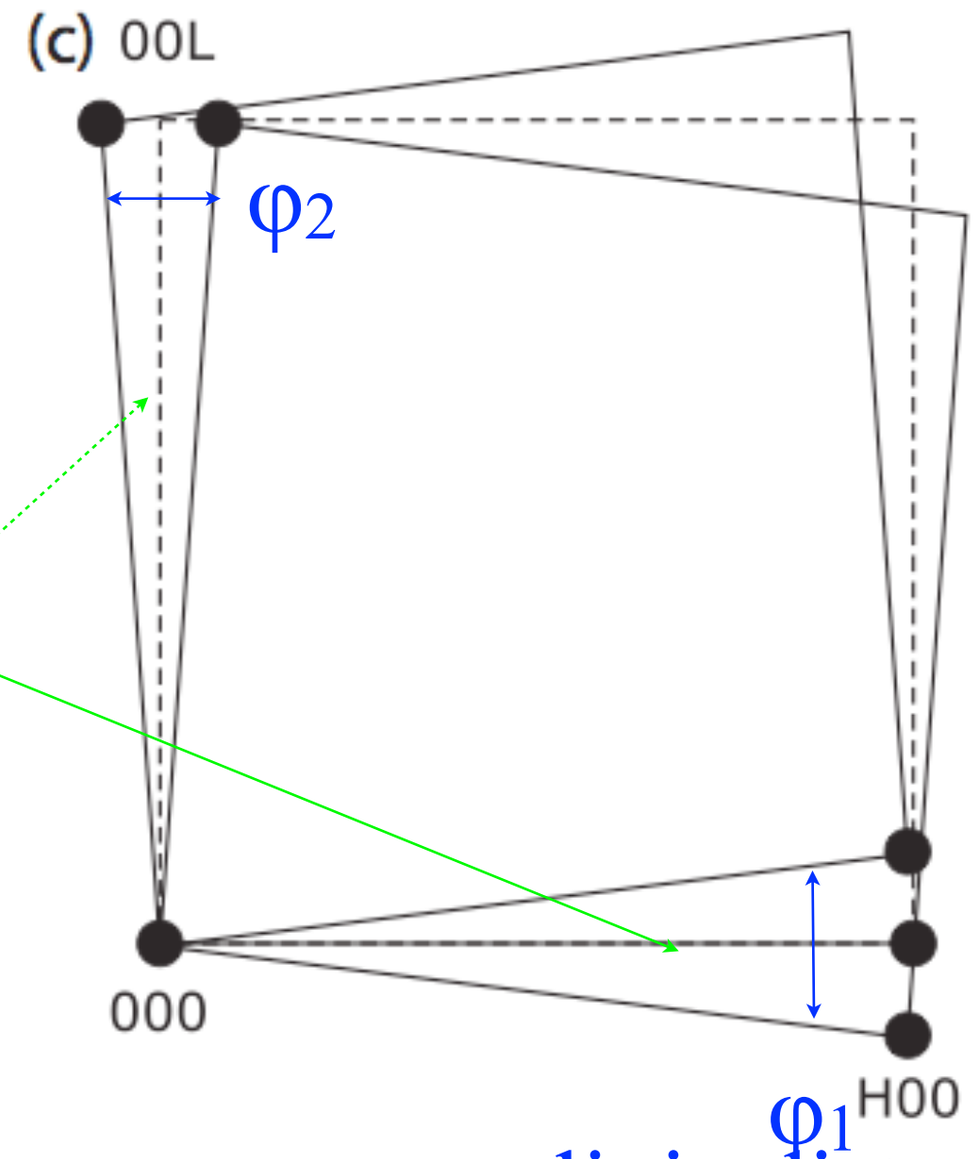

$\varphi_1 \neq \varphi_2$ --> monoclinic distortion

Powder neutron diffraction. Minority phase is shown by red line.

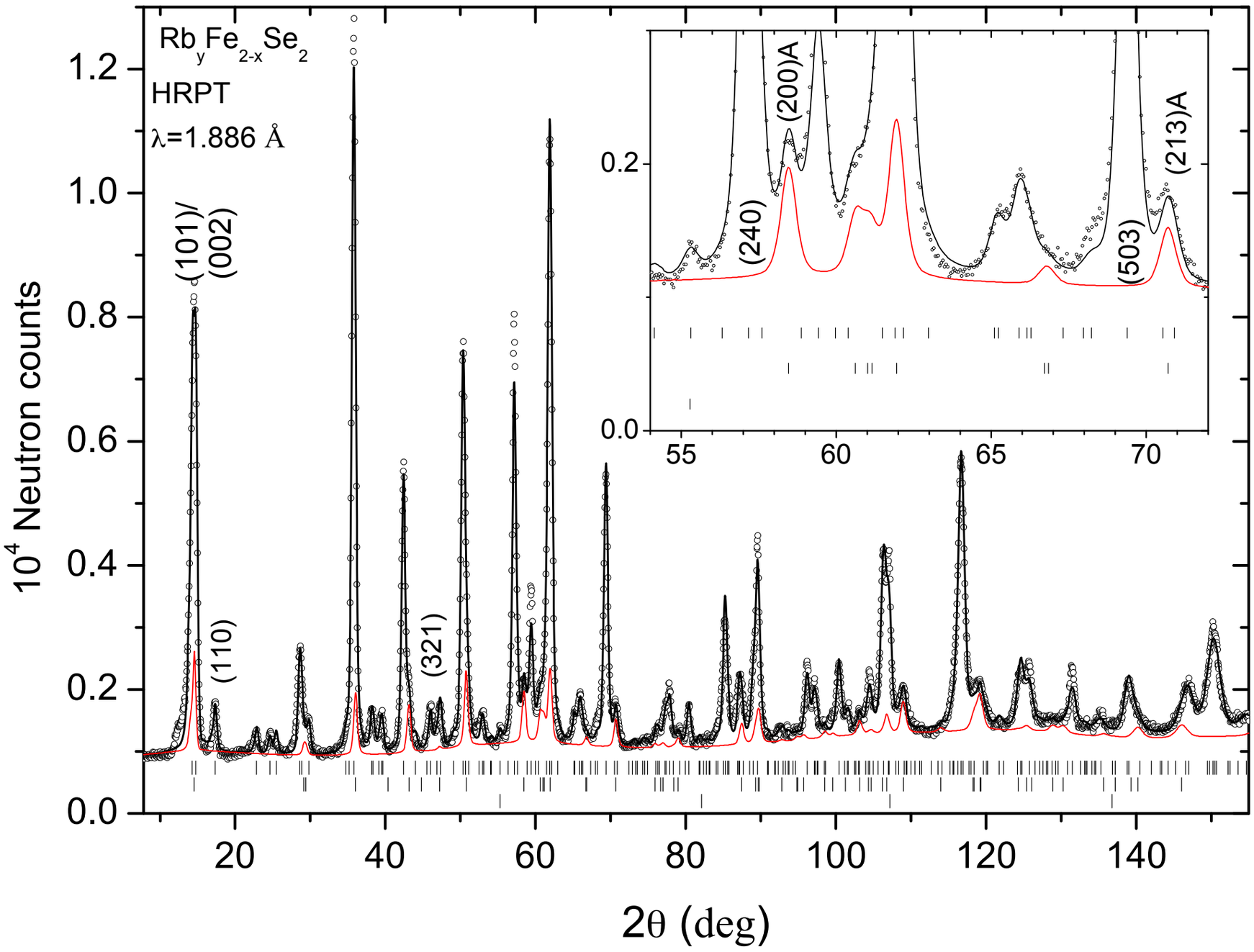

Structure model for minority compressed phase B.

parent average vacancy disordered structure (*I4/mmm* space group)* with the refined stoichiometry $Rb_{0.60(5)}(Fe_{1.10(5)}Se)_2$.
The minority phase amounts to 8–10% mass fraction.
The unit cell volume of the minority phase is 3.2% smaller.

---

*we can not afford a better model for 10% of phase & powder diffraction data

Differential scanning calorimetry

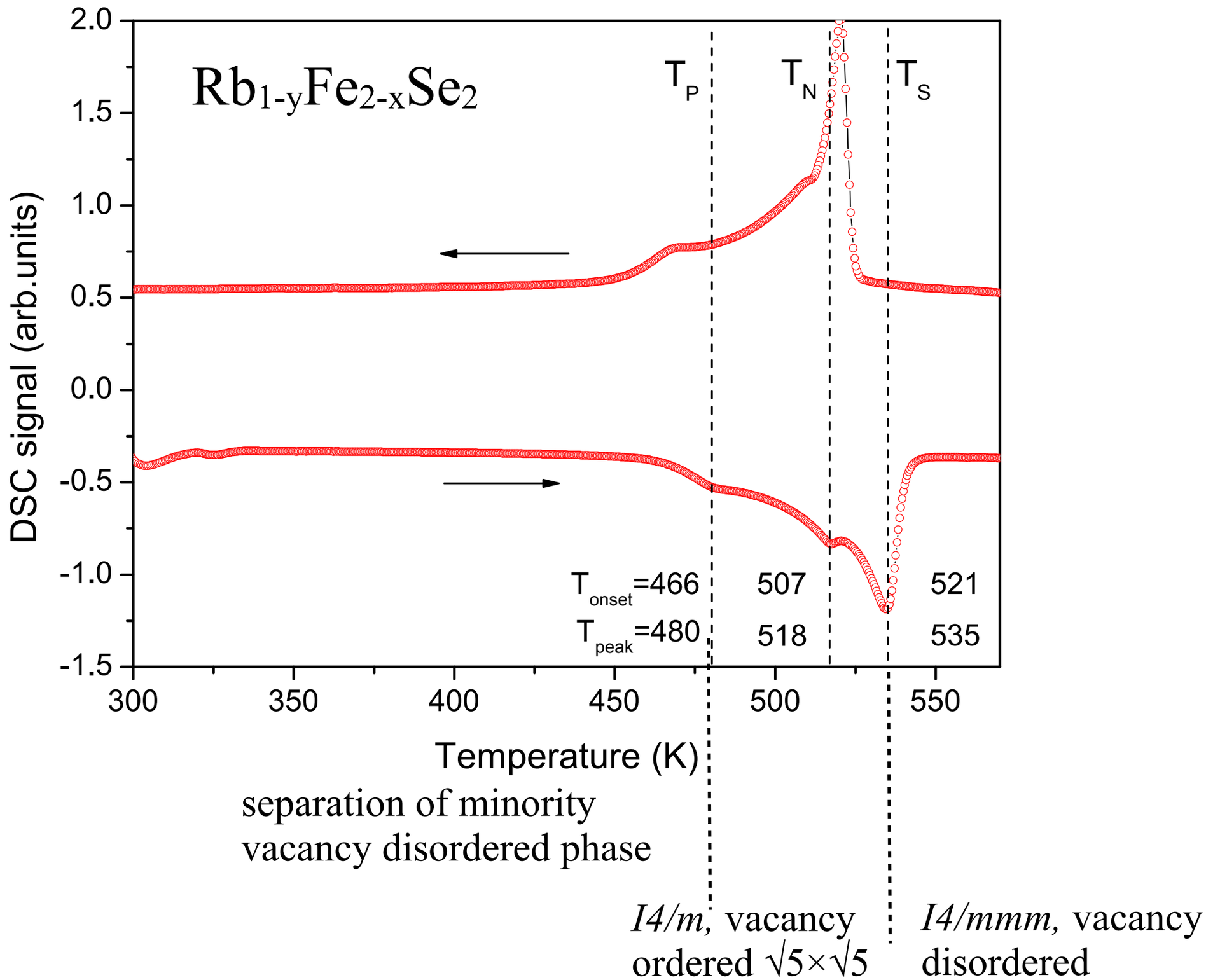

T-dependence of structure

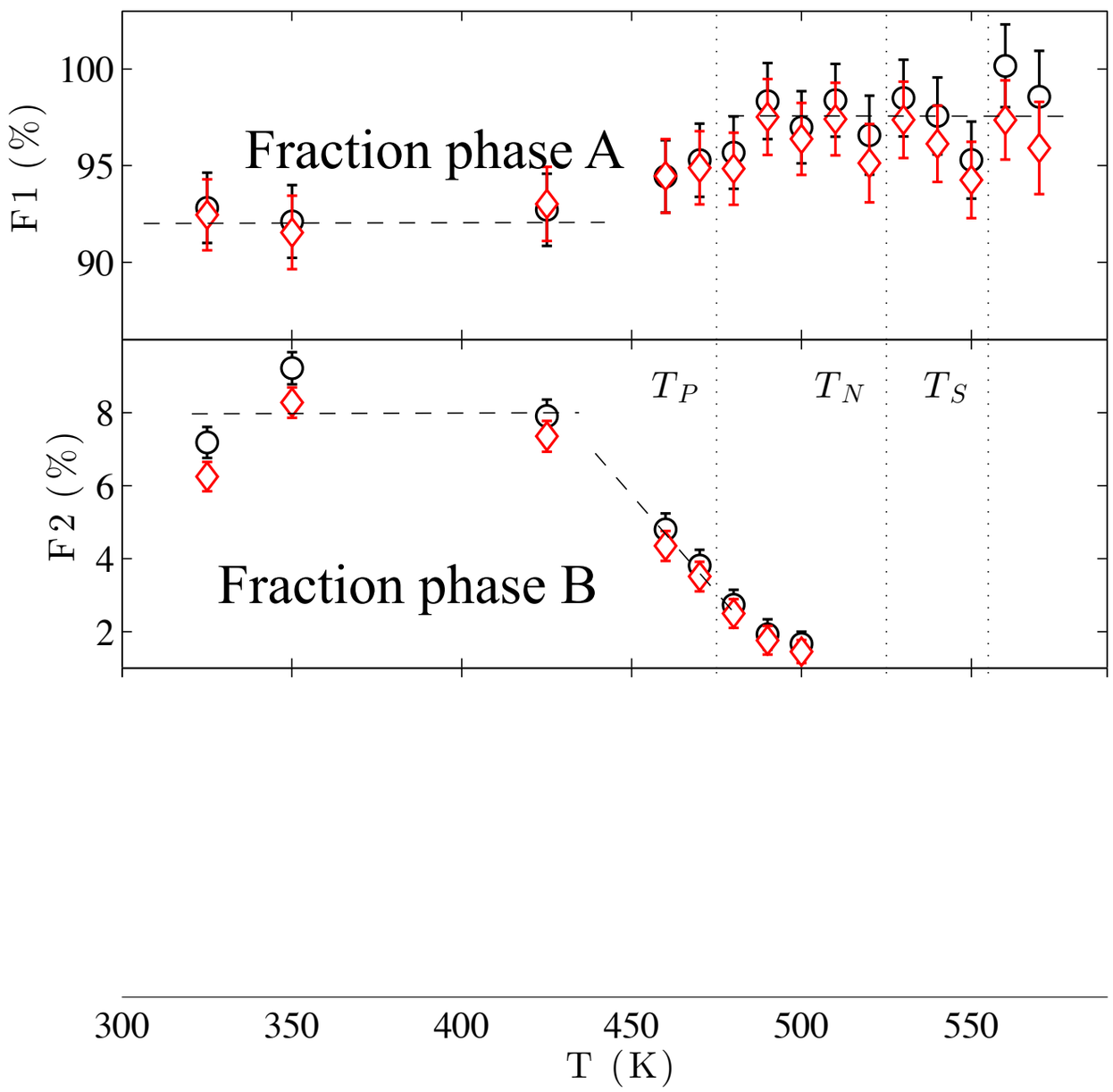

T-dependence of structure

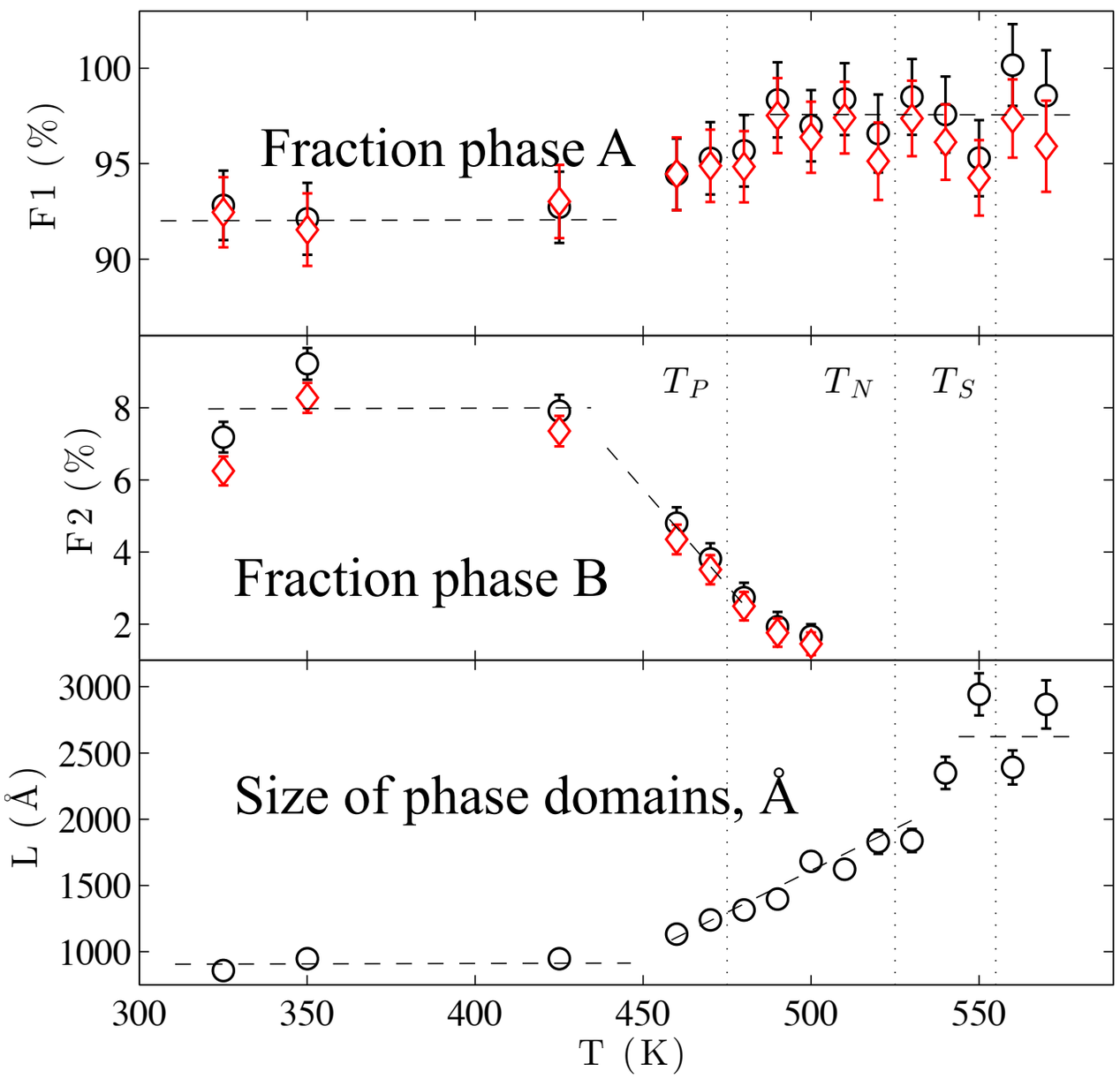

T-dependence of structure

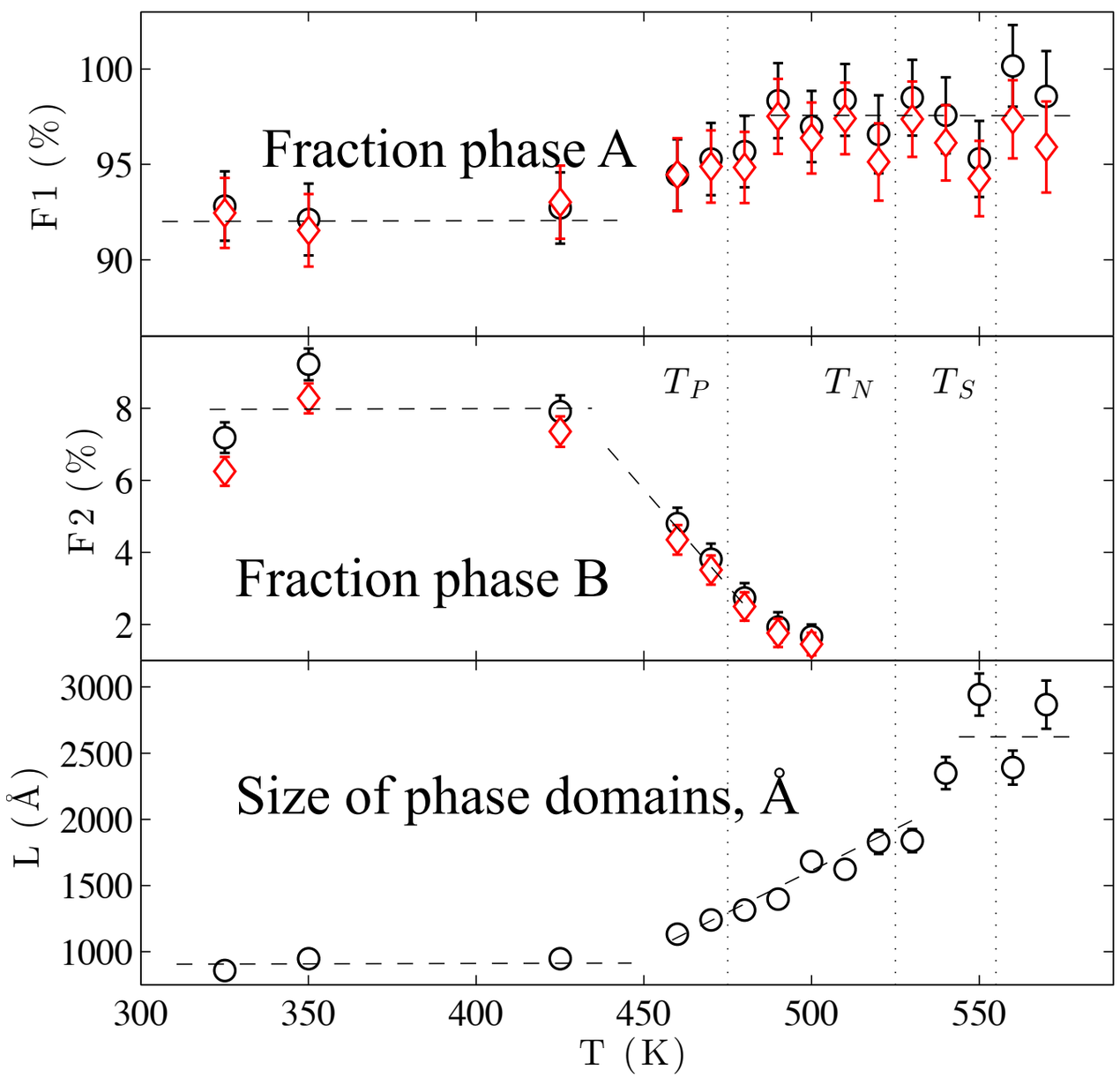

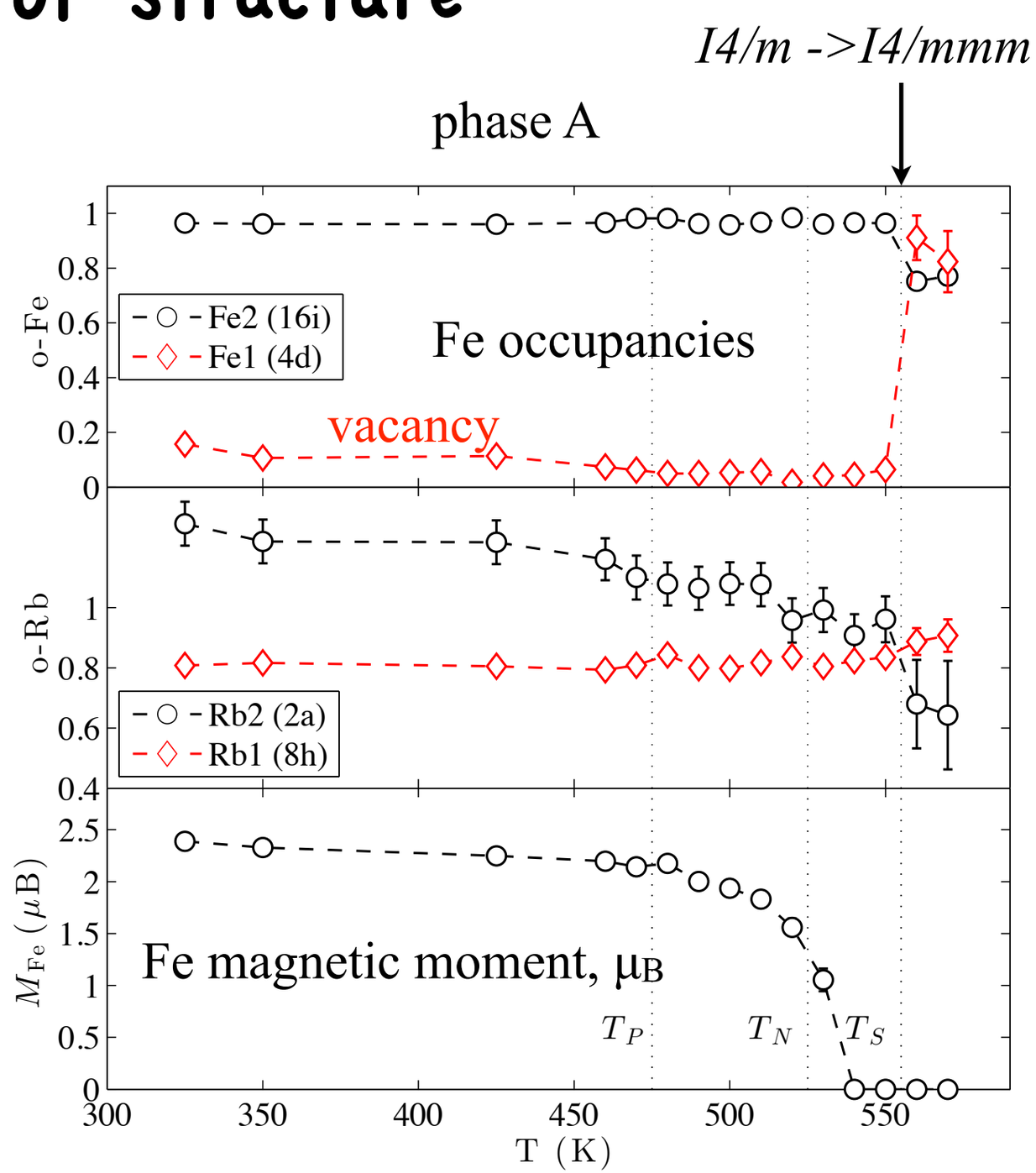

T dependence of phase separation. Single crystal synchrotron

Position	Max.Intensity	Int.Intensity	fwhm (Gaussian)	fwhm (Lorentzian)
24.70748 ± 0.00058	7583.4	623.0 ± 6.8	0.0772 ± 9E−4	0.0000
24.74645 ± 0.00074	4057.9	892.5 ± 7.9	0.2066 ± 0.0013	0.0000
25.03181 ± 0.00082	3217.1	691.4 ± 5.4	0.1209 ± 0.0022	0.0775 ± 0.0019

Int.Intens.Exp.	Bg(Pos)	dBg/dx
2172.2 ± 6.9	444.8 ± 4.9	227 ± 13

Monitor 1
* χ^2 3.787

Temperature= 300K

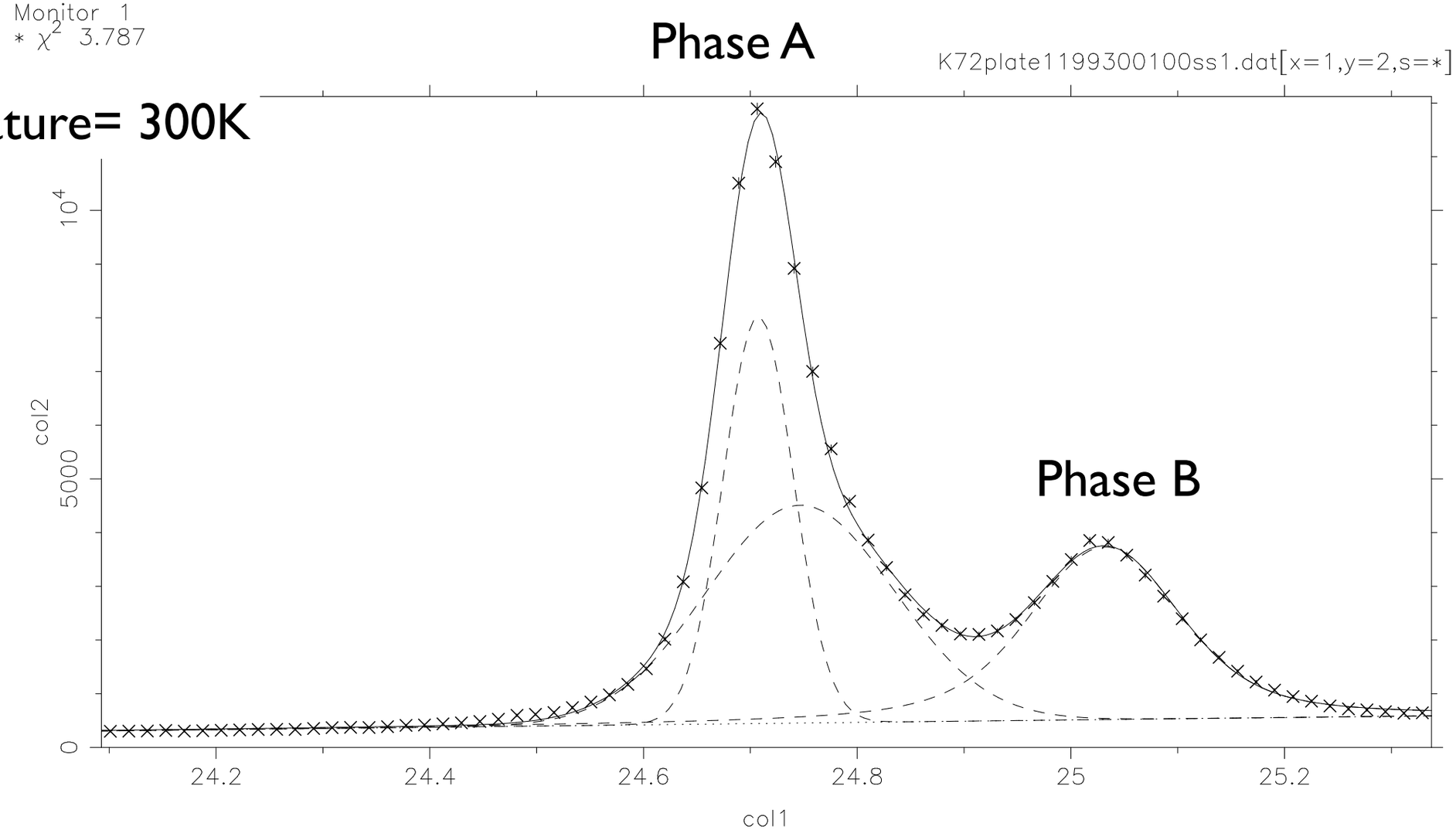

T dependence of phase separation. Single crystal synchrotron

Position	Max.Intensity	Int.Intensity	fwhm (Gaussian)	fwhm (Lorentzian)
24.6318 ± 3E−4	6484.5	531.8 ± 4.9	0.0770 ± 7E−4	0.0000
24.6738 ± 7E−4	4031.3	876.6 ± 8.5	0.2043 ± 0.0019	0.0000
24.9578 ± 0.0011	2410.1	514.3 ± 6.0	0.1304 ± 0.0021	0.0681 ± 0.0022

Int.Intens.Exp.	Bg(Pos)	dBg/dx
1904.7 ± 6.6	452.3 ± 4.6	207 ± 11

Monitor 1
* χ^2 3.584

Temperature= 424K

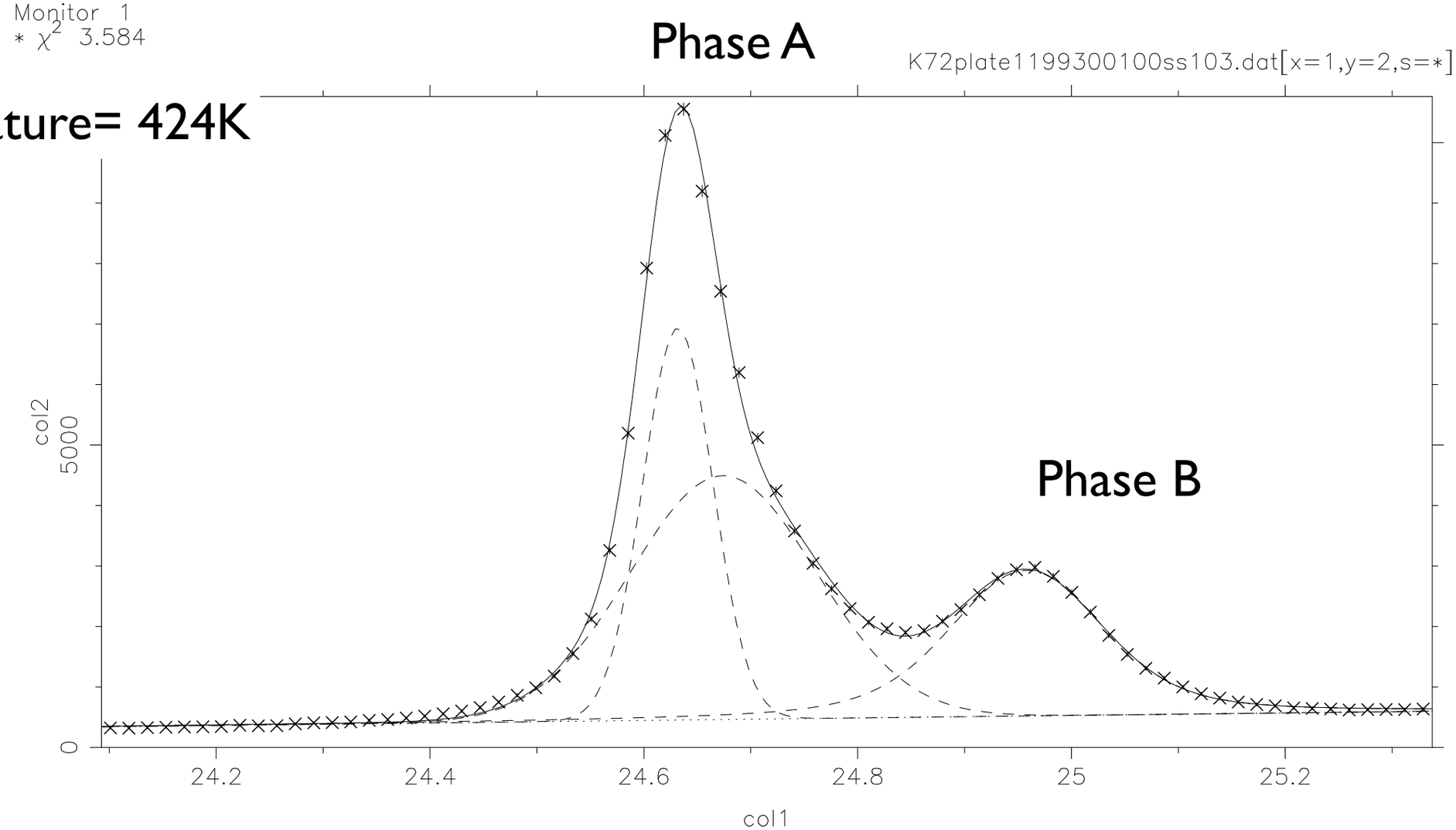

V. Pomjakushin, Phase separation in AFeSe JEMS '13

T dependence of phase separation. Single crystal synchrotron

Position	Max.Intensity	Int.Intensity	fwhm (Gaussian)	fwhm (Lorentzian)
24.5912 ± 3E−4	6878.6	622.7 ± 5.2	0.0850 ± 5E−4	0.0000
24.6719 ± 9E−4	3020.6	850.5 ± 5.7	0.2645 ± 0.0018	0.0000
24.9224 ± 0.0013	1458.4	326.1 ± 4.6	0.1056 ± 0.0052	0.0966 ± 0.0024

Int.Intens.Exp.	Bg(Pos)	dBg/dx
1783.8 ± 6.4	457.3 ± 4.2	187.4 ± 7.9

Monitor 1
* χ^2 2.823

Temperature= 482K

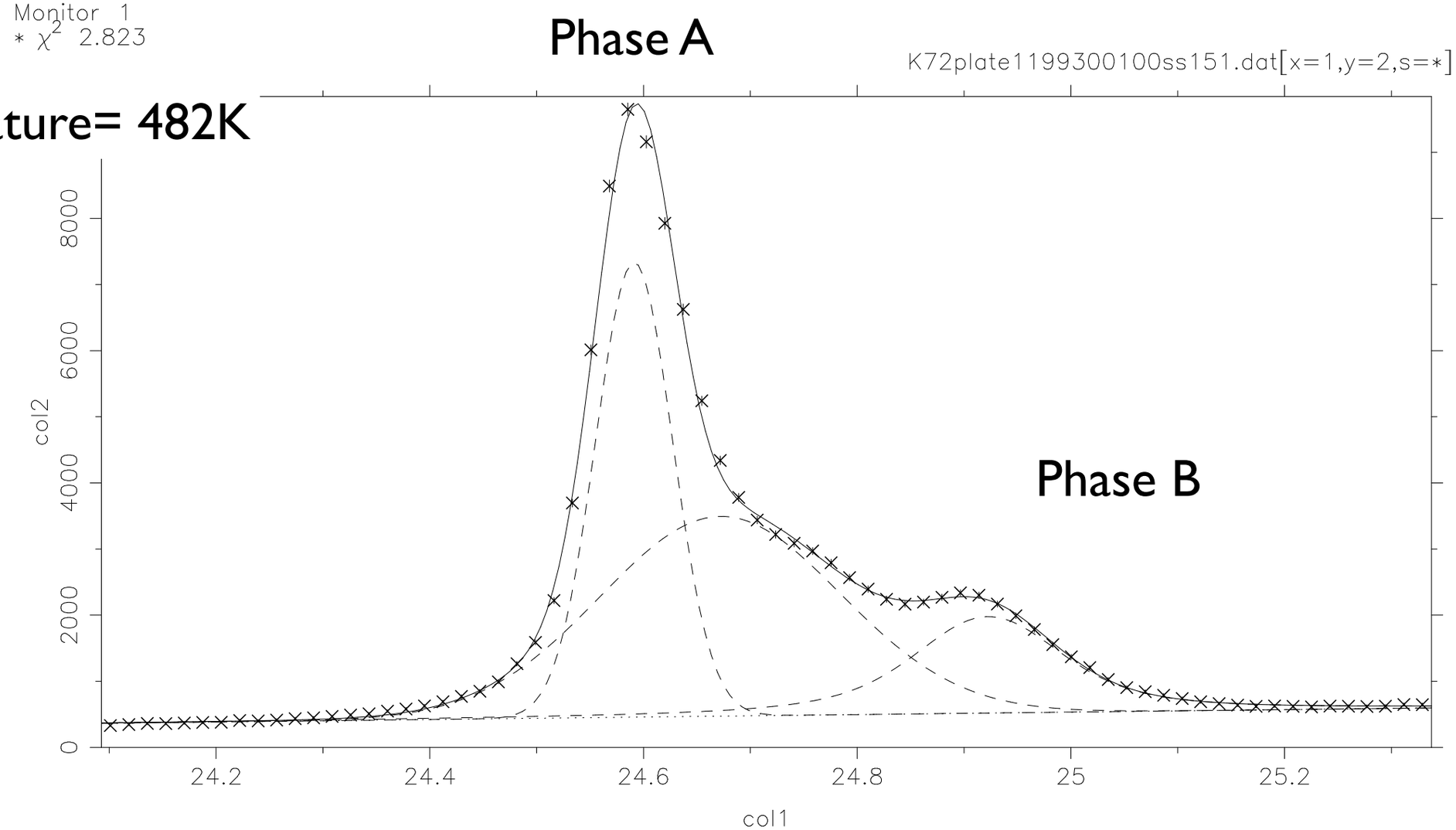

V. Pomjakushin, Phase separation in AFeSe JEMS '13

T dependence of phase separation. Single crystal synchrotron

Position	Max.Intensity	Int.Intensity	fwhm (Gaussian)	fwhm (Lorentzian)
24.5864 ± 3E−4	6672.6	583.8 ± 5.0	0.0822 ± 6E−4	0.0000
24.6804 ± 9E−4	3277.4	951.9 ± 6.3	0.2729 ± 0.0020	0.0000
24.9355 ± 0.0019	1158.4	236.4 ± 4.3	0.0849 ± 0.0061	0.0964 ± 0.0033

Int.Intens.Exp.	Bg(Pos)	dBg/dx
1761.8 ± 6.4	461.0 ± 4.1	193.0 ± 10.6

Monitor 1
* χ^2 2.705

Temperature= 485K

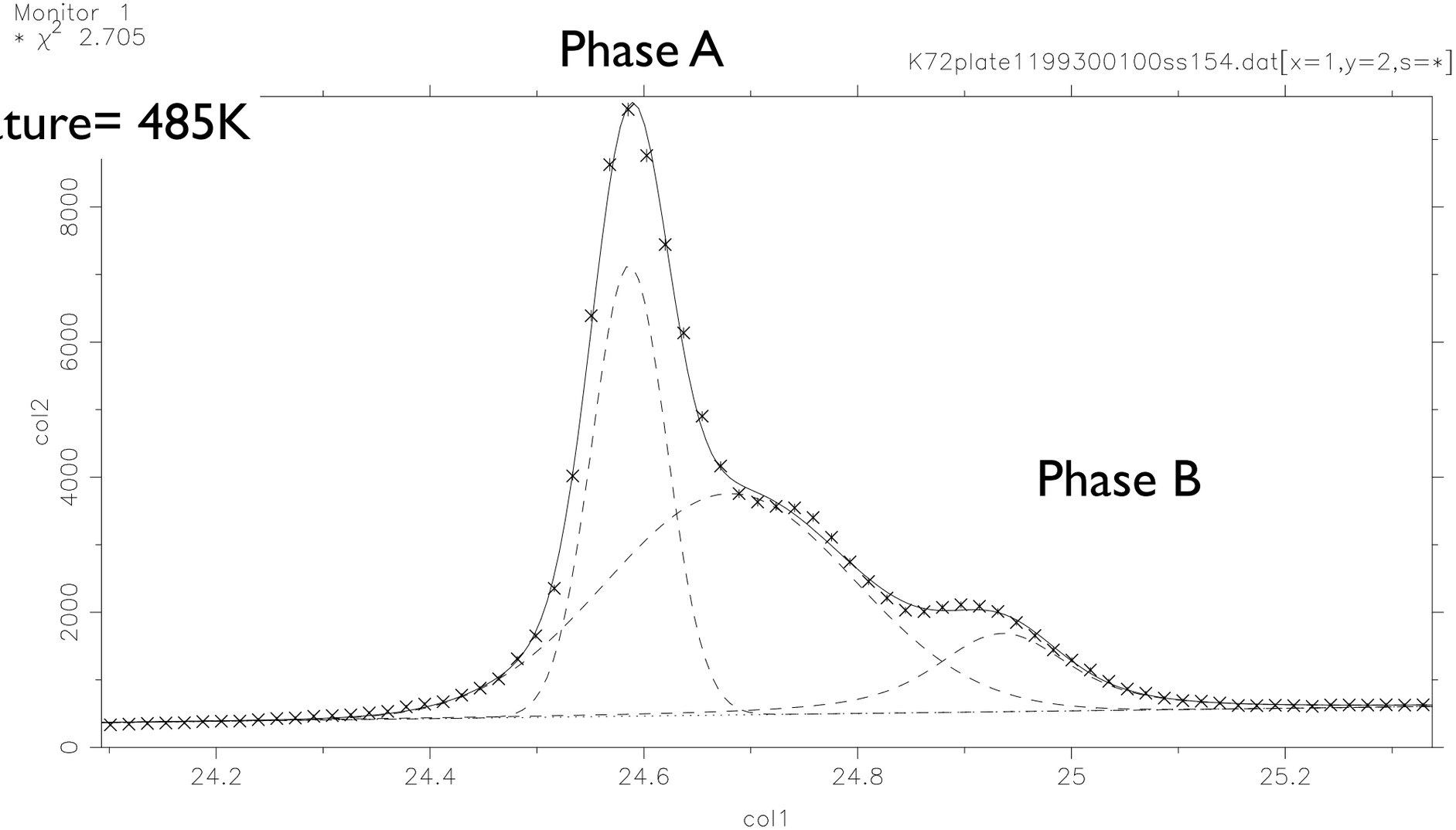

T dependence of phase separation. Single crystal synchrotron

Position	Max.Intensity	Int.Intensity	fwhm (Gaussian)	fwhm (Lorentzian)
24.5725 ± 3E−4	5779.1	424.1 ± 3.0	0.0689 ± 7E−4	0.0000
24.6725 ± 6E−4	4342.0	1155.3 ± 7.1	0.2500 ± 0.0015	0.0000
24.9435 ± 0.0026	783.3	142.7 ± 3.4	0.1150 ± 0.0041	0.0550 ± 0.0038

Int.Intens.Exp.	Bg(Pos)	dBg/dx
1720.3 ± 6.4	477.7 ± 3.8	204.3 ± 8.9

Monitor 1
* χ^2 2.505

Temperature= 495K

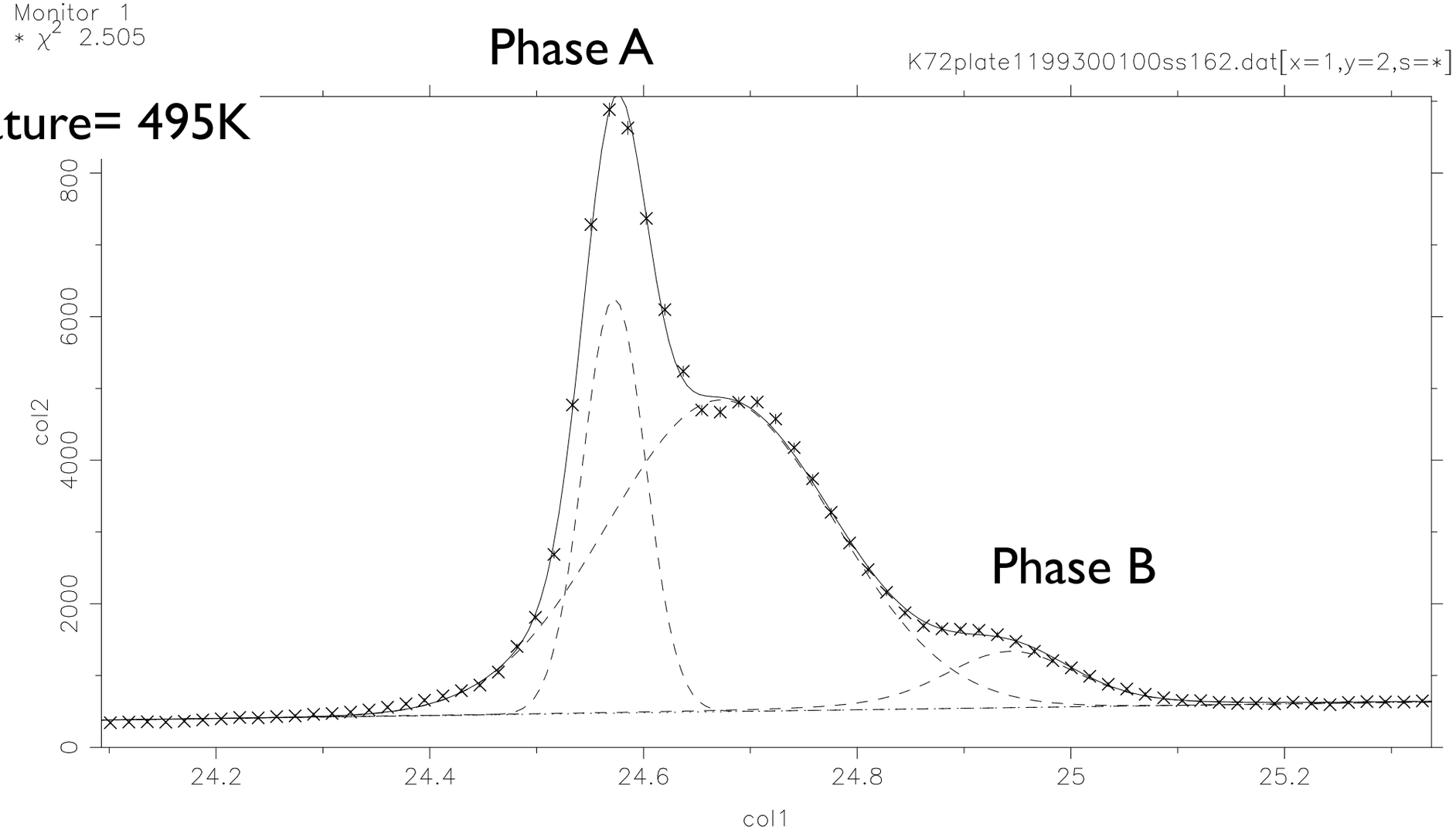

T dependence of phase separation. Single crystal synchrotron

Position	Max.Intensity	Int.Intensity	fwhm (Gaussian)	fwhm (Lorentzian)
24.5641 ± 3E−4	4947.1	323.6 ± 3.0	0.0615 ± 6E−4	0.000000
24.6626 ± 5E−4	5014.5	1262.1 ± 6.1	0.2365 ± 0.0013	0.000000
24.9347 ± 0.0030	618.6	109.7 ± 3.2	0.1652 ± 0.0054	0.001442 ± 0.005661

Int.Intens.Exp.	Bg(Pos)	dBg/dx
1698.1 ± 6.4	481.7 ± 3.4	214.4 ± 7.5

Monitor 1
* χ^2 2.091

Temperature= 500K

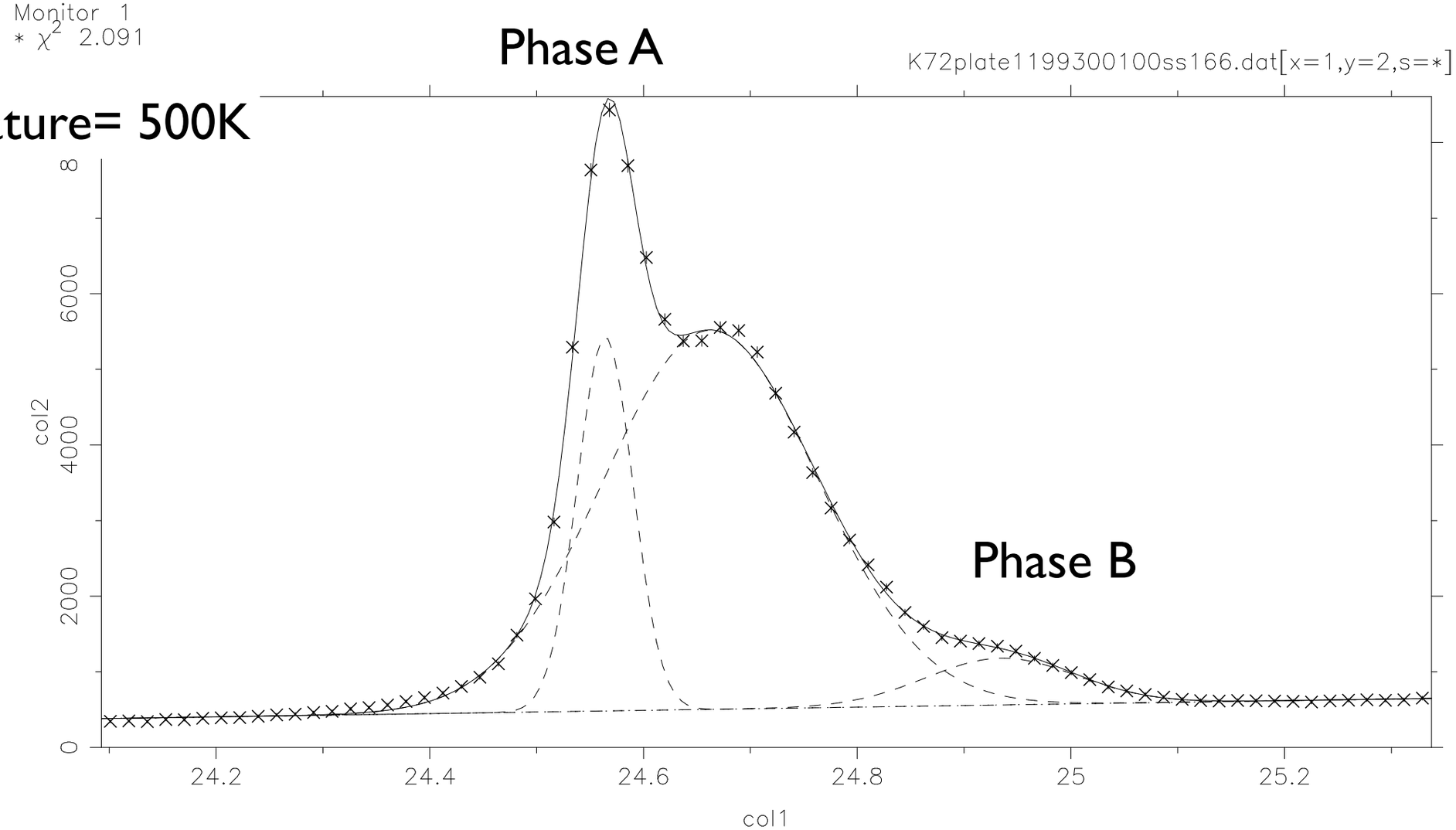

T dependence of phase separation. Single crystal synchrotron

Position	Max.Intensity	Int.Intensity	fwhm (Gaussian)	fwhm (Lorentzian)
24.5544 ± 6E−4	3711.7	200.9 ± 3.6	0.0509 ± 9E−4	0.0000000
24.6483 ± 5E−4	5831.3	1306.9 ± 7.6	0.2105 ± 0.0011	0.0000000
24.8678 ± 0.0030	637.0	161.2 ± 3.5	0.2377 ± 0.0045	3E−7 ± 0.003301
Int.Intens.Exp.	Bg(Pos)	dBg/dx		
1673.2 ± 6.4	480.9 ± 4.4	201 ± 10		

Monitor 1
* χ^2 3.265

Temperature= 500K

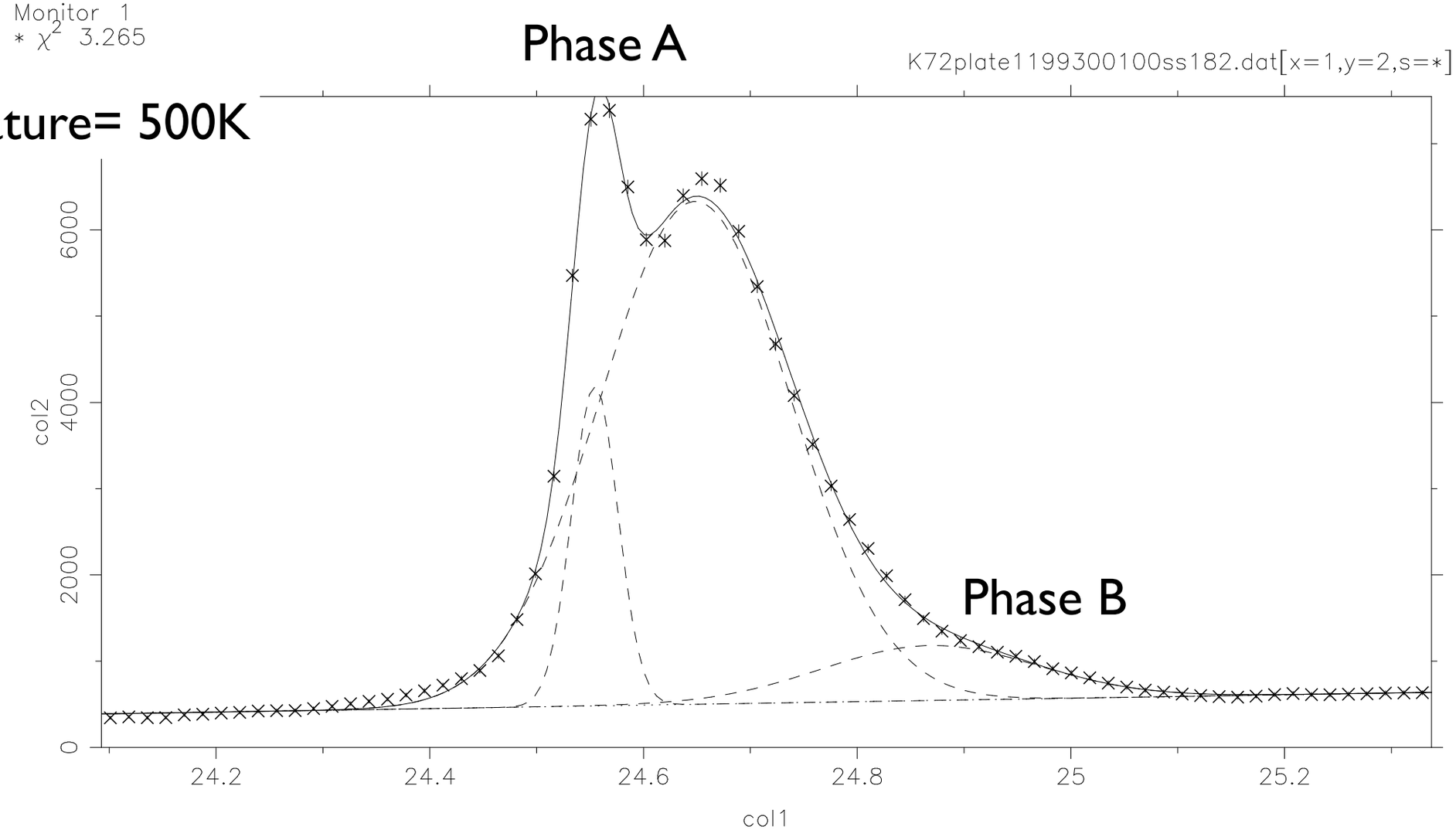

T dependence of phase separation. Single crystal synchrotron

Position	Max.Intensity	Int.Intensity	fwhm (Gaussian)	fwhm (Lorentzian)
24.55290 ± 0.00018	3721.6	214.6 ± 1.2	0.0542 ± 3E−4	0.000000
24.64952 ± 0.00026	4674.7	848.9 ± 2.7	0.1706 ± 5E−4	0.000000
24.70446 ± 0.00069	1546.8	611.2 ± 2.7	0.3707 ± 0.0014	0.000580 ± 0.001195

Int.Intens.Exp.	Bg(Pos)	dBg/dx
1675.8 ± 6.3	451.0 ± 1.4	220.5 ± 2.3

Monitor 1
* χ^2 1.3685

Temperature= 500K

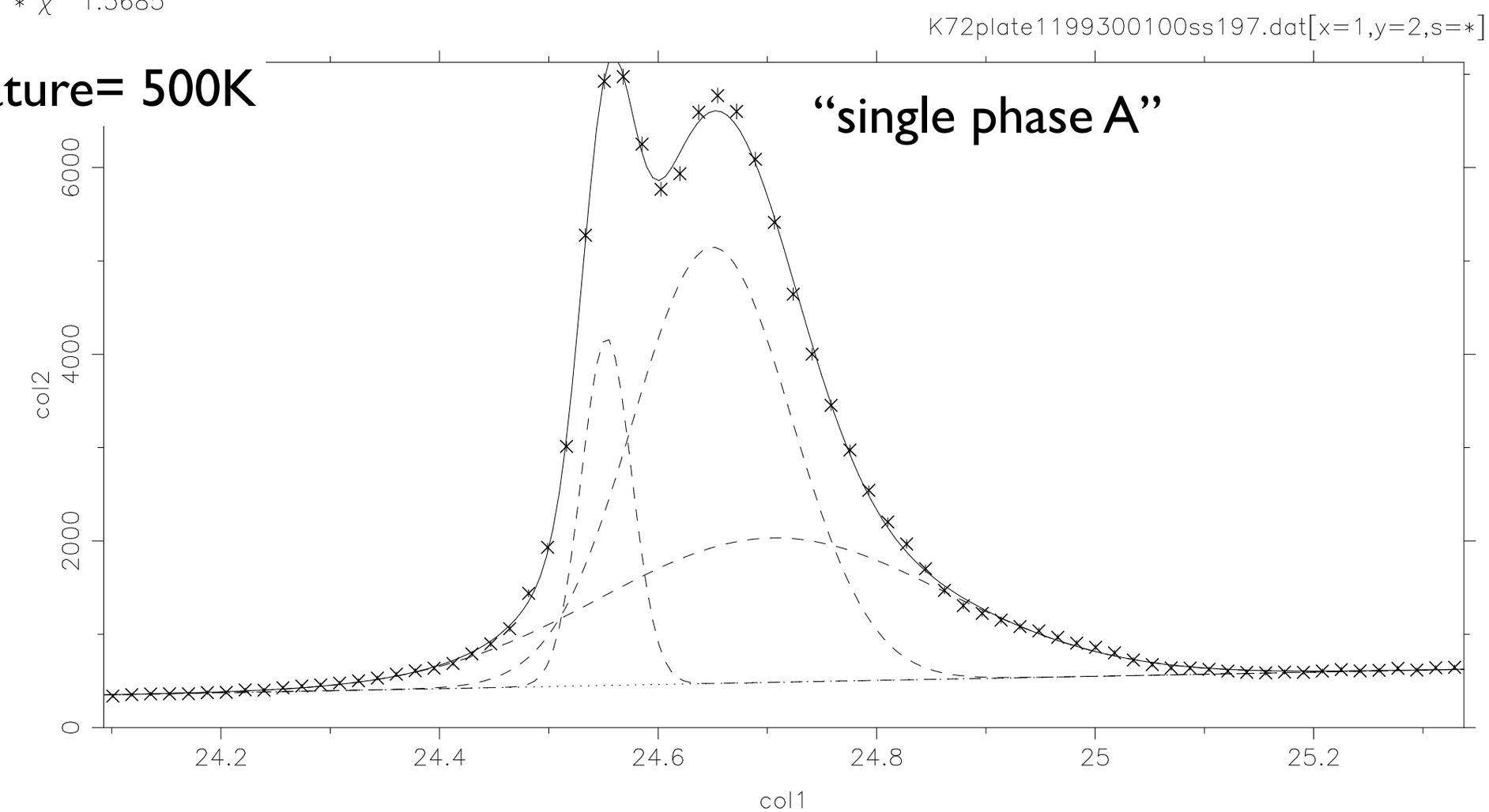

T dependence of phase separation. Single crystal synchrotron

Position	Max.Intensity	Int.Intensity	fwhm (Gaussian)	fwhm (Lorentzian)
24.55225 ± 0.00036	3274.5	184.7 ± 2.0	0.0530 ± 7E−4	0.0000000
24.65080 ± 0.00038	4651.7	795.9 ± 4.1	0.1607 ± 0.0010	0.0000000
24.70249 ± 0.00100	1700.7	642.2 ± 4.1	0.3546 ± 0.0024	0.0001565 ± 0.0013105

Int.Intens.Exp.	Bg(Pos)	dBg/dx
1624.2 ± 6.2	450.3 ± 2.8	217.9 ± 6.5

Monitor 1
* χ^2 1.3716

Temperature= 500K

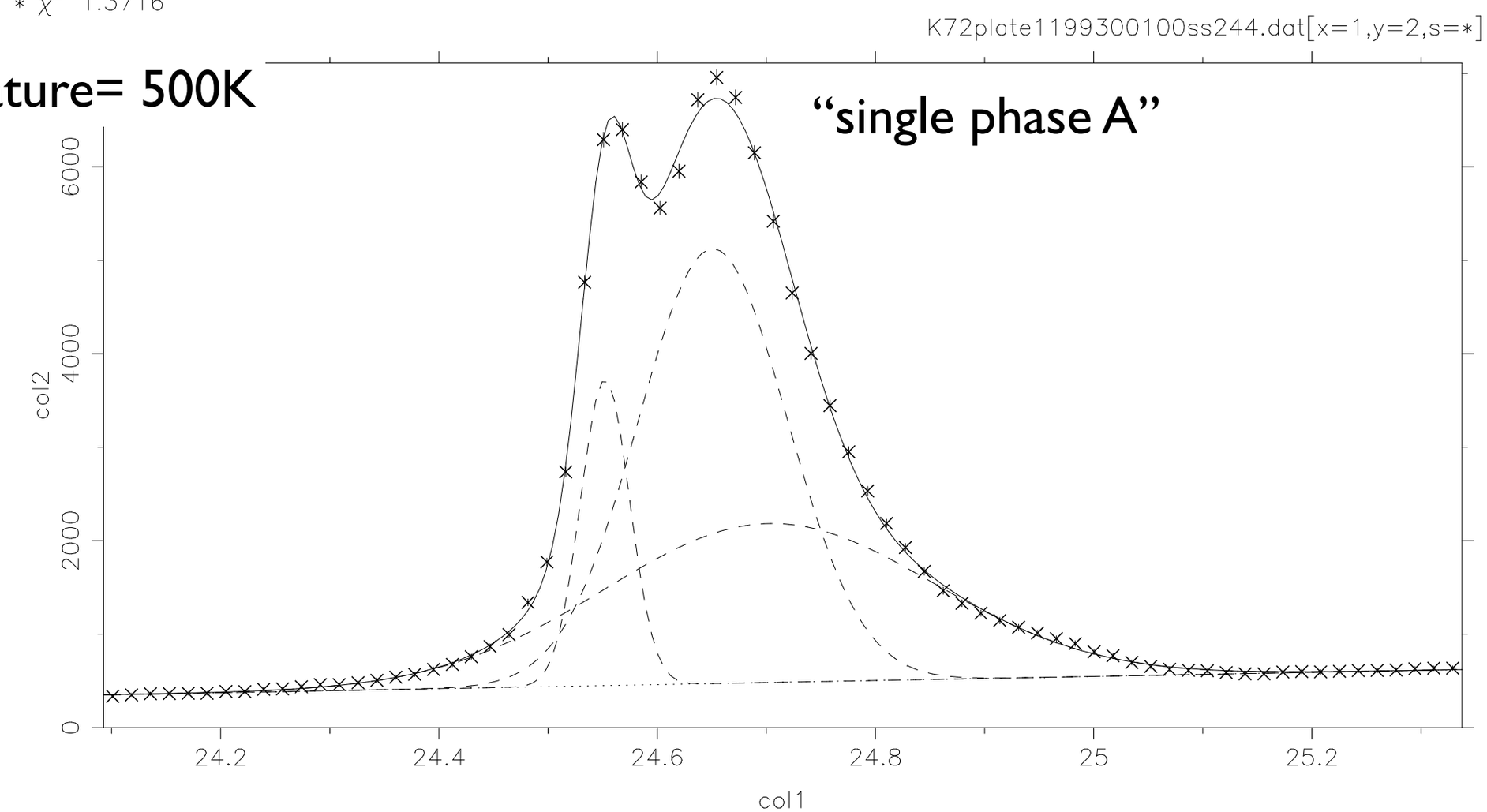

T dependence of phase separation. Single crystal synchrotron

Position	Max.Intensity	Int.Intensity	fwhm (Gaussian)	fwhm (Lorentzian)
24.55251 ± 0.00018	2959.6	153.4 ± 0.8	0.04868 ± 0.00036	0.00000
24.63731 ± 0.00015	4766.7	591.5 ± 1.3	0.08408 ± 0.00035	0.03229 ± 0.00034
24.67583 ± 0.00047	1587.6	446.3 ± 1.4	0.26407 ± 0.00084	0.00000

Int.Intens.Exp.	Bg(Pos)	dBg/dx
1183.4 ± 4.9	421.6 ± 1.2	282.3 ± 3.1

Monitor 1
* χ^2 1.1773

Temperature= 500K

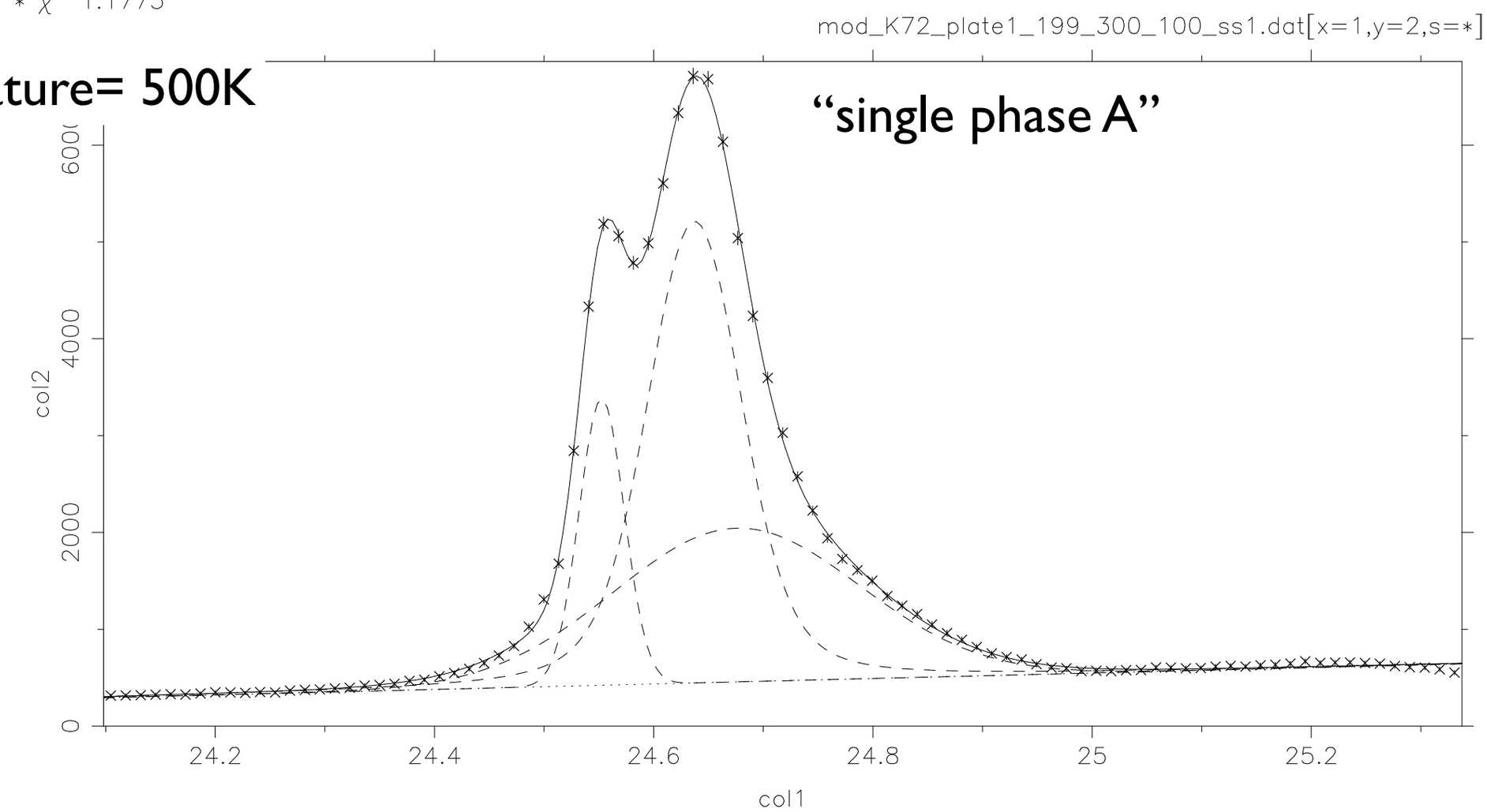

T dependence of phase separation. Single crystal synchrotron

Position	Max.Intensity	Int.Intensity	fwhm (Gaussian)	fwhm (Lorentzian)
24.5570 ± 4E−4	3362.5	191.2 ± 2.5	0.0534 ± 6E−4	0.00000
24.6450 ± 3E−4	5921.6	951.0 ± 3.8	0.0617 ± 1E−3	0.07936 ± 0.00048
24.7591 ± 0.0016	655.8	134.9 ± 2.0	0.1933 ± 0.0025	0.00000

Int.Intens.Exp.	Bg(Pos)	dBg/dx
1239.2 ± 4.9	373.2 ± 2.7	299.4 ± 6.4

Monitor 1
* χ^2 1.7885

Temperature= 492K

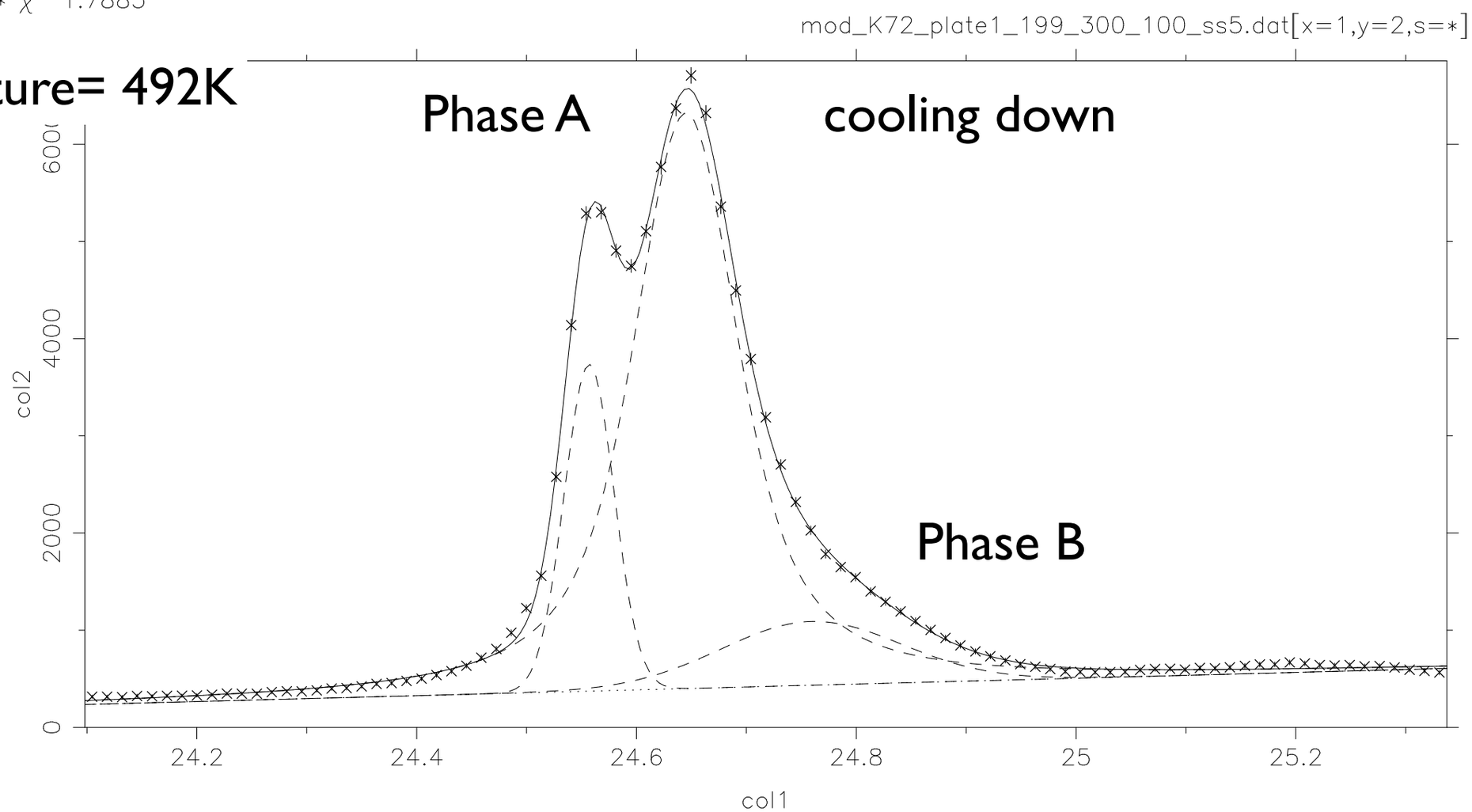

T dependence of phase separation. Single crystal synchrotron

Position	Max.Intensity	Int.Intensity	fwhm (Gaussian)	fwhm (Lorentzian)
24.5654 ± 4E−4	4101.2	258.8 ± 2.6	0.0593 ± 6E−4	0.00000
24.6611 ± 3E−4	5631.3	950.6 ± 4.2	0.0571 ± 0.0011	0.08833 ± 0.00059
24.8075 ± 0.0017	529.9	80.8 ± 1.6	0.1433 ± 0.0027	0.00000

Int.Intens.Exp.	Bg(Pos)	dBg/dx
1248.0 ± 4.9	370.9 ± 2.8	297.7 ± 5.5

Monitor 1
* χ^2 1.8746

Temperature= 484K

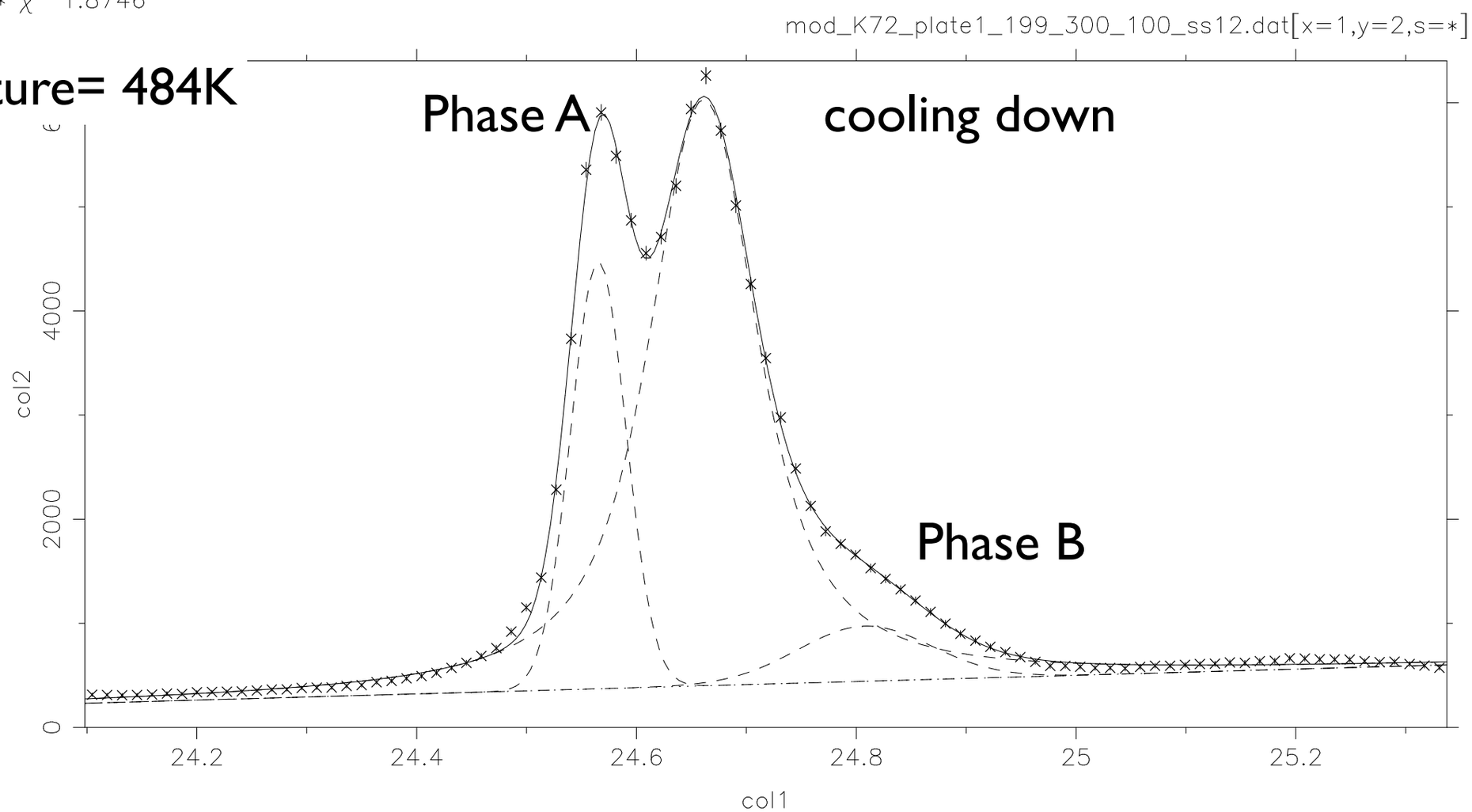

T dependence of phase separation. Single crystal synchrotron

Position	Max.Intensity	Int.Intensity	fwhm (Gaussian)	fwhm (Lorentzian)
24.5715 ± 3E−4	4633.1	315.4 ± 2.4	0.0640 ± 5E−4	0.00000
24.6720 ± 3E−4	5072.5	900.7 ± 3.8	0.0530 ± 0.0013	0.09702 ± 0.00063
24.8217 ± 0.0013	594.1	75.7 ± 1.4	0.1197 ± 0.0034	0.00000

Int.Intens.Exp.	Bg(Pos)	dBg/dx
1248.0 ± 4.9	373.4 ± 2.7	291.8 ± 4.9

Monitor 1
* χ^2 1.934

Temperature= 479K

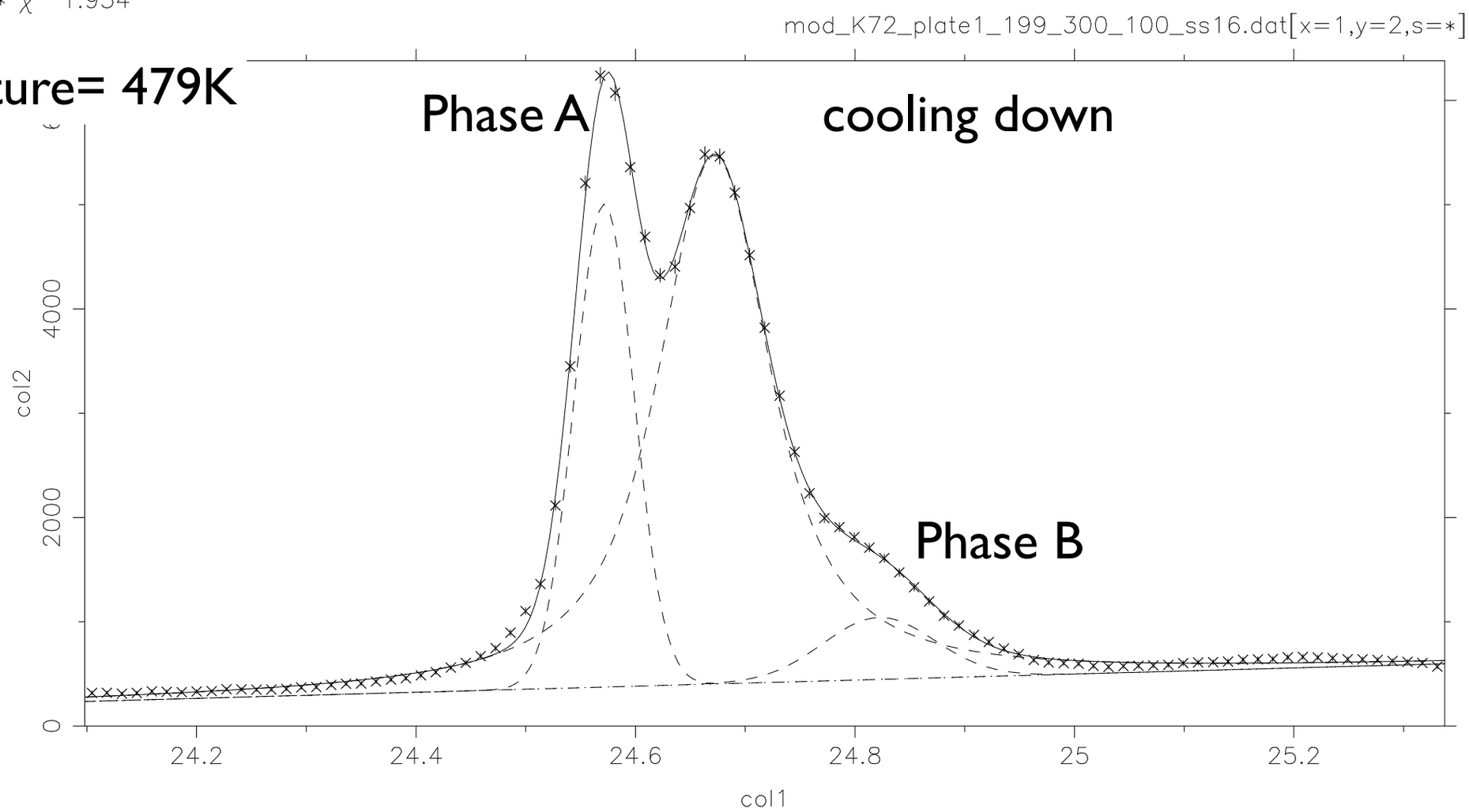

T dependence of phase separation. Single crystal synchrotron

Position	Max.Intensity	Int.Intensity	fwhm (Gaussian)	fwhm (Lorentzian)
24.5793 ± 3E−4	5217.7	390.6 ± 3.6	0.0703 ± 8E−4	0.00000
24.6842 ± 8E−4	4130.0	820.0 ± 4.5	0.0466 ± 0.0023	0.11490 ± 0.00082
24.8217 ± 0.0011	799.3	94.4 ± 1.7	0.1110 ± 0.0019	0.00000

Int.Intens.Exp.	Bg(Pos)	dBg/dx
1258.2 ± 4.9	371.9 ± 3.1	297.9 ± 7.6

Monitor 1
* χ^2 2.386

Temperature= 473K

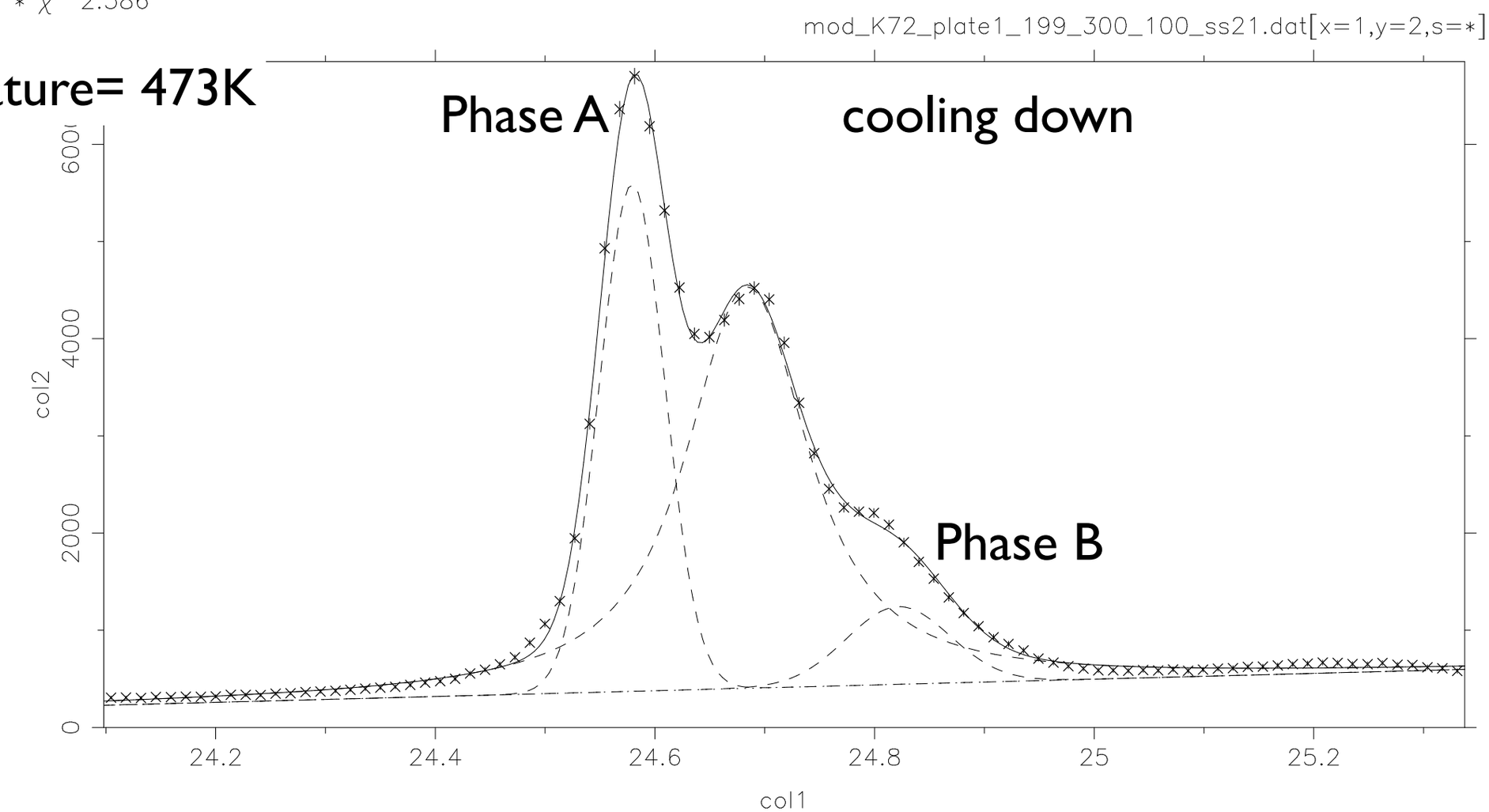

T dependence of phase separation. Single crystal synchrotron

Position	Max.Intensity	Int.Intensity	fwhm (Gaussian)	fwhm (Lorentzian)
24.58256 ± 0.00028	4616.2	314.9 ± 3.5	0.0641 ± 9E−4	0.00000
24.65116 ± 0.00077	3075.1	672.5 ± 3.3	0.1619 ± 0.0011	0.04407 ± 0.00081
24.80557 ± 0.00061	1472.9	230.1 ± 1.9	0.1468 ± 9E−4	0.00000

Int.Intens.Exp.	Bg(Pos)	dBg/dx
1204.3 ± 4.9	421.2 ± 2.6	309.2 ± 6.5

Monitor 1
* χ^2 1.8247

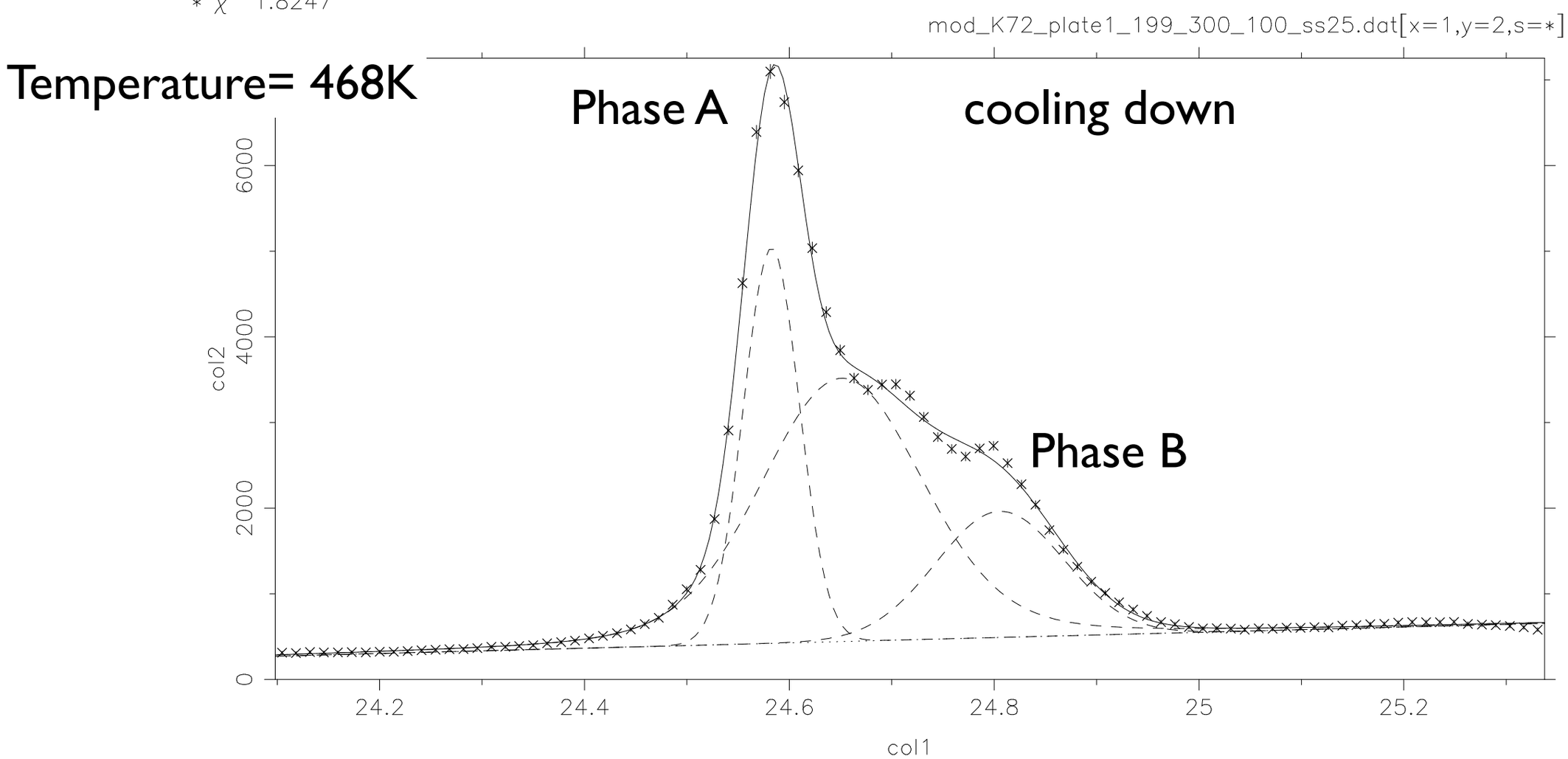

T dependence of phase separation. Single crystal synchrotron

Position	Max.Intensity	Int.Intensity	fwhm (Gaussian)	fwhm (Lorentzian)
24.58118 ± 0.00020	3401.6	205.1 ± 1.4	0.05665 ± 0.00036	0.00000
24.61286 ± 0.00019	4109.3	622.1 ± 1.8	0.09702 ± 0.00052	0.04439 ± 0.00045
24.78935 ± 0.00036	2330.9	387.3 ± 1.4	0.15610 ± 0.00043	0.00000

Int.Intens.Exp.	Bg(Pos)	dBg/dx
1201.9 ± 4.9	420.9 ± 1.5	321.2 ± 3.9

Monitor 1
* χ^2 1.5027

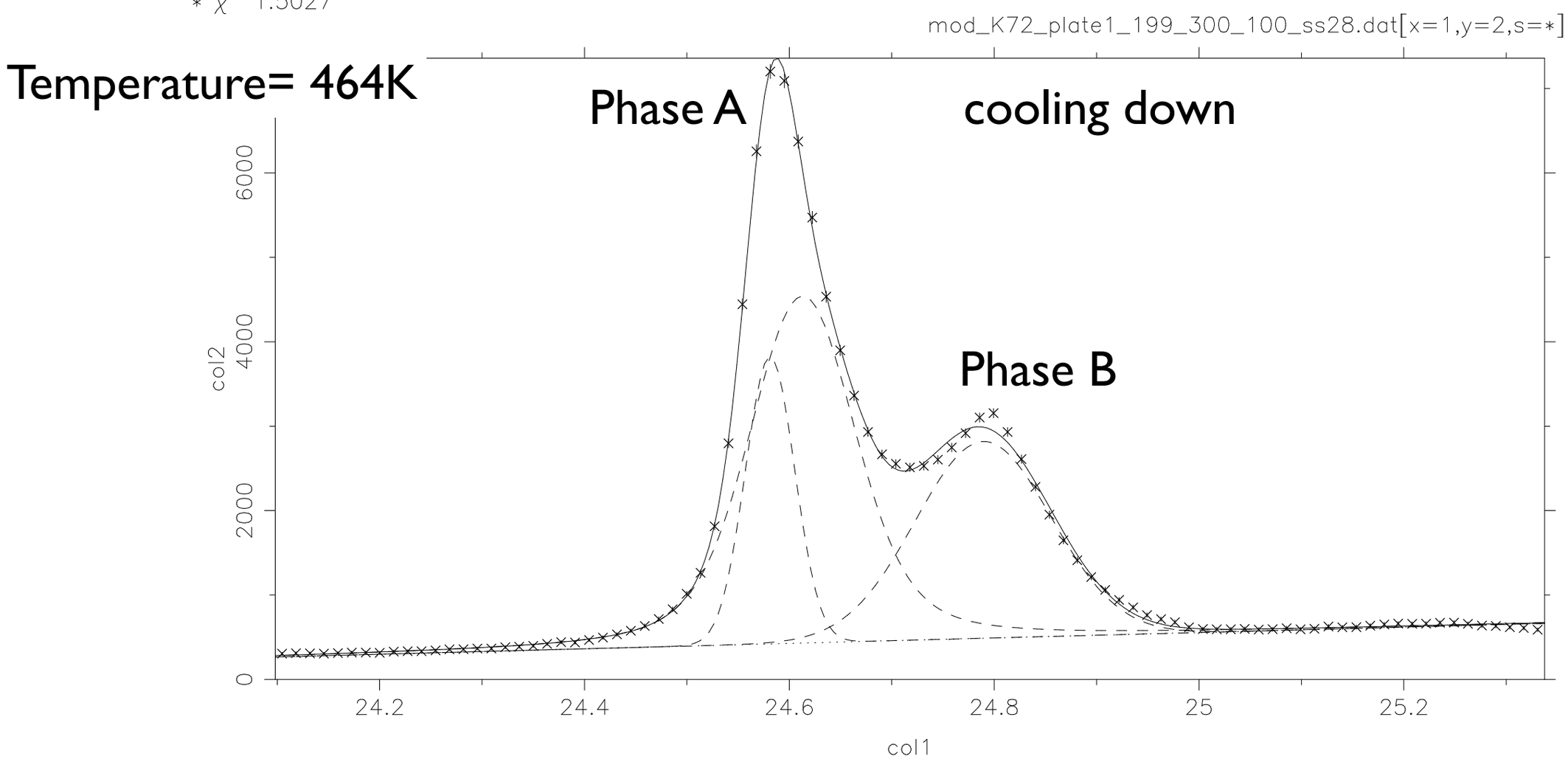

T dependence of phase separation. Single crystal synchrotron

Position	Max.Intensity	Int.Intensity	fwhm (Gaussian)	fwhm (Lorentzian)
24.61854 ± 0.00019	3775.9	249.0 ± 1.1	0.06196 ± 0.00026	0.00000
24.64470 ± 0.00017	4114.6	652.8 ± 1.9	0.11099 ± 0.00035	0.03805 ± 0.00034
24.85057 ± 0.00024	2289.9	343.3 ± 0.9	0.14083 ± 0.00031	0.00000

Int.Intens.Exp.	Bg(Pos)	dBg/dx
1233.0 ± 5.0	434.8 ± 1.1	341.6 ± 3.4

Monitor 1
* χ^2 1.1417

Temperature= 460K

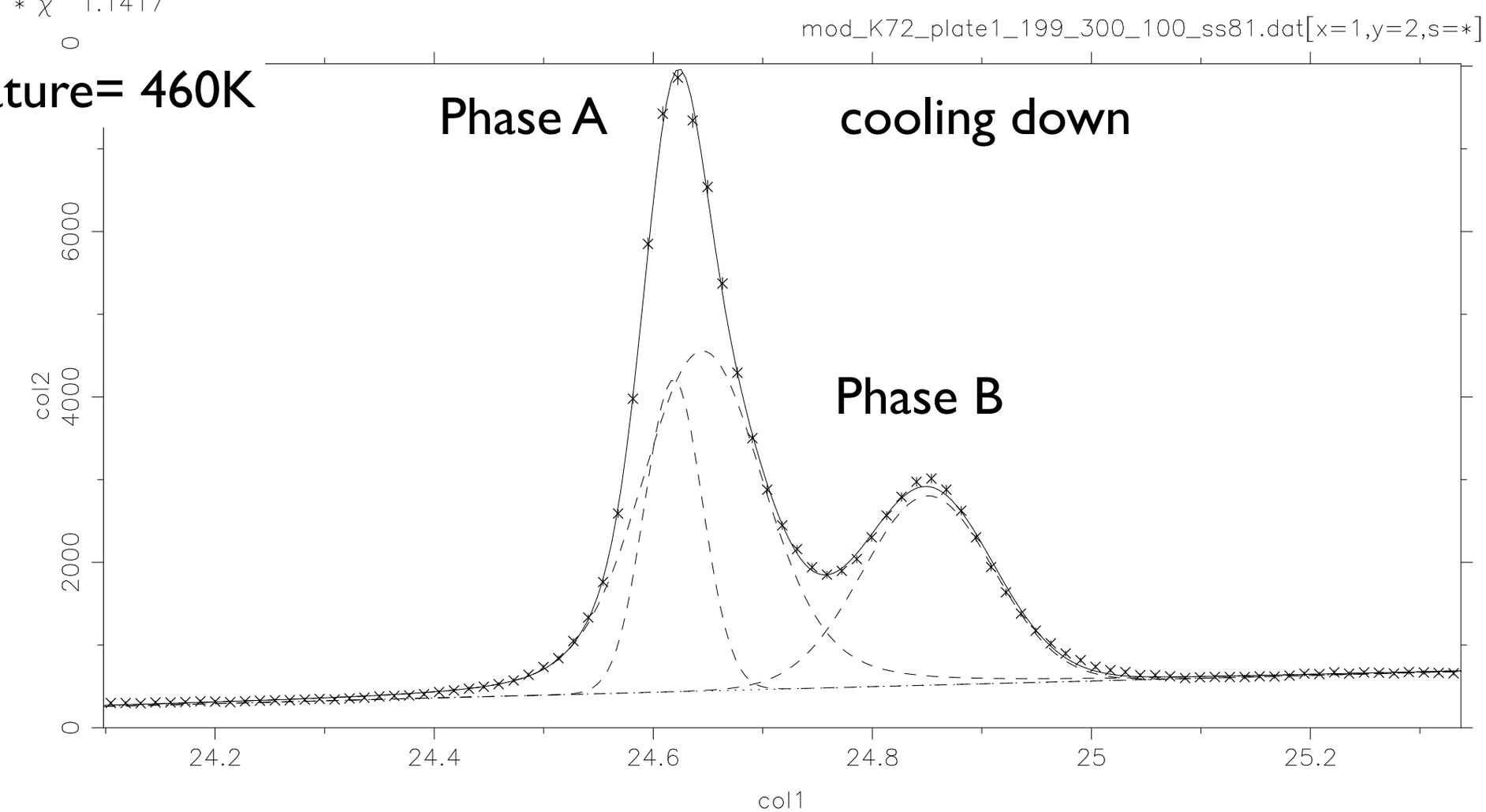

last frame

V. Pomjakushin, Phase separation in AFeSe JEMS '13

Summary on superconducting $A_{0.8}Fe_{1.7}Se_2$, X=K, Rb, Cs

- The ground state of the crystal is an intrinsically phase-separated state with two distinct-by-symmetry phases.
- The main phase has the iron vacancy ordered $\sqrt{5} \times \sqrt{5}$ *I4/M*-superstructure $Rb_{0.8}Fe_{1.5}Se_2$.
- The minority phase can be well approximated by *I4/mmm*-disordered structure with the refined stoichiometry $Rb_{0.60(5)}(Fe_{1.10(5)}Se)_2$. True symmetry is lower with 2D (ab)-plane ordering $\sqrt{2} \times \sqrt{2}$
- The minority phase merges with the main vacancy ordered phase on heating above the phase separation temperature $T_P \simeq 475K < T_S \simeq 530K$ (to average *I/mmm*)

Thank you!

Neutron diffraction patterns Rb, K, Cs

Magnetic contribution is in red

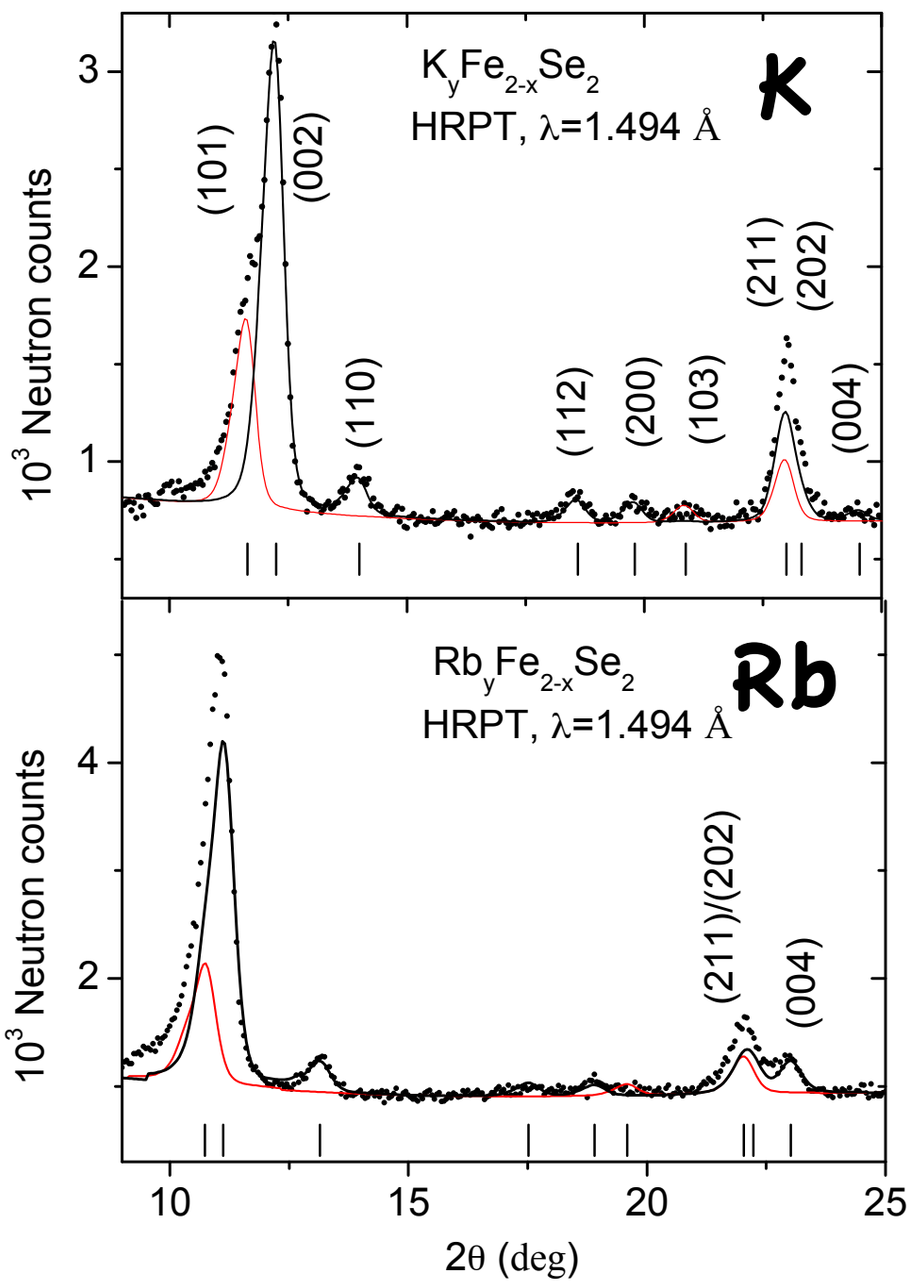

τ2 or t7 with spins along c

Comparison of different models.
Crystal structure is fixed by x-ray

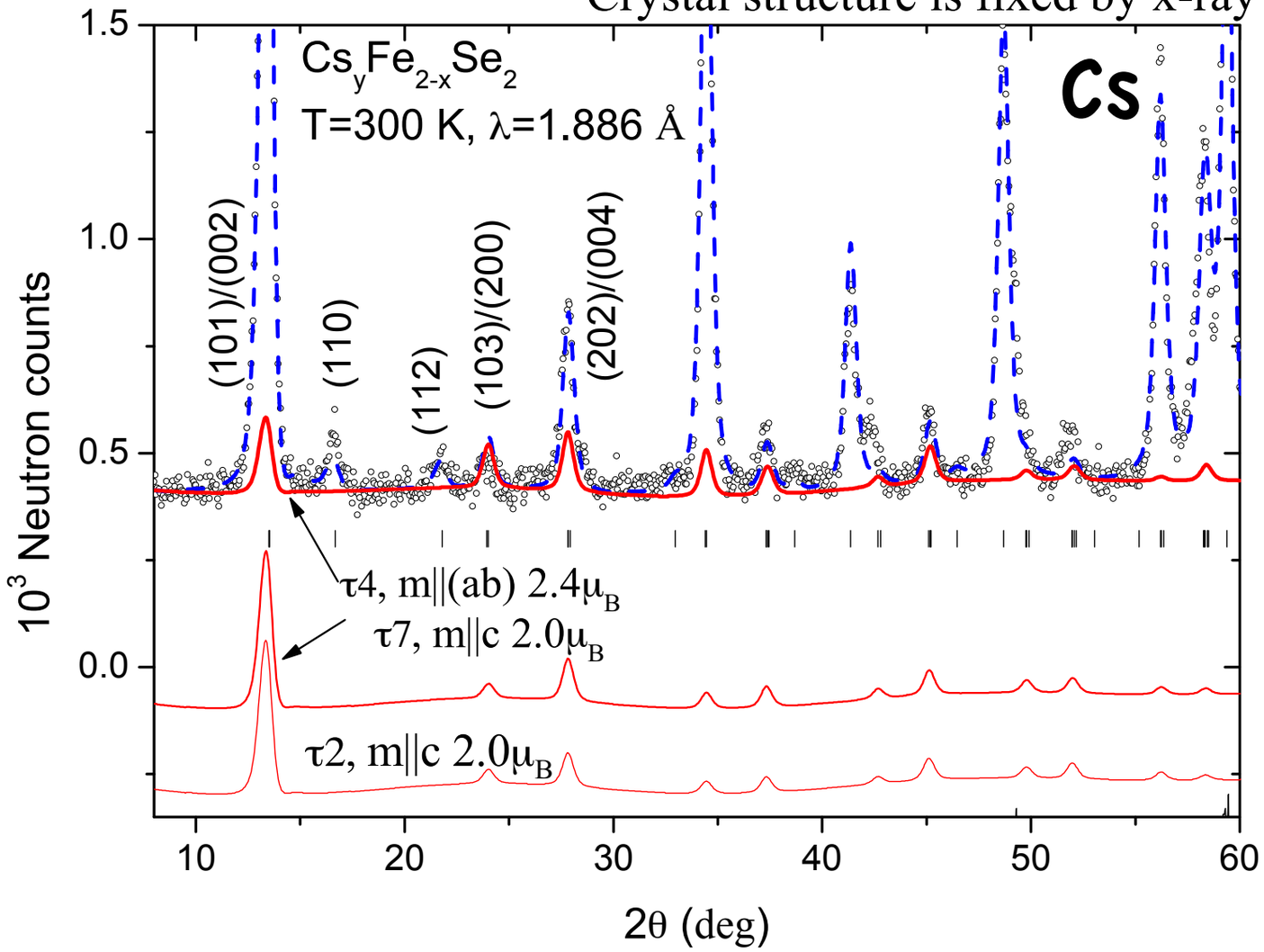

	K	Rb	Cs
a=	8.7302	8.7996	8.8582 Å
c=	14.1149	14.5762	15.2873 Å
$(c/a)^2$ =	2.6140	2.7438	2.9783≃3

is "difficult" for powder due to peak overlap

Magnetic representation. Symmetry adapted solutions.

I4/m, k=0 has 8 1D irreps τ_1,... τ_8.
4 real irreps <--> Shubnikov groups of *I4/m*
4 complex irreps

τ,ψ	h_1 1	h_{14} 4_z^+	h_4 2_z	h_{15} 4_z^-	h_{25} -1	h_{38} -4_z^+	h_{28} m_z	h_{39} -4_z^-
τ_2 *I4/m'*	1	1	1	1	-1	-1	-1	-1
τ_3	1	i	-1	$-i$	1	i	-1	$-i$
τ_5	1	-1	1	-1	1	-1	1	-1
τ_7	1	$-i$	-1	i	1	$-i$	-1	i

One unit cell with Fe

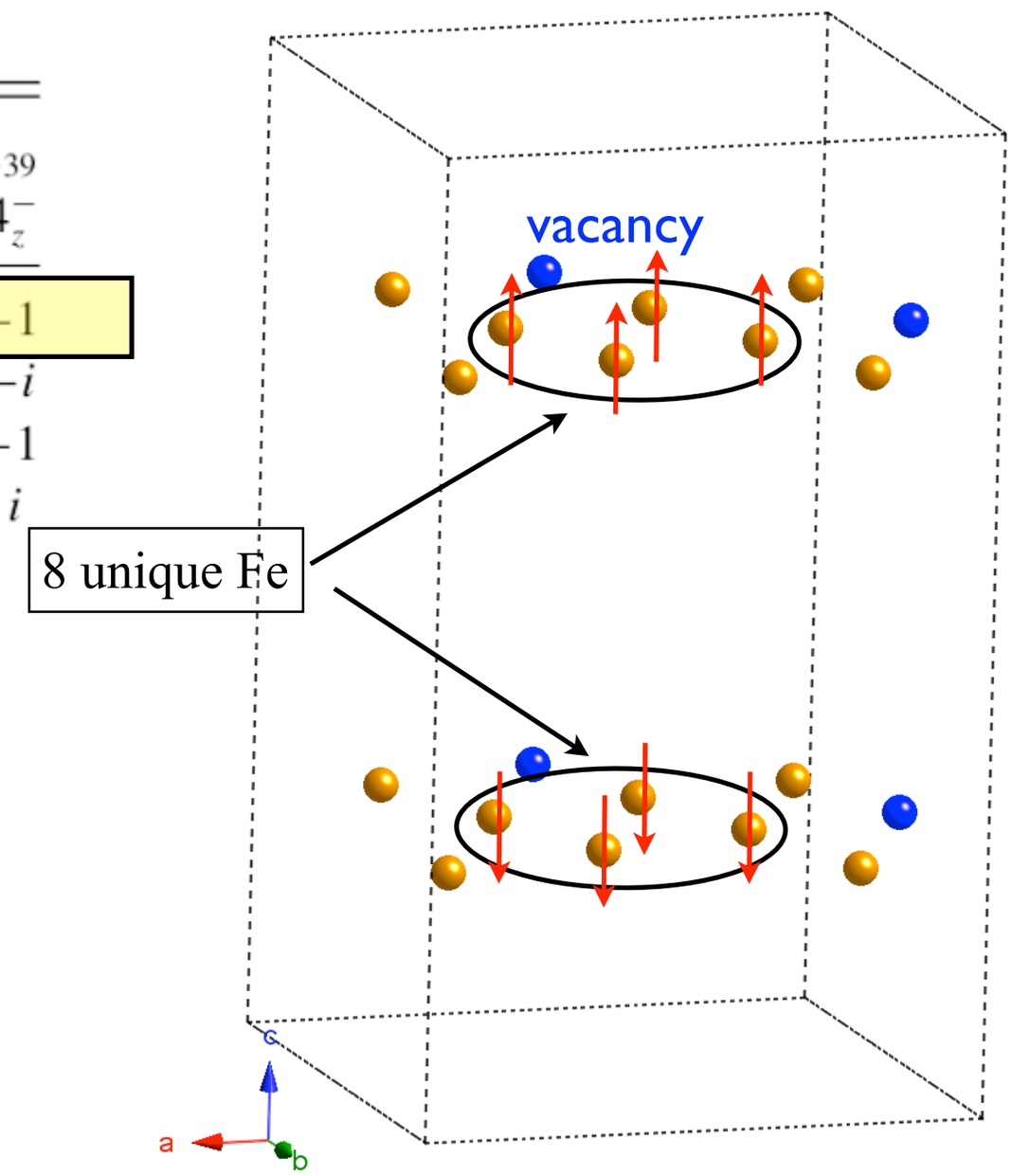

Fe Magnetic representation
(16i) (x,y,z): all eight irreps

$$\Gamma = 3\tau_1 \oplus 3\tau_2 \oplus 3... \oplus 3\tau_8$$

Magnetic structure of $X_{0.8}Fe_{1.6}Se_2$, X=K, Rb, Cs

I4/m cell shown by red square. One *(ab)* layer of Fe-atoms is shown. Fe spins are parallel (+) or antiparallel (-) to c-axis

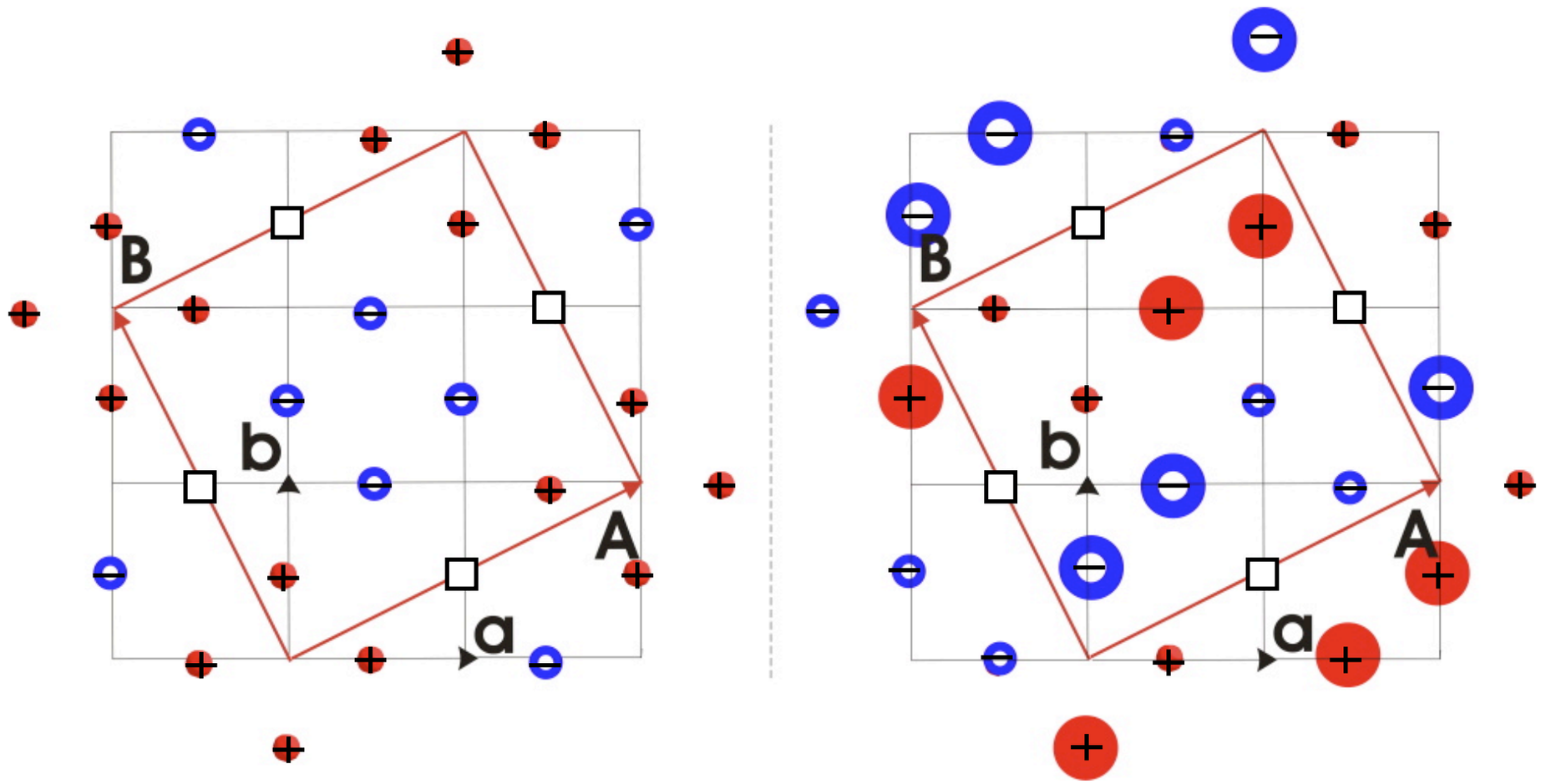

block checkerboard AFM
irrep τ_2, (Γ1-) *I4/m'*

zig-zag AFM
irrep τ_7/τ_3,(Γ4+/Γ3+), *C2'/m'*

Metric(T)

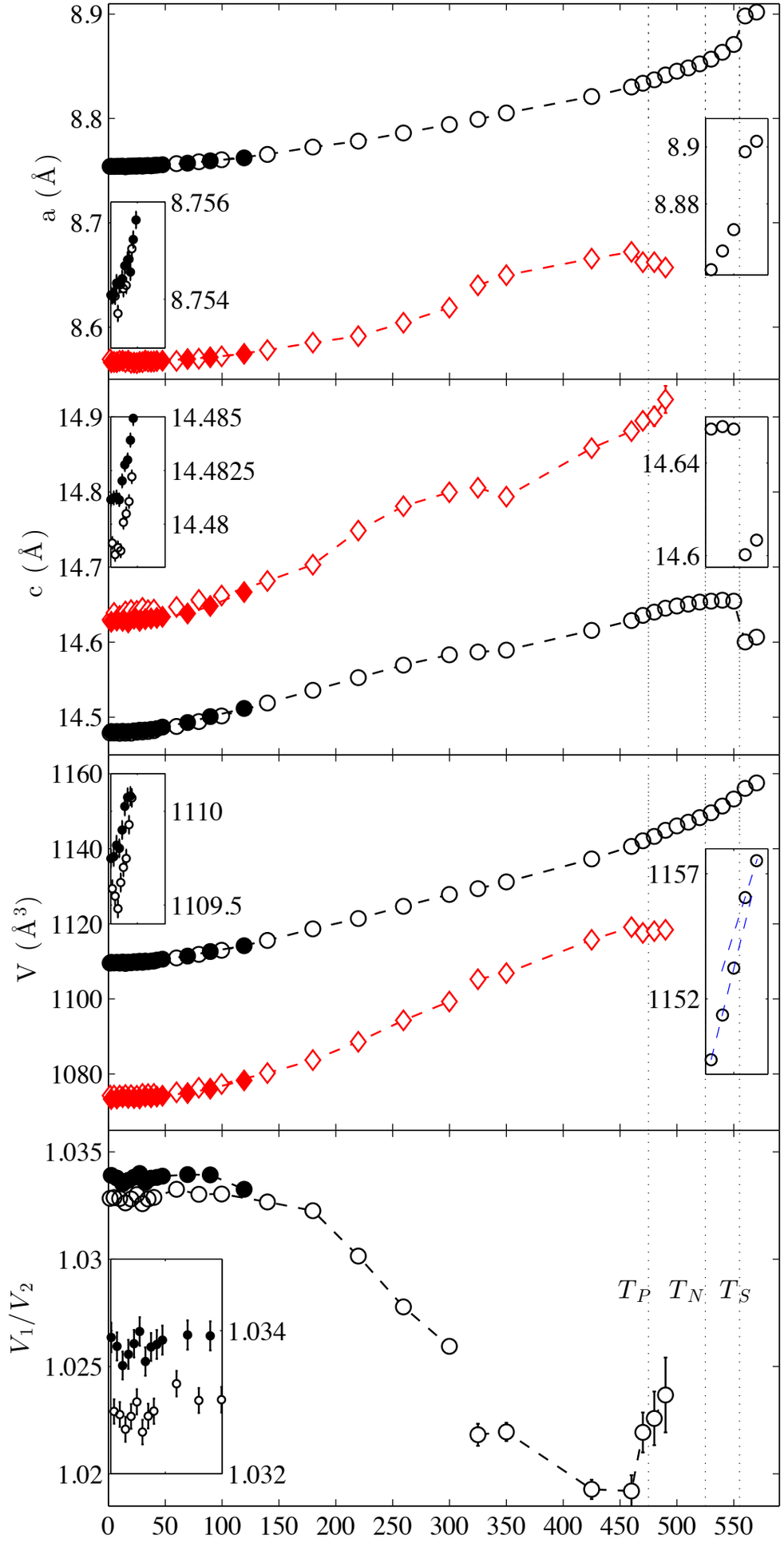

V. Pomjakushin, Phase separation in AFeSe JEMS '13

Yet another phase

Higher resolution: third phase (C) identification

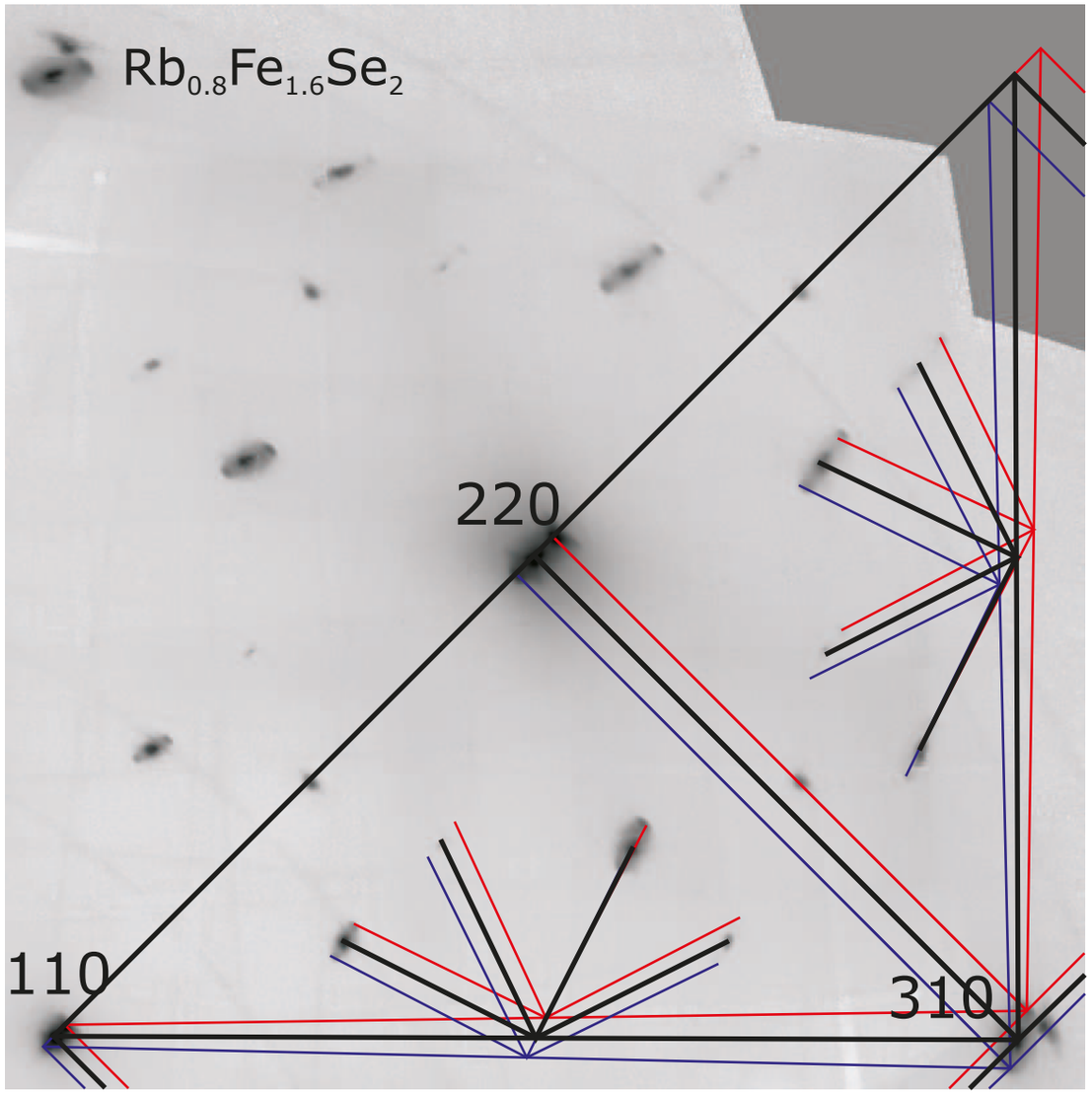

HK0 plane: logarithmic intensity

each reflection of main phase A is surrounded by weaker spots, corresponding to orthorhombic distortion in the basis a' = (a+b), b' = (a-b)

- the symmetry of minority phase C is not higher than orthorhombic
$a_C \sim 1.02a_0 2^{1/2}$, $b_C \sim 0.98a_0 2^{1/2}$, $c_C \sim c_0$
- vacancies ordering is similar to that of main phase
- no disorder-related component is present
- component C is more pronounced in Rb system

twinning motif recovery from 2D images is difficult

Different choice of equivalent propagation k-vectors in I4/mmm

arm of $\{\mathbf{k}_1\}$: $\mathbf{k}_1 = [\frac{2}{5}, \frac{1}{5}, 1]$

one can choose equivalent vector:

$$\mathbf{k}_1' = [-\frac{3}{5}, \frac{1}{5}, 0] = \mathbf{k}_1 + (-1, 0, 1)$$

Superstructure (HKL) can be built

Red: (HKL)=(h,k,**-1**)+ k

Blue: (HKL)=(h,k,**0**) + k'

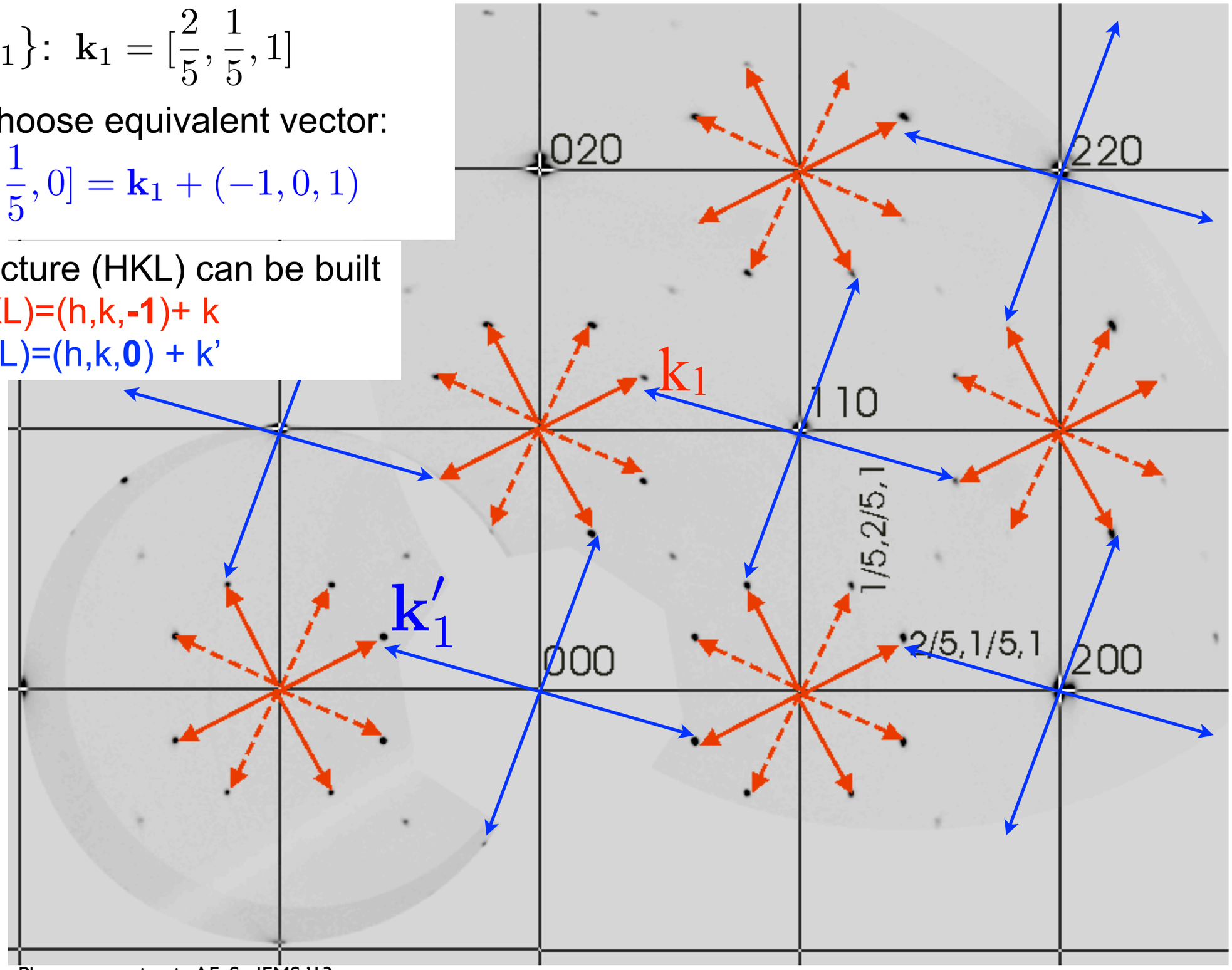

V. Pomjakushin, Phase separation in AFeSe JEMS '13

HOL slice. Supercell. Soft classification of peaks

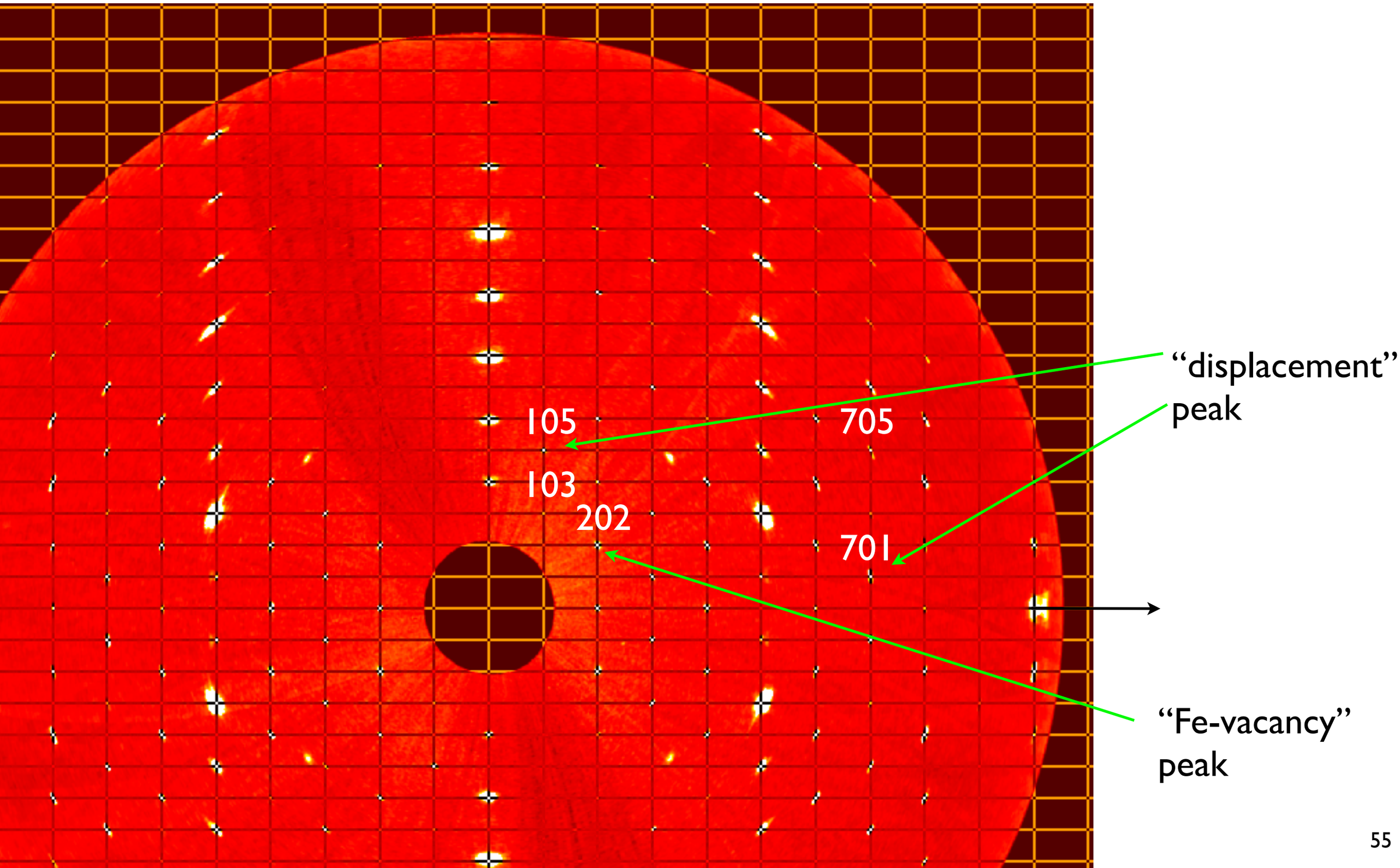

Crystal structure distortion in L=0 plane according to refined structure parameters

(HK0) parent cell

red, orange: forbidden
green, blue: allowed

(HK0) supercell

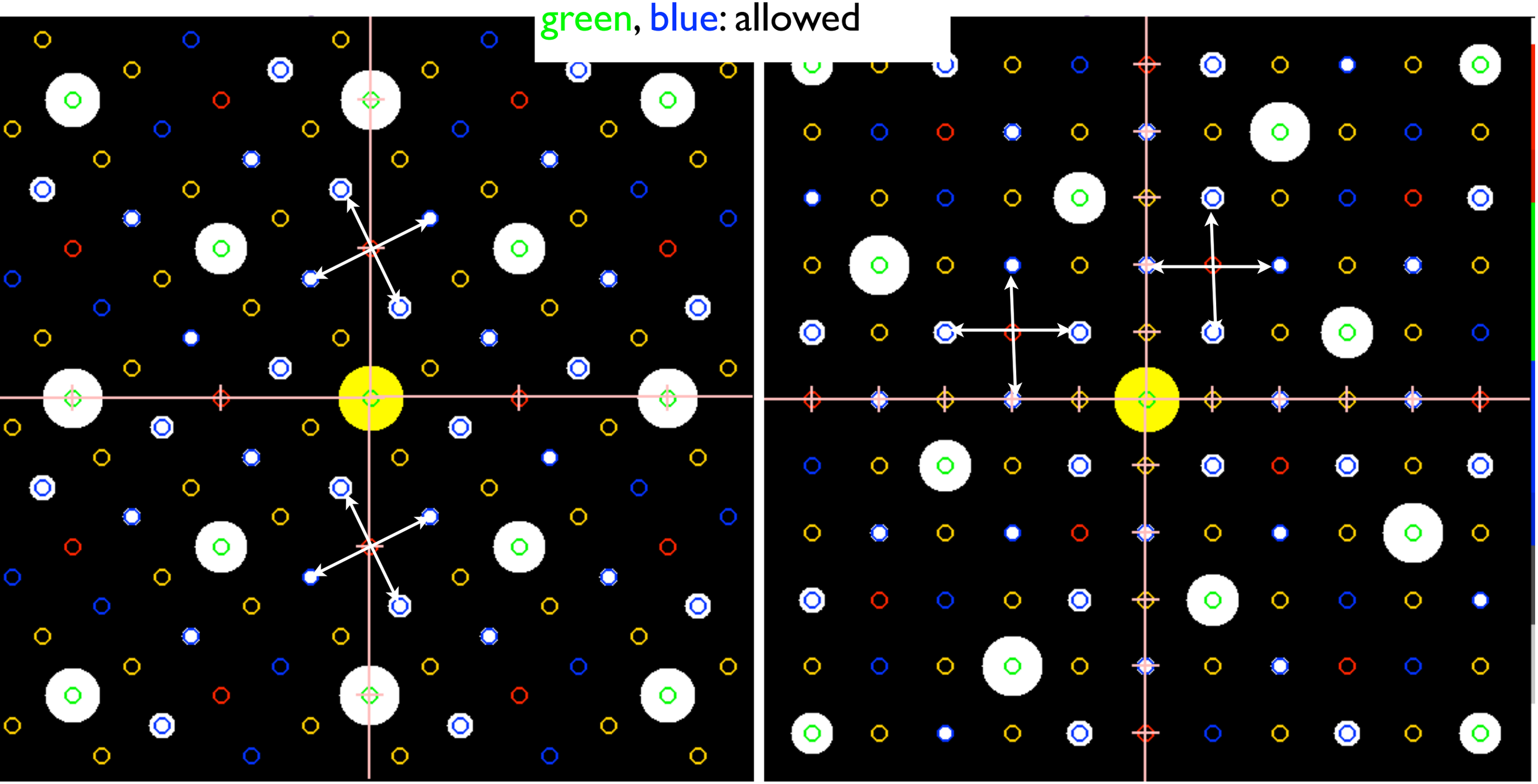

Crystal structure distortion in K=0 plane

(H0L) supercell

red, orange: forbidden
green, blue: allowed

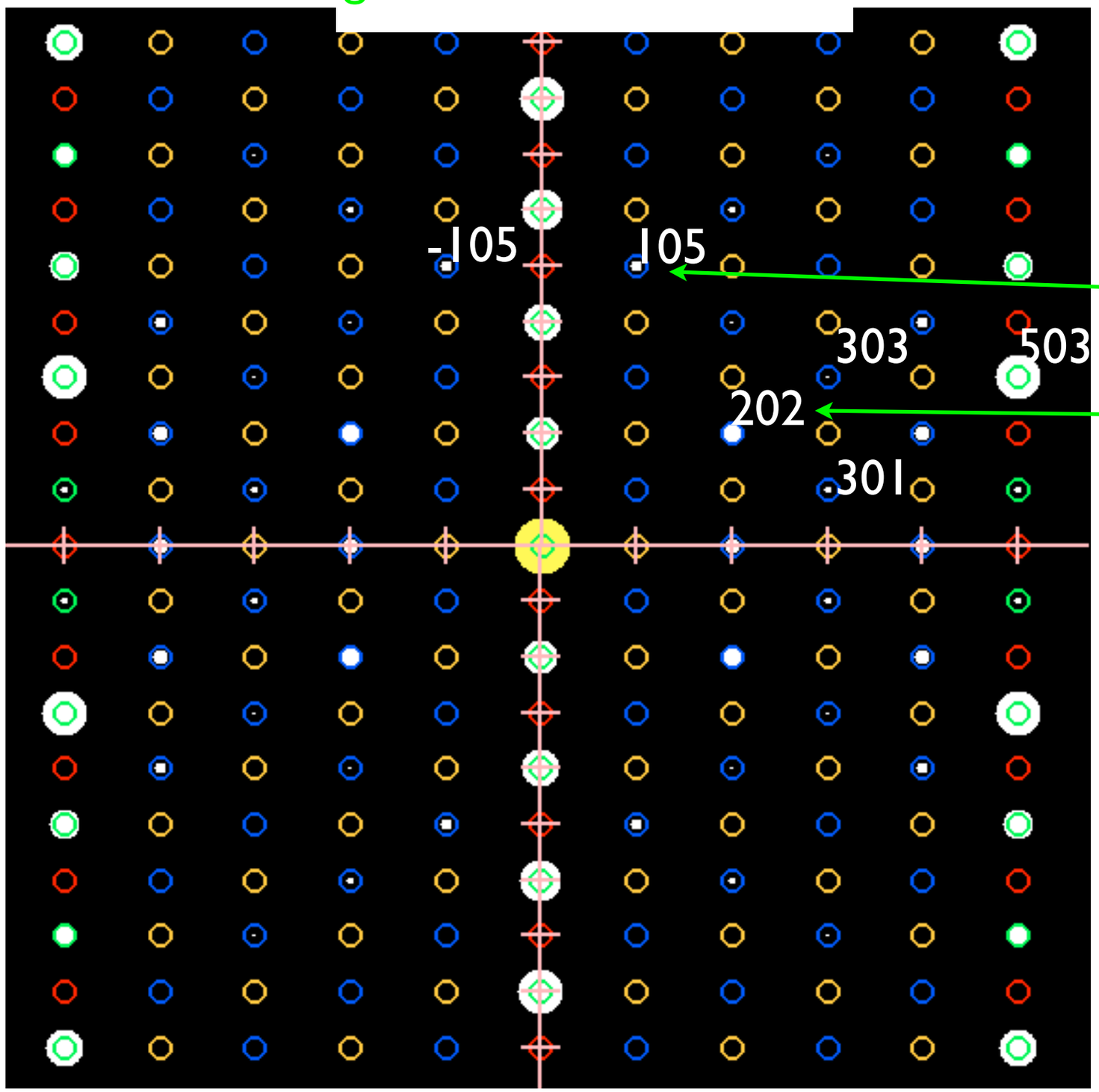

"displacement" peak

"vacancy" peak

No visible anomaly at T_c

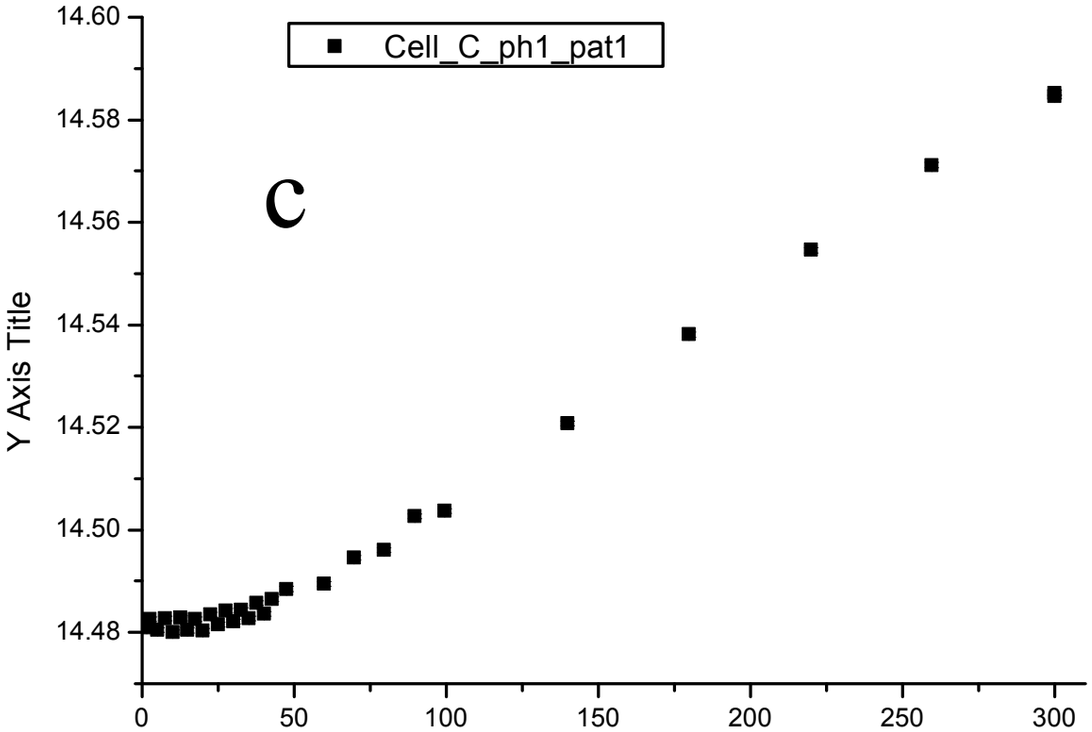

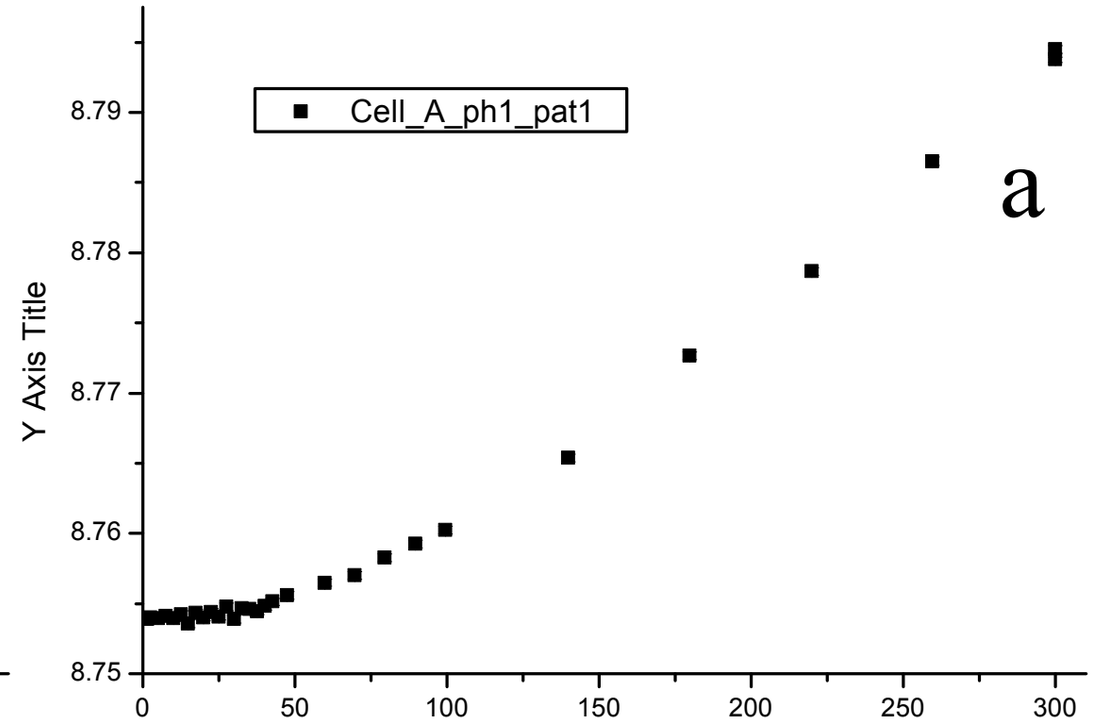

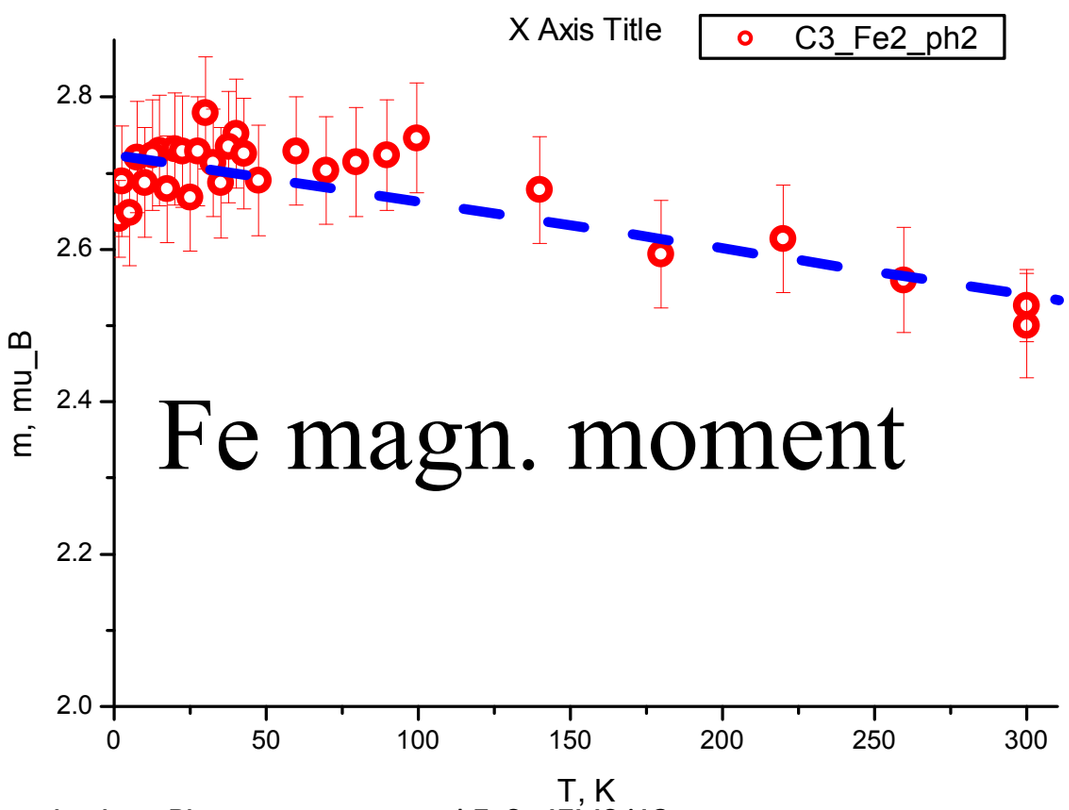

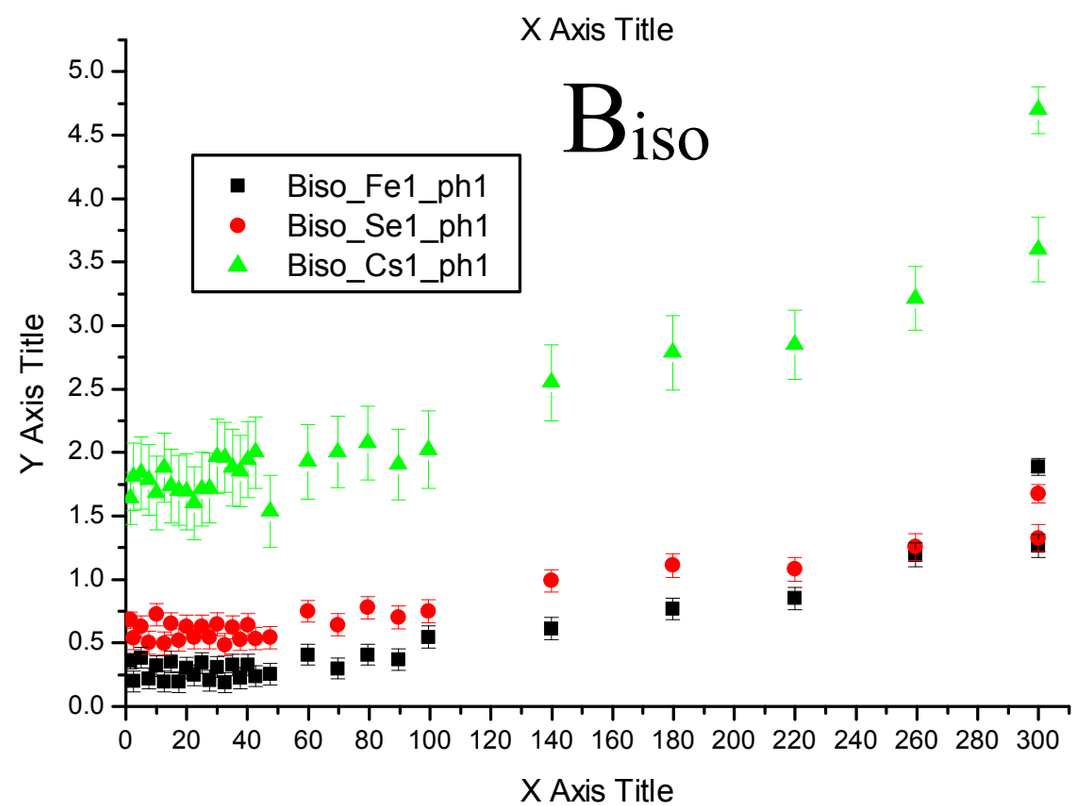

V. Pomjakushin, Phase separation in AFeSe JEMS '13

Parent compounds. $FeSe/Tl_y(Fe_{2-x}Se_2)$

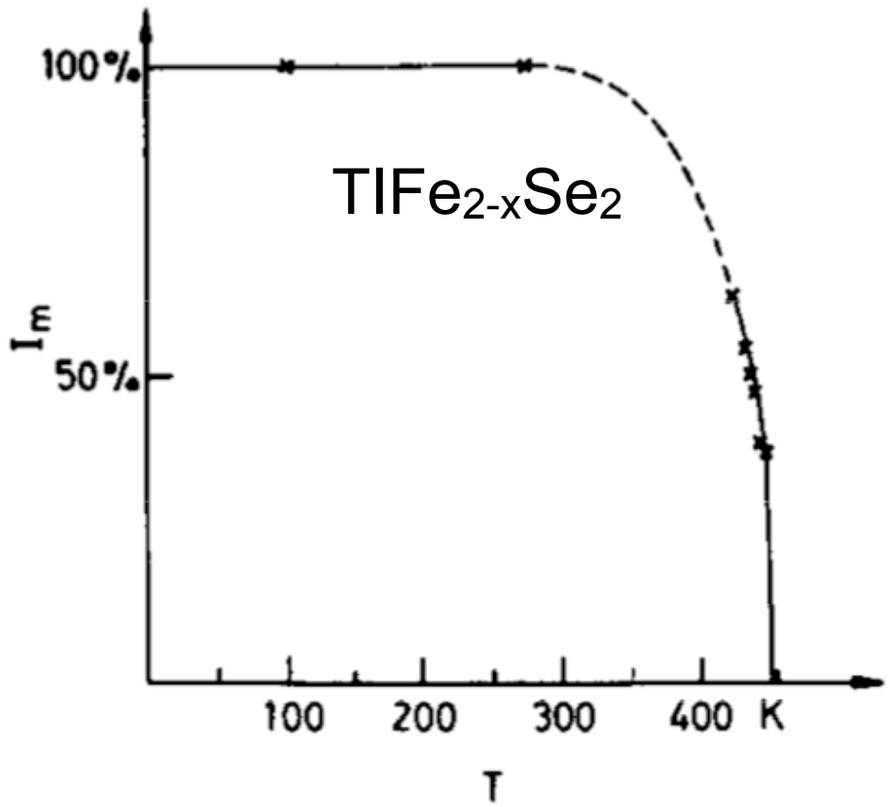

FIG. 5. Relative intensity of the magnetic main component as a function of temperature.

L. HÄGGSTRÖM, et al (1986)
H. Sabrowsky et al (1986)

Mossbauer and x-ray studies on a mosaic of single crystals of $TlFe_{2-x}Se2$

$Fe_1Se_{0.974(5)}$

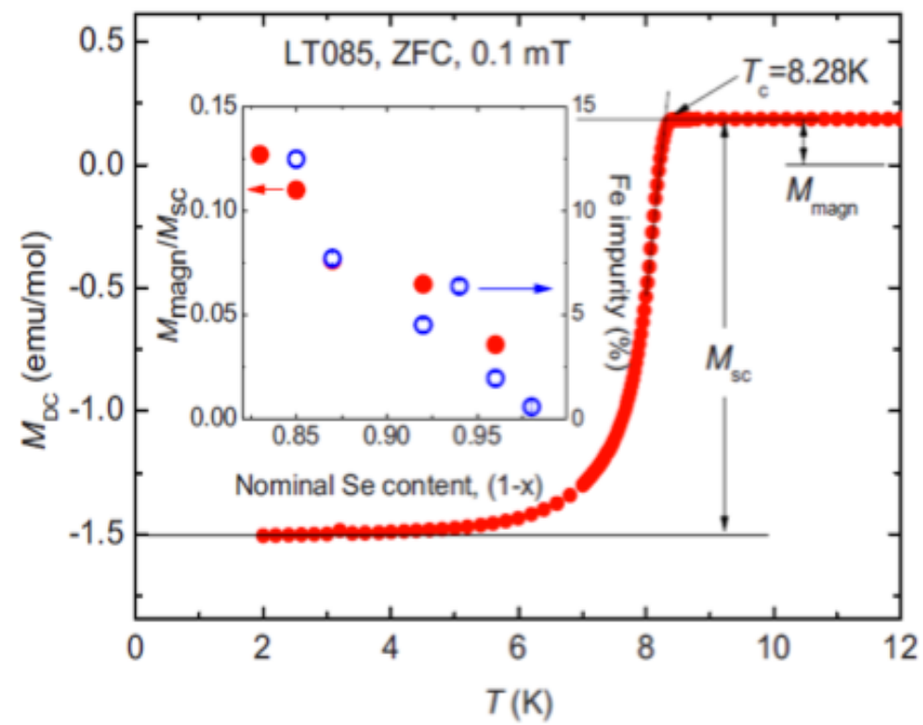

E. Pomjakushina et al (2009)